UNIVERSITY OF OSLO
Department of Geosciences
MetOs section

Simulated Changes in the Radiative Properties of Arctic Stratus due to Anthropogenic Forcing

Master thesis in Geosciences: Meteorology and Oceanography

Kari Alterskjær

1st September 2009

Abstract

Clouds in the Arctic differ from clouds elsewhere in that they have a net warming effect at the surface. This happens because the longwave (LW) radiation dominates the radiation regime due to large solar zenith angles throughout the year, combined with a high surface albedo. We have looked at how an increased amount of anthropogenic sulfate aerosols in Arctic clouds can modify the radiation budget in the region. In doing this we used both a one dimensional model based on the NCAR CCM3 radiation scheme and the three dimensional CAM-Oslo climate model. An increased amount of sulfate aerosols alters the clouds mainly through the first and the second indirect effect giving them smaller effective drop radii and higher liquid water paths. Elsewhere on Earth this would lead to an increased cooling effect, but given the LW dominance and the optically thin clouds in the Arctic it has been suggested that the change may lead to an increased warming by the clouds in this region. Studies by Garrett and Zhao (2006) and Lubin and Vogelmann (2006) have under certain conditions found an increase in the LW surface flux on the order of 3.3 to 8.2 W/m^2 due to indirect effects. We have studied these effects by using present and pre-industrial emission scenarios as well as a scenario with increased SO_2 emissions compared to present day. Our results suggest that cloud forcing is less susceptible to increased levels of pollution today than it was pre-industrially. The reduced sensitivity is caused by large amounts of aerosols already available to the clouds in present day. The increased aerosol levels from pre-industrial times until today leads to an annually averaged increase in the LW cloud forcing at the surface of 0.64 W/m^2. Although these simulated results are subject to uncertainties, the overall importance of the increase in LW surface flux seems significantly lower than the maximum possible increase in this quantity found in earlier studies. The annually averaged change in SW cloud forcing with indirect effects is -0.99 W/m^2, while the simulated net change in surface cloud forcing due to anthropogenic aerosols averages to -0.35 W/m^2. Due to LW dominance in winter, the average change in cloud forcing from October to May is positive (0.2 W/m^2), while the change in forcing averaged over the remaining months is negative (-1.4 W/m^2). We conclude that the overall effect of increased levels of anthropogenic sulfate aerosols under cloudy skies is a small *decrease* in the surface radiative flux.

Acknowledgements

First of all I want to thank my supervisor Jón Egill Kristjánsson for an interesting project, excellent guidance and for always making me feel welcome despite my many interruptions and knocks on his office door. I am grateful for the opportunity he gave me to present results from this work at the MOCA-09 Climate Conference in Montreal this July. Attending this conference gave me valuable experience. I would also like to thank Corinna Hoose for helping me handle the CAM-Oslo climate model, for good comments and for creating input files needed for simulations in this project. Thanks to Alf Kirkevåg, Kjell Andresen and Gunnar Wollan for their help with technical problems and to Surabi Menon for her input on the possible influence of the vertical resolution of our three dimensional model. Thanks also to Inger-Lise Aasen for proof reading and commenting on the written work.

The last year would not have been possible without the positive environment created by the girls at my study hall, or without the patience and kind words from friends and family. Last, but not least, I would like to thank Ståle for valuable discussions and for making it possible to maintain my sanity throughout most of the time spent working on this project.

Contents

1 Introduction

The Intergovernmental Panel on Climate Change (IPCC) leaves little doubt that we now experience a warming of the global climate: "Warming of the climate system is unequivocal, as is now evident from observations of increases in global average air and ocean temperatures, widespread melting of snow and ice, and rising global average sea level" (IPCC, 2007). They further state with *very high confidence* that this warming is caused by human activity.

The Arctic region is particularly sensitive to climate change (Wang and Key, 2005) and the increase in air temperature in the bottom layers of the atmosphere is almost twice as large here as in the rest of the world. This phenomenon is called the 'Arctic Amplification' (eg. Graversen et al. (2008)). Due to the rapid changes found in this region, there has been an increasing scientific interest in the Arctic in general. This was made evident by the onset of the International Polar Year (IPY) in 2007.

In projections of future climate published in the Fourth Assessment Report by the IPCC, changes in clouds due to human activity are among the major sources of uncertainty. An increased understanding of clouds and aspects related to change in clouds due to anthropogenic forcing is therefore important.

Clouds in the Arctic differ from clouds elsewhere in that they have a net warming effect at the surface - there is positive cloud forcing. Elsewhere on Earth clouds block more shortwave (SW) radiation than the longwave (LW) radiation they return to the Earth-atmosphere system (eg. (Liou, 2002)). In the Arctic, however, the sun is absent for large parts of the year, and when it returns in summer it is at large solar zenith angles. Additionally, the Arctic surface has a relatively high surface albedo. Depending on season, the fraction of solar radiation reflected by the Arctic surface may therefore be nearly the same as the fraction reflected by overlaying clouds. Because of this, the LW radiation plays a much more important role in this region than at lower latitudes and the greenhouse effect of clouds in the LW leads to a net warming by clouds in the Arctic.

In 2006 two empirical studies were published in Nature dealing with changes in Arctic clouds due to human activities (Garrett and Zhao (2006) and Lubin and Vogelmann (2006)). They both study the influence of anthropogenic emissions of pollution on thin, non-opaque clouds. Results from these studies suggest that LW surface warming by clouds increases significantly in the presence of large anthropogenic emissions.

The motivation behind this study lies in the large changes observed in the Arctic climate, combined with the general uncertainty regarding changes in clouds with pollution and results found in the empirical studies mentioned

above. In this thesis we will study how an increased amount of anthropogenic sulfate aerosols in the Arctic clouds can modify the radiation budget in the region. We will focus mainly on changes occurring in the surface forcing, and only briefly describe what occurs at the top of the atmosphere. To study this phenomenon we have used both a one dimensional (1D) model based on the radiation scheme from the National Center for Atmospheric Research Community Climate Model version 3 (NCAR CCM3) and the three dimensional (3D) CAM-Oslo climate model (Community Atmosphere Model). We will focus on the following questions.

- For what clouds is the forcing most susceptible to change with pollution?
- Can we reproduce the findings of earlier studies using the 1D model?
- How does the simulated surface LW cloud forcing change with pollution?
- How do the average changes in surface LW cloud forcing compare to earlier findings?
- How does the simulated surface SW cloud forcing change with pollution?
- What is the overall effect of increased amounts of anthropogenic sulfate aerosols interacting with clouds on the radiative balance at the Arctic surface?

The next chapter gives some background information on the earlier studies on interaction of Arctic clouds and aerosols. Chapter 3 goes into theory behind the influence of clouds on the radiative balance and how increasing aerosol levels may alter this influence. The models and methods used in this thesis are described in chapter 4. Results and discussions concerning the one dimensional model and the three dimensional model are presented in chapters 5 and 6 respectively. In the last chapter we summarize our findings and conclude.

2 Background

In this chapter we will briefly describe the background for studying the change in cloud forcing with pollution. We will also present articles by Garrett and Zhao (2006) and Lubin and Vogelmann (2006) which study changes in cloud radiative properties with increased aerosol concentrations. These articles form a basis for this thesis.

Climate change in the Arctic may be caused by several factors, among these is the increased surface radiative flux resulting from anthropogenic greenhouse gas emissions and soot deposition on snow. Soot deposition decreases the surface albedo and increases the amount of solar radiation absorbed by the snow covered surface. The articles by Garrett and Zhao and Lubin and Vogelmann mentioned above discuss another possible factor resulting from human activity that influences the Arctic climate - the increase in surface radiative flux when large amounts of pollution interact with the Arctic clouds.

Traditionally there has been a focus on how aerosols may change clouds to reflect more shortwave radiation (eg. Twomey (1974)). This effect has been observed for instance when ship tracks form in maritime stratus (Garrett et al., 2002). The change in cloud properties has not been considered to affect the longwave radiation properties as these clouds have been seen as black bodies in the longwave (Twomey, 1974). Following the increased focus on the Arctic region, there has been an increased interest in how aerosols may change the thinner, nonopaque clouds that are common in this region. Observations have shown that in addition to the increased cooling effect by the clouds in the shortwave, we may expect increased warming by these clouds in the longwave.

Aerosol concentrations influence the radiative forcing of clouds because they may act as cloud condensation nuclei. Through what is know as the indirect effects, increased aerosol levels influence the size of cloud particles and the amount of water held in a cloud. Both the size of particles and the water amount is affecting the cloud LW emissivity and the SW cloud albedo and therefore the cloud radiative properties. Changes in cloud parameters with pollution will be described in greater detail in section 3.4.

Garrett and Zhao (2006) study the surface radiative balance under cloudy skies for different concentrations of anthropogenic aerosols. Their work is based on measurements of aerosol concentrations and cloud properties obtained near Barrow, Alaska. They compare episodes of "clean air" to episodes when the air is more polluted and approximates these as the upper and the lower quartile thresholds of cloud condensation nuclei concentrations. They reduce the uncertainty of their study by only looking at cases with single

layer clouds with tops below 1.5 km altitude, and study a total of 9440 cloud samples from the year 2000 to 2003. When comparing the average polluted to the average clean case, they find a 3.3 to 5.2 W/m^2 increase in the surface net flux under cloudy skies.

The study by Lubin and Vogelmann (2006) is also based on observations obtained in northern Alaska. They use six years of data (not complete sets) of aerosol condensation nuclei (CN) and cloud properties. Like Garrett and Zhao they consider episodes where the CN values are below the lowest quartile threshold clean and above the upper threshold polluted. They further study only samples coincident with clouds that are not black bodies in the LW.

In their article they study the radiative LW effect of reductions in the size of cloud droplets due to high levels of pollution. They find that under cloudy skies such changes in cloud droplet size lead to an increase of an average of 3.4 W/m^2 in the LW flux at the surface. Changes in both cloud droplet size and water amount with pollution lead to an average increase of 8.2 W/m^2 in the same flux.

The findings of both Garrett and Zhao (2006) and Lubin and Vogelmann (2006) are of magnitudes believed to be climatologically significant. For comparison, the increased flux resulting from anthropogenic emissions of green house gases is approximately 2.3 W/m^2 (IPCC, 2007). Based on this it is therefore important to study this phenomenon closer and find the overall importance of changes in radiative properties of Arctic clouds with pollution.

3 Theory

3.1 Radiation Theory and Clouds

In this thesis the term long wave (LW) radiation is used for the thermal infrared (IR) radiation emitted at temperatures found in the earth-atmosphere system (λ=5 to 100 μm). The short wave (SW) radiation describes the solar radiation reaching our system (λ=0.1 to 5 μm).

The net longwave flux varies within this system because of changes in both temperature and characteristics of the emitting bodies with location and time. The reason for this variation can be seen using the Stefan-Boltzmann law. It gives the flux density emitted by a body:

$$F = \epsilon \sigma T^4 \tag{1}$$

where ϵ is the emissivity of that body and σ the Stefan-Boltzmann constant (σ = 5.67 * 10^{-8} J m^{-2} s^{-1} K^{-4}) (Liou, 2002). The emissivity of a given wavelength is defined as the ratio of the emitted intensity to the maximum possible emitted intensity at that wavelength. If the emissivity approaches unity, the emitting surface is close to a black body. Liou states in his book "An Introduction to Atmospheric Radiation" (p 384) that the emissivity of the Earth surface in thermal IR is close to one.

From the Stefan-Boltzmann law it is clear that warmer bodies with higher emissivities emit more energy. The law also makes it clear that if the mean temperature and emissivity of the sun are taken to be approximately constant, the shortwave flux reaching our system is constant as well.

Clouds affect the longwave and the shortwave radiation balance through different processes. In the longwave, some or all of the energy radiated from the surface and the atmosphere below the cloud layer is absorbed by the cloud. The portion of energy absorbed depends on the cloud absorptivity, the ratio of absorbed intensity to the incident intensity at that wavelength. At the same time the cloud itself emits radiation, the amount of which depends on the cloud emissivity and temperature. Kirchhoff's Law states that in order to have thermodynamic equilibrium in a medium, the absorptivity must be equal to the emissivity (Liou, 2002). This is valid below 60-70 km and is a good approximation for the part of the atmosphere studied in this thesis.

The longwave cloud emissivity is a function of liquid water path (LWP), cloud phase and size of the cloud particles. LWP is the integrated amount of liquid water in a column above a certain area (units of g/m^2). The LW cloud emissivity can be defined as (NCAR CAM3.0 documentation):

$$\epsilon \;=\; 1 - e^{-1.66 * k_{abs} * LWP} \tag{2}$$

Cloud phase and particle size affects the emissivity through the absorption coefficient, k_{abs}:

$$k_{abs} = k_{abs,liquid} * (1. - fice) + k_{abs,ice} * fice \quad (3)$$

Here fice is the fraction of cloud particles that are frozen. Both $k_{abs,liquid}$ and $k_{abs,ice}$ are inversely proportional to cloud particle size, although for liquid particles this is only for droplets larger than 10 μm. For droplets smaller than 10 μm the wavelength of the LW radiation is larger than the droplet size and the absorption efficiency is small (Garrett et al., 2002). For droplets over a certain size the absorption coefficient thus increases with decreasing cloud particle size.

From equation 2 it is clear that the longwave emissivity increases with liquid water path in the cloud. This corresponds well with general expectations, that clouds containing more water are optically thicker and hence emit and absorb more energy. The exponential form of this equation however tells us that when a certain water amount is reached, changes in LWP become less significant as the exponential term may already be approximated by zero and the emissivity is very close to unity. For smaller water amounts, however, the emissivity is also sensitive to the size of cloud particles, both droplets and ice particles, through the absorption coefficient. Smaller particles correspond to higher k_{abs} and higher emissivity.

To see what water amount is necessary for the cloud to be optically thick in the LW we go back to equation 2. If we assume that a black body is defined as having an emissivity above 0.99 we get an expression for the minimum LWP required for the cloud to reach this limit:

$$\epsilon = 1 - e^{-1.66*k_{abs}*LWP} > 0.99 \quad (4)$$

$$\Leftrightarrow e^{-1.66*k_{abs}*LWP} < 0.01 \quad (5)$$

$$\Leftrightarrow k_{abs} * LWP > -\frac{1}{1.66} ln 0.01 \quad (6)$$

$$\Leftrightarrow LWP > \frac{1}{k_{abs}} 2.77 \quad (7)$$

Inserting for average absorptivity coefficients gives the data set shown below (see table 1). The data presented is based on results from the one dimensional model used in this study. Notice how the necessary water amount increases with effective radius. This is because larger radii lead to smaller absorption coefficients and the LWP must increase for the exponential term of equation 2 to approach zero.

The shortwave radiation is affected by clouds through a different process. The energy is to a much smaller degree absorbed by the cloud, unlike the longwave case, but rather scattered or reflected by the cloud particles. In fact, for water clouds absorption of SW radiation increases with water amount and levels off between 10 and 12 percent for high liquid water paths (Slingo, 1989). The cloud reflectivity also increases with water amount, but reaches values as high as 75 to 80 percent for LWP important to this thesis (Slingo, 1989). Clouds in that manner mainly work to change the direction of the incoming solar radiation and by back-scattering prevent some of the energy from reaching the surface.

The cloud albedo, A, is the ratio of flux reflected by the cloud back towards space to the incoming solar flux (Liou, 2002), and hence tells us how much of the solar energy is kept from reaching the environment below the cloud. Twomey (1974) shows that the cloud albedo is a function mainly of cloud optical thickness, asymmetry factor and single-scattering albedo. The single-scattering albedo, $\tilde{\omega}$, gives the fraction of energy not absorbed in a single scattering event. Water clouds have very little absorption in the visible region, which is located at the peak of the Planck curve for solar radiation. One therefore often assumes $\tilde{\omega} \approx 1$. The albedo of a cloud can then be approximated by the optical thickness and the asymmetry factor alone (Meador and Weaver, 1980):

$$\begin{aligned} A &= \frac{(1-g)\tau}{1+(1-g)\tau} \\ &= \frac{1-g}{\frac{1}{\tau}+(1-g)} \end{aligned} \tag{8}$$

The asymmetry factor, g, gives the direction of the scattered radiation, where g = 1 indicates pure forward scattering and g = -1 pure back-scattering. It is calculated as the average value of the cosine of the scattering angle (Hobbs, 1993). According to Twomey (1974) for warm clouds most of the energy scattered by cloud droplets is scattered forward and g is close to 0.8

Table 1: Liquid water path corresponding to optically thick clouds in the LW: emissivity ≈ 1.

	Summer (fice = 0)	Winter (fice $\approx$ 0.3)
Re $\leq 10\mu$m	LWP$>$ 36.9 g/m^2	LWP$>$ 52.3 g/m^2
Re = 11μm	LWP$>$ 40.7 g/m^2	LWP$>$ 57.7 g/m^2
Re = 12μm	LWP$>$ 44.7 g/m^2	LWP$>$ 63.0 g/m^2
Re = 13μm	LWP$>$ 47.8 g/m^2	LWP$>$ 67.5 g/m^2

- 0.9. Slingo and Schrecker (1982) go further and show that for these clouds g depends on the effective radius, $\bar{r}$, of cloud droplets, and the wavelength of the incoming radiation, λ. Larger sizes lead to higher valued asymmetry factors.

$$g = e(\lambda) + f(\lambda)\bar{r} \tag{9}$$

where e(λ) and f(λ) are parameters > 0. In addition, g depends on cloud phase as well, because the size and the shape of ice particles differ from those of water clouds.

For water clouds two of the three quantities comprising the cloud albedo can be approximated and the importance of the cloud optical thickness, τ, becomes evident. From equation 8 it is clear that higher τ corresponds to higher cloud albedo. The optical thickness of a cloud layer indicates that a fraction $1-e^{-\tau}$ of the incident vertical SW radiation beam has been scattered at least once in passing through the layer. τ is given by (Twomey, 1977):

$$\begin{aligned} \tau &= \int_{z_b}^{z_t} k_E dz \\ &= \pi \int_{z_b}^{z_t} \int_0^{\infty} Q_e(r/\lambda) r^2 n(r,z) dr dz \\ \tau &\approx 2\pi N \bar{r}^2 \Delta z \end{aligned} \tag{10}$$

Here k_E is the extinction coefficient and n(r)dr the number of drops per unit volume with radius in the interval (r, r + dr). N is the total number concentration of droplets and Q_e the extinction efficiency. The latter may be approximated by $Q_e \approx 2$ for wavelengths in the visible where $\lambda << $ r (Liou, 2002). In the simplified expression we have assumed that the cloud droplet radii can be approximated by the effective radius, $\bar{r}$. This is a mean of droplet size where the droplet cross section is included as a weighting factor. It is given by (Liou, 2002)(page 372):

$$\bar{r} = \frac{\int \pi r^3 n(r) dr}{\int \pi r^2 n(r) dr} \tag{11}$$

We have also assumed that Δz represents the depth of a homogeneous cloud layer. All model layers are homogeneous and the above assumption is therefore suited for our purposes. In a homogeneous cloud layer the liquid water content, $LWC = \frac{4}{3}\pi\rho_L \bar{r}^3 N$, will be constant with height. This leads to a

simplified expression for the liquid water path:

$$\begin{aligned} LWP &= \int_{z_b}^{z_t} LWC dz && (12) \\ &\approx LWC * \Delta z && (13) \\ &= \frac{4}{3}\pi\rho_L \bar{r}^3 N \Delta z && (14) \end{aligned}$$

Inserting this into the above expression for τ one is left with a very simple expression for the optical thickness of warm clouds as a function of liquid water path and effective radius:

$$\tau = \frac{3}{2}\frac{LWP}{\rho_L \bar{r}} \quad (15)$$

From this equation, it is evident that τ increases with increasing LWP and decreasing $\bar{r}$. The same relation is used by Zhang, Stamnes and Bowling in their study of "Impact of Clouds on Surface Radiative Fluxes and Snowmelt in the Arctic and Subarctic" (1996) (see also Liou (2002) and Slingo and Schrecker (1982)).

For ice clouds the optical depth is given as a function of ice water path (IWP), a mean effective crystal size (D_e) and parameters depending on crystal type (c and b) (Liou, 2002):

$$\tau \approx IWP(c + \frac{b}{D_e}) \quad (16)$$

The IWP can be approximated as IWC*Δz, the mass of ice per unit volume of air times the depth of the cloud layer. For ice columns c$\approx$-6.656*10^{-3} and b$\approx$3.686 (Liou, 2002). From this equation we see that ice and water clouds have similar characteristics. Increasing the ice water path or reducing the effective crystal size in ice clouds leads to an increase in the cloud optical depth.

In addition to what is mentioned above the wavelength of the incoming radiation is also of importance to the cloud albedo.

3.2 Cloud Forcing

Clouds in the Arctic region differ from clouds elsewhere in that they have a net warming effect on the surface environment - there is positive cloud forcing (CF). Cloud forcing is defined as "the radiative impact that clouds have on the atmosphere, surface, or top-of-the-atmosphere (TOA) relative to clear skies" (Shupe and Intrieri, 2004). It tells you how much more energy

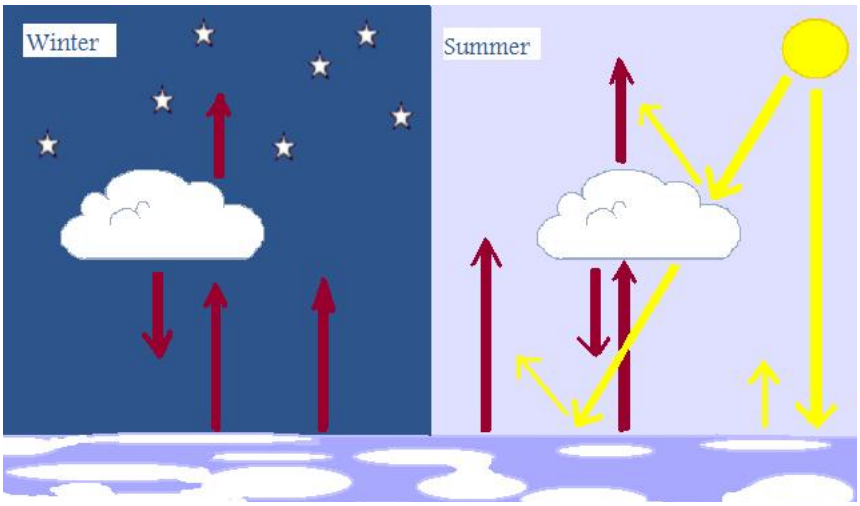

Figure 1: Cloud forcing mechanisms in the Arctic environment. SW radiation in yellow and LW radiation in dark red.

is received at a certain level in the atmosphere with clouds present than without. Assuming all fluxes are defined as positive towards the surface, cloud forcing is defined as:

$$
\begin{aligned}
CF_{LW} &= Netflux_{LW,allsky} - Netflux_{LW,clear} && (17)\\
&= F{\downarrow}_{LW,allsky} - F{\uparrow}_{LW,allsky} - F{\downarrow}_{LW,clear} + F{\uparrow}_{LW,clear} && (18)\\
CF_{SW} &= Netflux_{SW,allsky} - Netflux_{SW,clear} && (19)\\
&= F{\downarrow}_{SW,allsky} - F{\uparrow}_{SW,allsky} - F{\downarrow}_{SW,clear} + F{\uparrow}_{SW,clear} && (20)\\
CF &= CF_{LW} + CF_{SW} && (21)\\
& && (22)
\end{aligned}
$$

In general CF is calculated using the true atmospheric state including clouds which we call allsky, and using a hypothesized clear sky atmosphere. The latter is simulated through numerical modeling. The best estimate of the true state of the atmosphere is used as input and the clouds then removed. The radiation fluxes are then calculated to give the clear sky net fluxes. (Some claim that the water vapor amount in a vertical column of the atmosphere is larger when clouds are present than when they are not. Simply removing the clouds is in that case not a good approximation of the clear sky state as water vapor interferes with the radiative fluxes. Ignoring such an effect will lead to an underestimation of the cloud forcing.)

The sign and magnitude of the cloud forcing depends on several factors. First we will consider the cloud forcing at the surface. The longwave part of

this forcing is positive and reflects the warming effect caused by downward longwave radiation emitted at the cloud base. This radiation increases the LW allsky net flux, and hence the cloud forcing. The increase in LW allsky net flux is larger the higher the cloud base temperature, T_b, is relative to the surface temperature. However, higher surface temperatures, T_s, increase the cloud forcing as this increases the clear sky upward flux. The magnitude of the LW cloud forcing (LWCF) is thus larger for both high $\frac{T_b}{T_s}$ ratio and for high T_s. The two effects dominate at different times of the year.

In the Arctic the longwave cloud forcing experiences little annual variability. During the SHEBA campaign (Surface Heat Budget of the Arctic Ocean) a 30 W/m^2 annual variability was observed in the net LW flux (Intrieri et al., 2002a). The components that comprise the forcing change with season. In winter, the net allsky flux can be close to or even larger than zero. This happens because of temperature inversions and the cloud base being warmer than the surface (the $\frac{T_b}{T_s}$ ratio is high). Assuming that the clouds are black bodies, the ground thus receives more energy from the cloud than it emits itself (see equation 1). The net clear sky flux is rather small because of low surface temperatures but it gives a positive contribution to the LW cloud forcing at the surface.

In summer observations show a LW cloud forcing of comparable magnitude to the winter case. This is caused by different phenomena. In summer, inversions are not as common, and the net flux in a cloudy atmosphere is negative - the ground receives less radiation from the cloud base than it emits itself. However, the clear sky upward flux is larger during summer than in winter because of higher surface temperatures. This contributes to increase the LWCF. The sum of decreased allsky net flux and decreased net clear sky flux makes the LWCF approach the same level as it does in winter. This argument clearly states the importance of cloud temperature. One should also mention that the Arctic usually has a larger cloud cover in summer, increasing the LW effect (Intrieri et al., 2002a).

The SW part of the cloud forcing is negative and thus leads to cooling by clouds in areas where this radiation dominates. Depending on the cloud albedo, a fraction of the incoming solar radiation is reflected to space and thus never reaches the environment below the cloud. Receiving less energy this environment becomes colder in the presence of clouds.

The shortwave cloud forcing is, unlike the longwave, strongly variable over the annual cycle because of change in incoming solar radiation and surface albedo. The contribution of solar radiation is smaller for high solar zenith angles because its path through the atmosphere is longer (Shupe and Intrieri, 2004). The radiation is therefore attenuated before hitting the clouds and the ground. The lack of solar radiation in winter (zenith angles above 90°)

leads to zero SW cloud forcing during this season. The solar zenith angle is therefore of crucial importance in calculating the cloud forcing.

The surface albedo also varies with season and influences the SWCF greatly. As mentioned above, the difference, or rather lack thereof, between the reflective properties of the clouds and the ground is part of what keeps the surface SWCF low in the Arctic. The large areas covered by ice and snow have an albedo very close to that of overlaying clouds. Therefore the energy absorbed by the surface may not change much in the presence of clouds. A decrease in surface albedo will increase the importance of clouds and the shortwave cloud forcing along with it. The surface ice cover is at its minimum in September (NSIDC, 2009a) and the surface albedo generally reaches a minimum simultaneously, even if it also depends on meteorological conditions such as presence of fresh snow, melt ponds on top of the ice etc.

The annual variability in shortwave cloud forcing will thus depend mainly on two factors. The solar radiation will increase towards summer solstice and decrease later in the summer season. From this one would assume that the SWCF was at its peak around late June. The surface albedo, however, will continue to decrease all the way into September and thus works to increase the SW cloud forcing throughout the summer. The sum of these effects makes the shortwave cloud forcing generally reach its peak in July, depending somewhat on meteorological conditions. The peak in cloud cover in August also affects the SW effect.

On a smaller time scale, the magnitude of both the longwave and the shortwave contribution strongly depends on the microphysics and water content of each cloud. In the longwave case, cloud longwave emissivity is of crucial importance. If the cloud is not optically thick in the LW it will emit less radiation and less radiation will reach the ground. The allsky net flux is then reduced, and so is the LW surface cloud forcing. An emissivity less than unity is mainly a consequence of a low cloud liquid water path (see equation 2).

Cloud microphysics and water content are of importance also in the short wave case. These parameters are what decide the cloud albedo and hence to what extent the cloud influences the incoming solar radiation. Some claim that this is especially important for thick clouds as they are already saturated in the LW, but are not so in the SW (Shupe and Intrieri, 2004) - the albedo continues to increase in the SW after it is saturated in the LW, and thus makes the short wave contribution to the cloud forcing increasingly important (Figure 2).

The same physics applies in the case where we consider the top of the atmosphere (TOA). The main difference between results at the surface and at this level, is that at the surface, the cloud forcing is a measure of how

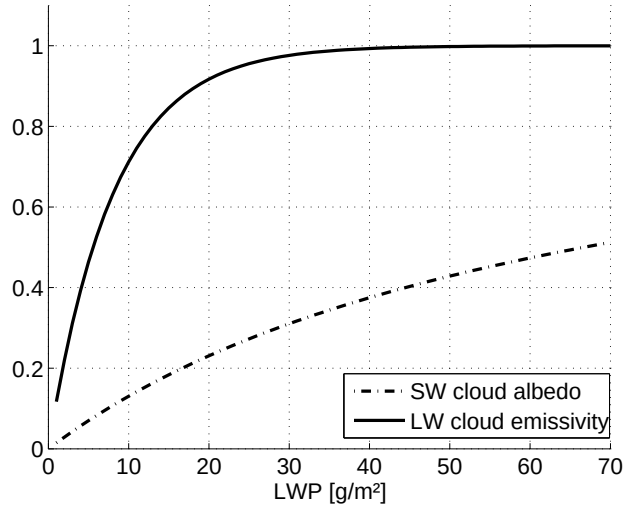

Figure 2: Cloud SW albedo and LW emissivity as a function of liquid water path. (Cloud ice fraction = 0 and effective radius = 10 μm)

much the clouds influence the radiation budget at that specific level. At the top of the atmosphere, however, the cloud forcing indicates how the energy available to the entire earth-atmosphere system has changed. It thus comprises all levels of the atmosphere.

The sign of LW forcing at the TOA will depend on whether the cloud top emits more or less energy than the underlying surface. In winter the cloud top is often warmer than the surface. This leads to negative cloud forcing if the cloud emissivity is high. More energy is then leaving the earth-atmosphere system than it would without clouds present. In an atmosphere without temperature inversions the cloud top will be colder than the surface and the LWCF at the top of the atmosphere is positive.

In the SW the sign of the forcing will depend on whether the cloud has a higher albedo than the earth surface. A higher albedo means more reflected radiation and negative cloud forcing - the clouds in this case force more energy to leave the system. If on the other hand the cloud albedo is lower than the surface albedo (not very common), the SWCF at the top of the atmosphere will be positive.

3.3 Pollution

Most cloud condensation nuclei in the Arctic are believed to be sulfate particles from marine and pollution sources (Curry and Ebert, 1992). According

to Quinn et al. (2008) the tropospheric aerosol concentrations in this region show a marked increase during late winter and early spring. This is a result of transport patterns and meteorological conditions. Aerosols are transported to the Arctic mainly from mid-latitude Eurasia. Barrie (1986) explains how east-west pressure gradients exist for long periods of time between the semi-persistent Siberian high and low pressure centers over northern Europe at this time of year. These are associated with large scale eddies that result in surges of polluted air from Eurasia into the Arctic region. Also worth mentioning is the fact that the pollution in this case travels mainly over snow covered land-ice areas and hence is not much affected by precipitation. There is also a pathway leading from the east coast of North America into the Arctic (Barrie, 1986). However, the pollution travelling along this pathway crosses the north Atlantic, an area prone to heavy precipitation. This removes much of the pollution before the air mass reaches the Arctic.

A change in transport in summer exists because of a shift in the polar air mass and the pressure patterns. In Eurasia the mean flow in the lower troposphere shifts from southwest to northeast and there is little transport into the Arctic region.

The increase in aerosol concentration during winter is also a consequence of the aerosols having longer atmospheric lifetimes during winter. As mentioned above temperature inversions are common in the Arctic during winter. This is associated with a stably stratified environment which inhibits turbulent transfer and thus removal through dry deposition (Quinn et al., 2008). In addition to this the Arctic troposphere is dry and there is little precipitation, most of which falls during the summer (Barrie, 1986). This results in very little wet deposition during winter and spring. During summer temperature inversions are less common and precipitation is heavier, leading to increased removal by both dry and wet deposition during the warmer half of the year.

3.4 The First and Second Indirect Effect

Pollution and the presence of tropospheric aerosols may affect the Arctic climate in several ways. The direct effect relates to how aerosols scatter or absorb incoming solar radiation. Scattering leads to a decrease in the radiation reaching the environment below the aerosols and hence the radiation reaching the surface. However, the Arctic surface has a relatively high albedo and the increased reflection to space by aerosols may only be a minor contribution. SW absorption by the aerosols is potentially of greater importance as the aerosols emit longwave radiation towards the surface, which has an emissivity close to unity for these wavelengths (Quinn et al., 2008). Aerosols may also affect the terrestrial radiation directly if they are hygroscopic and

grow large, or affect the surface albedo if they are deposited to snow and ice surfaces. The focus of this study however is how aerosols lead to climate forcing through interacting with clouds, known as the indirect effects. For this to happen, it is crucial that periods with high pollution levels coincide with periods prone to certain cloud types.

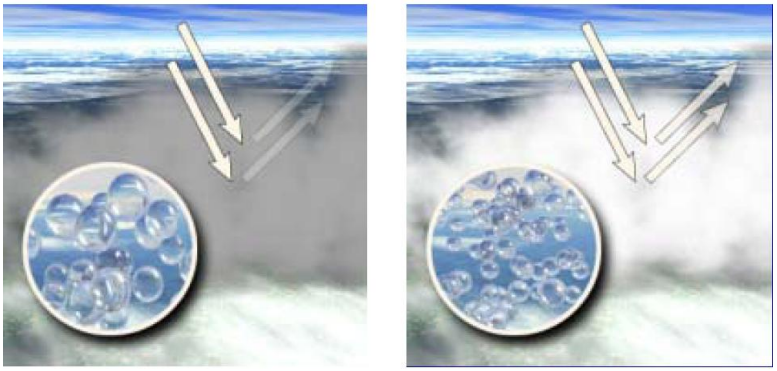

Figure 3: Change in cloud properties with pollution. Left) clean, non-opaque cloud with few large droplets. Right) Polluted cloud, more optically thick with numerous small droplets. From Lohmann (2005).

3.4.1 The First Indirect Effect

The first indirect effect has been described as an increase in the SW cloud albedo through decreased effective radius and increased number concentration of the cloud droplets (Twomey, 1977). These changes result from pollution leading to an increased number concentration of cloud condensation nuclei (CCN). The first indirect effect assumes that the cloud liquid water content is held constant and that the water in the cloud is divided between an increased number of droplets, each having a smaller radius.

It is previously shown that the albedo increases with optical depth, τ. One can see directly from equation 15 ($\tau = \frac{3}{2}\frac{LWP}{\rho_L \bar{r}}$) that reducing the effective radius while holding the water amount constant will lead to a higher τ and therefore increase the cloud albedo.

From equation 10 it is clear that it is the total droplet cross-section, $\sigma = \pi r^2 N$, not the volume that determines the impact of clouds on shortwave

radiation.

$$\tau \approx 2\pi\bar{r}^2 N\Delta z \quad (23)$$
$$= 2\sigma\Delta z \quad (24)$$

This fact is what leads to increased albedo with smaller and more numerous droplets. A given volume of a population of droplets, $V = \frac{4}{3}\pi\bar{r}^3 N$, corresponds to several optical depths depending on the effective radius of the droplets. Expressing the total droplet cross section in terms of this volume gives $\sigma = \frac{3}{4}\frac{V}{\bar{r}}$. For a given V, σ increases with decreasing $\bar{r}$. The optical depth and the albedo increase along with it.

This increase in the shortwave albedo will reduce the net radiative flux in the environment below the cloud if it is located over a low albedo surface. The effect should reach a peak when the surface albedo is low, but the solar radiation still high. Like the SW cloud forcing, we expect the influence of the indirect effect to reach a maximum sometime in July. One should mention that the shortwave first indirect effect will be smaller in this region than elsewhere on earth as the Arctic receives relatively little sunlight and has highly reflective surfaces.

As mentioned earlier the main focus of changes in cloud microphysics with pollution has been on how it influences properties related to shortwave radiation. It is evident, however, that reducing the effective radius of a cloud changes properties in the longwave as well.

Keeping the LWP constant, the longwave emissivity is affected only through changes in the absorptivity coefficient (see equation 2). For radii greater than 10 μm, the absorption coefficient will increase with a decrease in $\bar{r}$, while for $\bar{r} < 10\mu$m $k_{abs,liquid}$ is constant with $\bar{r}$. The emissivity thus either increases with decreasing $\bar{r}$ or remains constant depending on the average size of the particles in the cloud. Reductions in cloud particle size through the first indirect effect may therefore influence the longwave radiation balance. Equation 2 shows, as before, that if the LWP is large, the emissivity is already close to unity. For there to be a longwave first indirect effect it is therefore crucial not only that the effective radius of the cloud is larger than 10 μm, but also that the cloud is not already optically thick in the longwave.

An increase in longwave emissivity will result in stronger LW cloud forcing and warming of the areas below the cloud and can influence the Arctic climate throughout the year. Because of the LW dominance and the thin non-opaque clouds common in this region, the longwave first indirect effect may be of large importance here.

3.4.2 The Second Indirect Effect

The second indirect effect is an increase in the SW cloud albedo and LW emissivity following an increased liquid water path in the cloud. The water path increases because the larger number concentration of CCN leads to smaller more numerous drops and thus increases the amount of water the cloud can hold without the onset of precipitation. Precipitation starts as droplets reach a certain size. This is mainly because the auto conversion increases greatly as the effective radius increases above 10 to 15 μm due to large collection efficiencies.

From equation 15 and equation 2 we know that an increased LWP increases not only the shortwave cloud albedo but also the longwave emissivity, assuming the cloud is not already a black body in the given wavelength ranges. Thus the second indirect effect may bring changes to the longwave radiation budget as well as to the shortwave.

In addition to the above it has been suggested that the suppression of precipitation will lead to a cloud lifetime effect, allowing the cloud to persist longer. However, this has not been confirmed by observations (Menon et al., 2002).

3.4.3 Increased Pollution

For there to be changes in the cloud properties as a result of pollution, there must be an increase in the number concentration of CCN in the Arctic atmosphere. As clouds in low layers usually have higher temperatures than clouds at higher altitudes, we will focus on changes at low levels.

Garrett and Zhao (2006) show that the amount of anthropogenic sulfate particles released into the atmosphere today should be sufficient to affect cloud LW emissivity. They calculate that increasing the concentration of CCN in the lowest 4 km of the Arctic atmosphere by 5 cm^{-3} requires about 5 kt of material. They further state that this is enough to ensure a nominal increase in emissivity of about 0.01. With a characteristic lifetime of these particles up to 39 days, it requires about $\frac{365}{39} * 5kt = \sim 50$ kt of material to sustain such an increase in CCN throughout one year. Including the uncertainty of this calculation Garrett and Zhao (2006) suggest that a long range transport of 10 to 100 kt of material into the Arctic each year would suffice to affect the cloud forcing in the region. This is only about 1 per cent of the SO_2 emitted north of 60° in the Eurasian region alone. If pollution affects the LW emissivity, it would also affect the SW cloud albedo as it depends on the same parameters as ϵ.

Hobbs (1993) (p.43) shows that even when assuming a CCN lifetime of only 2 days, anthropogenic emissions of sulfur should be affecting cloud properties.

4 Model Tools and Methods

To study the first and the second indirect effect we have used both a one dimensional (1D) model based on the NCAR CCM3 radiation scheme and the three dimensional (3D) CAM-Oslo climate model. The 1D model was used to study how specific changes in effective radius and liquid water path alter the cloud forcing in the Arctic at different times of the year. It was also used to look at what clouds are most sensitive to indirect effects and to investigate whether we could reproduce the findings of earlier studies. The 3D model was run to study how changes in anthropogenic aerosol pollution affect the cloud forcing depending on time and location.

4.1 Model Modification - LW Emissivity as a Function of Effective Radius

When the models were used to simulate clouds at lower latitudes, the calculations in the longwave part of the spectrum did not depend on cloud droplet radius. This is because this dependence is insignificant when shortwave radiation is dominating the radiation regime. In the Arctic however, LW radiation is much more important, and we can no longer neglect the LW emissivity dependence on cloud droplet size. If this was ignored we would see no first indirect effect in the LW. We therefore deduced an expression for LW emissivity that depends on cloud droplet size. We then reprogrammed both the 1D and the 3D model to use this expression and thus increased the accuracy of these models, especially when used to simulate Arctic conditions.

In order for the longwave cloud emissivity to depend on droplet size, the liquid water mass absorption coefficient ($k_{abs,liquid}$) is expressed in terms of effective radius. The absorption coefficient for liquid particles is given by:

$$k_{abs,liquid} = \frac{\beta_a}{LWC} \tag{25}$$

where β_a is the volume absorption coefficient for liquid droplets and LWC is the liquid water content of the cloud in units of mass per volume. These components will be examined closer in order to show how this coefficient depends on droplet size.

The volume absorption coefficient is given by:

$$\beta_a = \pi \int_0^\infty n(r) r^2 Q_a(r) dr \tag{26}$$

where n(r) is the cloud droplet size distribution as a function of radius, r, and Q_a is the absorption efficiency. Q_a is approximately constant and equal

to 1.0 for effective radius, $\bar{r}$, greater than 10μm. For $\bar{r}$ smaller than 10μm, Q_a increases linearly with $\bar{r}$: $Q_a = Q_a(\bar{r}) = 0.1\bar{r}$. These relations are based on findings by Garrett et al. (2002). The absorption efficiency depends on wavelength. Here the wavelength of terrestrial radiation is assumed to be constant at the peak of its intensity between 10 and 12 μm.

The effective radius is constant in the population of droplets and $Q_a(\bar{r})$ can be taken outside the integral.

For $\bar{r} < 10\mu m$:

$$\beta_a = \pi Q_a(\bar{r}) \int_0^\infty n(r) r^2 dr \tag{27}$$

For $\bar{r} \geq 10\mu m$:

$$\beta_a = \pi Q_a \int_0^\infty n(r) r^2 dr \tag{28}$$

We simplify these equations by expressing the integrals in terms of LWP and $\bar{r}$. The liquid water path is given by Liou (2002)(p. 373). Each vertical layer in the model is homogeneous and one can therefore assume a vertically homogeneous cloud layer.

$$LWP = \int LWC dz \tag{29}$$

$$\approx \Delta z LWC \tag{30}$$

$$= \Delta z \frac{4}{3} \pi \rho_L \int r^3 n(r) dr \tag{31}$$

Dividing through by effective radius (equation 11) we are left with an integral on the similar form as the ones found in equation 27 and 28:

$$\frac{LWP}{\bar{r}} = \frac{\Delta z \frac{4}{3} \pi \rho_L \int r^3 n(r) dr}{\int \pi r^3 n(r) dr} \int \pi r^2 n(r) dr \tag{32}$$

$$= \frac{4}{3} \Delta z \pi \rho_L \int r^2 n(r) dr \tag{33}$$

$$\Rightarrow \int n(r) r^2 dr = \frac{3}{4} \frac{1}{\Delta z \pi \rho_L} \frac{LWP}{\bar{r}} \tag{34}$$

Inserting into β_a:

$$\beta_a = \frac{3}{4} \frac{Q_a}{\rho_L \Delta z} \frac{LWP}{\bar{r}} \tag{35}$$

As mentioned above, the liquid water content can be approximated by $LWC \approx \frac{LWP}{\Delta z}$. The mass absorption coefficient for liquid droplets then becomes:

$$k_{abs,liquid} = \frac{\beta_a}{LWC} \approx \beta_a \frac{\Delta z}{LWP} \tag{36}$$

$$= \frac{3}{4}\frac{Q_a}{\rho_L \Delta z}\frac{LWP}{\bar{r}}\frac{\Delta z}{LWP} \tag{37}$$

$$= \frac{3}{4}\frac{Q_a}{\rho_L \bar{r}} \tag{38}$$

$$k_{abs,liquid} = \frac{3}{4}\frac{Q_a}{\rho_L \bar{r}}, \begin{cases} Q_a = 0.1 * \bar{r} & for \quad \bar{r} < 10\mu m \\ Q_a = 1.0 & for \quad \bar{r} \geq 10\mu m \end{cases} \tag{39}$$

Thus the mass absorption coefficient may depend on droplet effective radius. This is the coefficient used in the model simulations for this thesis.

4.2 The One Dimensional Model

Using a one dimensional model involves great simplifications, but it allows us to look at specific atmospheric conditions and thus gives valuable insight into the mechanisms we want to study. The main advantage of using such a model is of course just this simplicity. We can easily create conditions highly adapted for our study and make changes in them to study certain effects. One might question whether the conditions we specify are realistic. We do not worry about this, however, as we are using this model mainly to check how certain changes in effective radius and LWP influence the Arctic radiation balance and to see what magnitude of change is possible under these conditions. However, we are basing our input on observational studies performed in the Arctic and on model runs for this area. This suggests that our results are plausible.

Another advantage of using this model is that its radiation scheme is similar to that of the three dimensional model. If results from the 1D model show changes in cloud forcing with indirect effects we know that if similar conditions appear in the 3D model simulations, we should see similar changes in the forcing.

In addition to this, the flexibility of the model allows us to insert specific values of effective radius and LWP and check whether we can recreate the findings of earlier studies.

The one dimensional model was created by Jón Egill Kristjánsson and Gunnar Myhre. The model uses the radiation scheme from the NCAR CCM3

model to give instantaneous values of radiation fluxes, and thus cloud forcing, in the atmosphere. Using the model input one can place a specific type of cloud in a preferred environment and study the instantaneous radiation effects of this cloud. The model input includes cloud parameters such as effective droplet radius, liquid water path, cloud cover, equivalent effective radius of ice crystals, cloud height and thickness etc. It also includes location given by latitude and time of the year, and gas and temperature profiles suited for the chosen environment. It returns an output averaged over the chosen latitude, equal to a 24 hour mean in the SW. In our study the model ran with 26 layers in the vertical.

4.2.1 1D Model Methods

In running the one dimensional model we chose to look at mid January as representative of the Arctic winter and mid July of the Arctic summer. We did this to capture the most extreme conditions in two model cases. In the winter case the solar radiation is absent, the surface albedo is high and the vertical profile is marked by inversions in temperature. The summer case includes solar radiation, has lower surface albedo and does not have temperature inversions. The cloud conditions modeled are specified for each run by choosing different effective radii and liquid water paths and will thus not depend directly on time of year chosen. The specific input also allows us to simulate both high and low pollution events.

Based on the findings of Intrieri et al. (2002b) from the SHEBA campaign the model runs for January included a single cloud layer. Their results show that during summer it is common to have multiple cloud layers, one and two layers being the dominant regimes. Based on this, the July simulations included both one and two model cloud layers. The SHEBA campaign ran for one year and the averages found may therefore not reflect the truly most common scenarios. However, because of lack of more comprehensive studies, we chose to use the results from this campaign as a guidance. Through the SHEBA results we know that the scenarios chosen are occurring in the Arctic region.

Each model run involves specifying several cloud parameters. This input is based on findings in the literature on Arctic clouds. Observational studies of clouds in the Arctic region are however limited. First of all there have been few research campaigns in this area. Secondly, the campaigns that have taken place were usually very limited in both time and space. Aside from the SHEBA campaign, few other studies last longer than a season. Most campaigns are centered over northern Alaska and the Beaufort Sea and thus do not necessarily give a detailed picture of the Arctic in general. Our input

may therefore not be representative for the true Arctic average, but will be included in the span of possible conditions in this region.

An example of such input is data describing the cloud droplet effective radius. Studies have found it to be anywhere between 7 and 13 μm on average (eg. Shupe et al. (2001) and Curry et al. (2000)). In the 1D simulations this parameter is therefore set between these values. The focus is however on values between 10 and 13 μm, assuming the smaller effective radii represent an atmosphere subject to pollution. This choice is supported by Garrett and Zhao (2006) who have observed an average decrease in effective radius from 12.9 to 9.9 μm when going from clean to polluted conditions under cloudy skies.

In studying the possible impact of indirect effects, another important input parameter is the liquid water path. A range of LWP from 5 to 150 g/m^2 were used in the 1D simulations. The lower values are based on the findings of Curry et al. (1996) which suggest that the LWP of Arctic stratus is often less than 20 g/m^2. The higher limit of liquid water paths is used to study the radiation effects as the increasing water amounts saturate clouds in the LW while they are of continued importance in the SW.

The equivalent effective radius of ice particles, Rei, was chosen based on an article by Kristjánsson et al. (2000) where ice particle effective radius is given as a function of temperature. In our case, this was only of importance in the winter case as the average summer cloud did not contain ice crystals because of high temperatures. In our runs Rei was between 110 μm and 140μm, being larger for larger temperatures.

The model runs were made with total cloud cover and cloud layers of different height and thicknesses. The output was then averaged to study general trends.

4.2.2 1D Model Modifications

The model was modified to better suit the simulations needed for this project. One challenge was to adapt it to the Polar region as it had not previously been used for calculations at these latitudes. The program code had to be modified and new gas and temperature profiles were needed.

The original gas profiles were based on the McClatchy profiles, and did not include Arctic profiles. Given the low number of observational studies in the Arctic it was difficult to get profiles based on measurements, especially since averages over long time periods at different times of the year were needed. In this study the profiles used are therefore based on output from the CAM-Oslo climate model averaged over the Arctic region. This region was taken to be north of the Arctic circle, 66.561°N.

The new profiles were also better suited for Arctic cloud simulations as they had better vertical resolution close to the surface than profiles found in the model originally. The program code was modified to run with changed vertical resolution.

Originally the model was written for calculations in a column above the open sea surface. To make it representative for the Arctic region as a whole the surface conditions were specified by changing the average surface albedo. Here we chose again to use the output from the CAM-Oslo model in order to have consistent input in our simulations. One drawback of using an averaged albedo like this is that it will contain values from large areas of open water, especially during summer, as the region extends far southwards. This will significantly decrease the surface albedo and thus increase the SW contribution to the cloud forcing. However, since we are looking at the Arctic as a whole, we choose to keep this albedo average. We are aware that the SW contribution in summer might be unrealistically large and will take this into account when studying the model output.

Both input profiles for gas and temperature and albedo averages were created for January and July separately. The model was also rewritten in order to make it possible for it to run with two separate cloud layers.

4.3 The Three Dimensional Model

Using a three dimensional (3D) model ensures a much more comprehensive study of the phenomenon. Such models are state of the art and the closest we get to true Arctic conditions. They include important aspects of and the variation in the atmospheric conditions, surface properties and radiative balances. Here we only specify different emission scenarios and let the model physics handle the rest - to transport the pollution into the Arctic region and to modify the clouds in the proper manner. The 3D model allows us to look at spatial differences in the influence of pollution. It may thus point to regions that are more sensitive to increased release of anthropogenic aerosols. As the 3D model does not only give instantaneous output one can study the effect of increased pollution over some time and in different seasons. A long term average tells us something about the overall importance of the phenomenon. A 3D model also makes it possible to look at vertical cross sections to study the vertical structure of the atmosphere in areas particularly interesting to our research.

The three dimensional model used in this thesis is the CAM-Oslo climate model. This model was developed at the University of Oslo based on the NCAR CAM3.0 model. The horizontal resolution is approximately 2.8° x 2.8° (T42), and there are 26 layers in the vertical. The vertical coordinate

is a hybrid coordinate that follows the terrain in the lower troposphere and gradually becomes pressure coordinates when entering the lower stratosphere (Rasch and Kristjánsson, 1998). A 20 minute time step is used for the model dynamics.

4.3.1 3D Model Methods

In this thesis three emission scenarios were used in order to study the effect of increased amounts of pollution on cloud forcing: One scenario describes present day emissions, hereby referred to as PRES, one scenario describes pre-industrial times, hereby referred to as PIND, and one scenario where present day emissions of SO_2 from fossil fuel have been doubled, referred to as 2SOx. The scenarios are based on the AEROCOM emissions.

We chose to modify the pre-industrial emission field. Originally this scenario included areas where the pre-industrial emissions from organic carbon and black carbon were higher than in the industrial case. This was based on an assumption that the emissions from forest fires were higher before man started to put them out. Some believe, however, that more forest fires occur today because of intervention of human beings, some even started deliberately. Because of this uncertainty we rewrote the PIND scenario so that the emissions prior to the industrial revolution were never higher than the present day scenarios.

All model versions were run for five years and the results shown in this thesis are averaged over these years. This helps exclude variations due to specific weather events. The summer season includes the months of June, July, August and September, while the winter season is an average of the remaining months.

The model was run both on-line and off-line. The first case involves letting the emission scenario in question be part of the evolution of the simulations through influencing the weather and creating feedback. Running the model off-line, on the other hand, involves the same meteorological evolution in all model runs. For each time step the model will calculate the influence of the emission scenario we wish to study and return fluxes of radiation, effective radius, liquid water path, etc. A specified background scenario will then be used to recalculate the properties of this time step. This will be the same for all model runs and is what will decide the simulated meteorological development.

Running the model off-line is an advantage because it allows us to study how the clouds are changed by different emission scenarios without changes in the meteorological situation. The change in cloud forcing with pollution simulated is then only a result of aerosols interacting with the clouds and we

avoid noise from other sources in our results.

4.3.2 3D Model Modifications

Several model modifications were made to better suit the model to the focus of our study, the most important being to let the LW absorption coefficient depend on effective radius (see section 4.1). It was also modified so that the off-line calculation of LW effects now depends on the effective radius resulting from increased pollution amounts. Previously this was not necessary as the LW emissivity calculations did not depend on the effective radius.

In order to use the off-line version of the 3D model it had to be rewritten to return output it did not previously return. To study the indirect effects only, we rewrote the model so that the optics of clear sky simulations did not change between different emission scenarios.

4.3.3 3D Model Verification

For model verification output from CAM-Oslo was compared to theory and observations. The latter was challenging because quantitative knowledge about Arctic cloud microphysics is extremely limited (Lin et al., 2001). In this section theory on air transport into the Arctic, as described in section 3.3, will be used to investigate whether the spacial pattern of pollution in the model is as can be expected. Observations are used to verify that the model cloud forcing and properties that affect its size compare to observational studies. At the end of this section we will suggest model modifications to enhance the validity of our study.

Observations taken during the SHEBA experiment are used to validate the model output. This campaign took place in the Beaufort and Chukchi Seas from October 1997 to October 1998. It only covers a small region of our area of interest, and measurements taken here do not verify the model over the entire Arctic region. We acknowledge that this leads to uncertainties in our results.

Patterns of Pollution

The annually averaged present day concentration of sulfate (SO_4) over the Arctic region is plotted in Figure 4(a). The concentration is largest over northern Eurasia, and gradually decreasing as we move away from this region. This is consistent with the main transport into the Arctic coming from Eurasia and suggests that the model transports pollution into the region in accordance with the theory presented in section 3.3. The annual concentrations of organic and black carbon follow the same pattern.

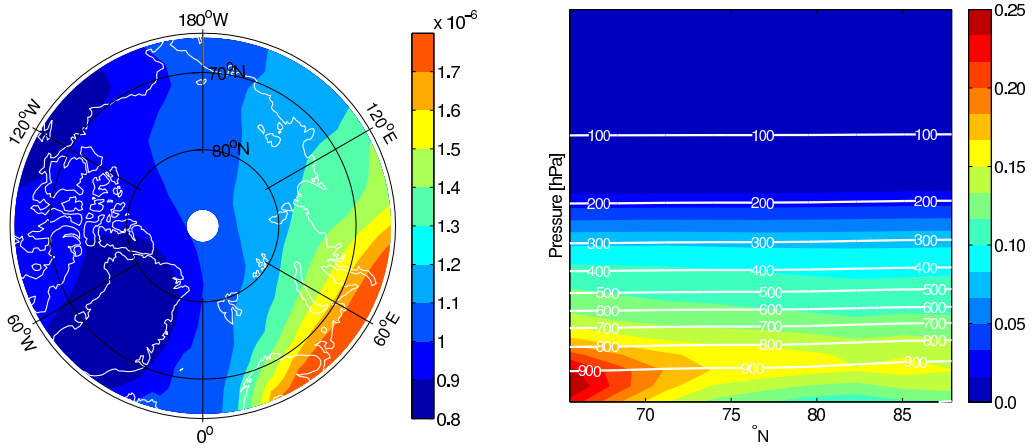

(a) (b)

Figure 4: Annually averaged sulfate concentrations in the Arctic region. a) Column SO_4 [kg/m^2], b) SO_4 concentration [μg/m^3].

In order for indirect effects to occur clouds and pollution must be co-located. The vertical distribution of aerosols, and especially sulfate, is therefore important. Comparing the CAM-Oslo simulated vertical profiles of SO_4 to observations is challenging. First of all, measurements of SO_4 in the Arctic are limited both in number and in geographical distribution. According to Scheuer et al. (2003) there is generally a lack of information on "spatial variability, both horizontally and vertically". There are not enough long term measures of the vertical SO_4 distribution to conclude on an " average Arctic vertical profile". Secondly, there is large variability in the observations, also when taken with short time intervals in the same regions (eq. Dreiling and Friederich (1997) and Scheuer et al. (2003)). This makes it difficult to compare these observations to our monthly averaged vertical profiles.

Figure 4(b) shows the concentration of sulfate with height in terms of μg sulfur per unit volume of air. The values are annually averaged over the Arctic region. Concentrations at the surface are consistent with measurements (Quinn et al., 2007), as is the seasonal variability of this quantity.

The vertical cross section shows that north of 70 to 75°N the largest concentrations are found in layers around 800 to 900 hPa. Although we have no average observed vertical profiles to verify the concentrations of this cross section by, 800 hPa is the height found by Dreiling and Friederich (1997) often to have the largest concentration of particles of all sizes. Our results show that concentrations are lower during summer than during winter, especially close to the surface. During summer there is a sharp positive gradient in

the concentration with height from the surface to the level of maximum concentration. This is consistent with findings of Talbot et al. (1992).

It should be mentioned that Treffeisen et al. (2005) suggests that the high variability of the Arctic aerosol distribution in both time and space can not be accounted for by coarse resolution global climate models. The coarse resolution of our model may thus lead to uncertainty.

Although we can not verify that the magnitude of sulfur concentration with height is accurate in the CAM-Oslo runs, we find no reason to assume otherwise. The surface concentrations are within the range of measured values and the trend in concentration with height in different seasons fits with earlier findings. However, lack of more comprehensive measurements of this quantity and therefore proper model verification does lead to uncertainty in our simulations.

Cloud Cover

The seasonal variation in Arctic cloud cover has a minimum occurring during winter time with values around 50 percent. A maximum occurs in late summer/early fall and peaks around 80 percent in August(Zhang and Lohmann (2002) and Rasch and Kristjánsson (1998)). This trend is reproduced well by the model, as shown by Figure 5.

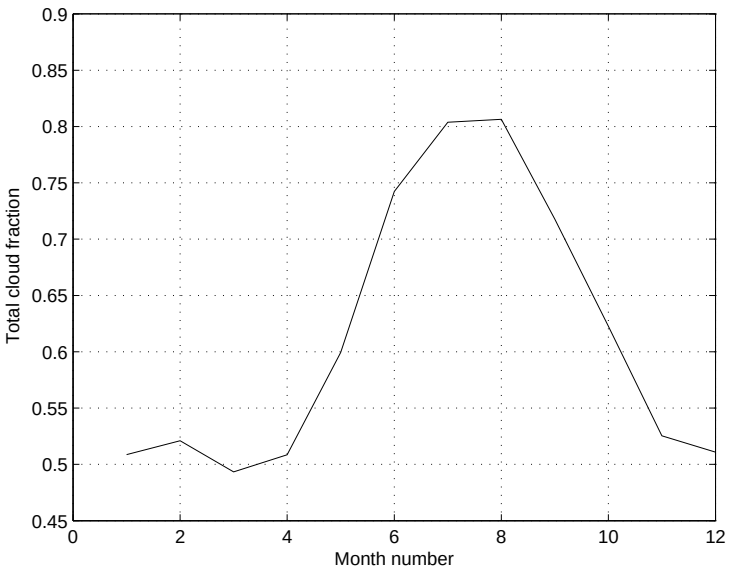

Figure 5: Simulated monthly variation in average Arctic cloud cover (CAM-Oslo)

Surface Albedo

The CAM-Oslo surface albedo was averaged over the SHEBA region for comparison with observations. There are, however, several differing sets of surface albedo measurements available from the campaign. This illustrates the difficulty of getting accurate measurements of this quantity. Intrieri et al. (2002a) use two sets from the campaign, but state that only one is expected to be quantitatively correct. This is a single sight albedo and is located precisely above an ice floe. In addition to these measurements, Curry et al. (2000) show aircraft measurements taken over the SHEBA region from May through July the same year.

The CAM-Oslo albedo is below the single sight SHEBA albedo for the entire summer season, although it lies closer to the observed values during the months that corresponds to the peak in cloud forcing; June through August. However, the CAM-Oslo results are consistent with the measurements taken from Curry et al. (2000). Rough monthly estimates of the aircraft measured albedos are 0.76, 0.67 and 0.50 for May, June and July respectively. CAM-Oslo results from the same region and time period are 0.79, 0.70 and 0.52. In this case, the model results are in fact somewhat higher than what was observed. Hence we can conclude that the model surface albedo is within reasonable range.

Effective Radius

The model effective radius of the clouds in the SHEBA region has an annual average of 10.0 μm (10.3 μm during winter and 9.4 μm during summer). This is a realistic value when compared to several Arctic observations (eg. Curry et al. (2000),Morrison et al. (2009)). However, Shupe et al. (2001) found a mean effective radius from April to July during SHEBA of 7.4 μm. Although this is comprised of measurements in all-liquid clouds only, it may suggest that the CAM-Oslo effective radius is somewhat too large.

Liquid Water Path

Measurements taken during the SHEBA campaign were used by Zhang and Lohmann (2002) to retrieve monthly averaged liquid water paths for this region. They reach a maximum of around 100 g/m^2 in August, when the cloud fraction reaches its peak value. This value seems to be in accordance with the typical range of Arctic LWP only seldom exceeding 150 g/m^2 (Löhnert et al., 2003). The monthly averaged LWP (including its uncertainty) retrieved from measurements is much lower than the output given by CAM-Oslo for the same area. In fact, the CAM-Oslo LWP for the SHEBA region

is overestimated by a factor 3 to 5, depending on season (see Figure 6).

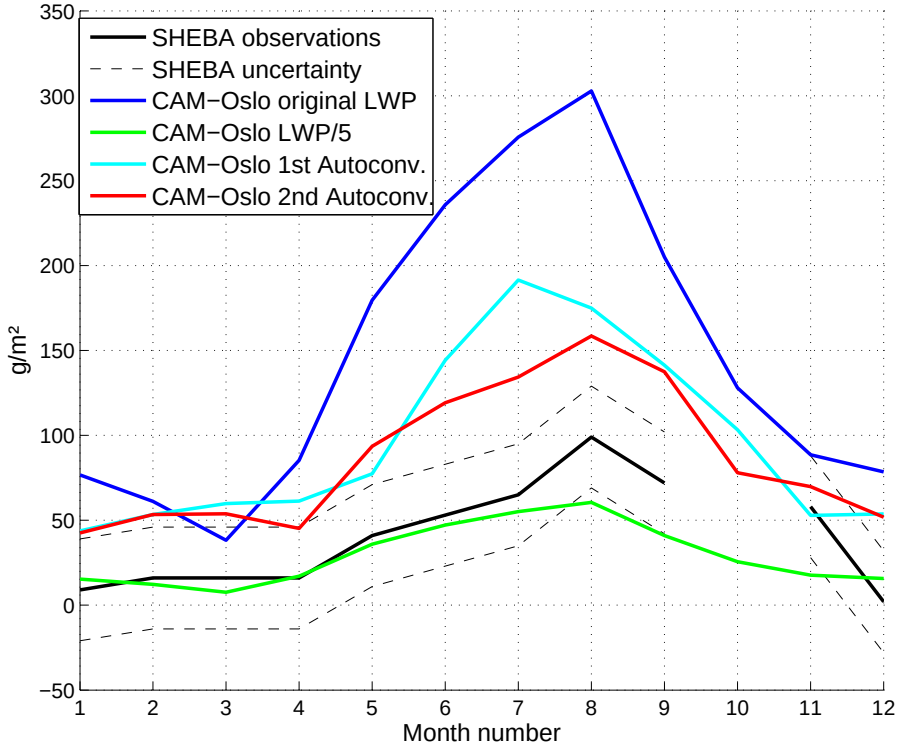

Figure 6: Monthly variation in average cloud liquid water path in the SHEBA region. Observed values reproduced from Zhang and Lohmann (2002).

Morrison et al. (2009) performed an intercomparison study of an observed versus modeled multilayer mixed-phase cloud from observations made during the ARM Mixed-Phase Arctic Cloud Experiment. A similar intercomparison was conducted by Klein et al. (2009) for a single-layer cloud. In both cases a single-column version of the CAM3 (SCAM3) was part of the analysis. Results show that the single-layer cloud was reproduced fairly well by the SCAM3, but the multilayer cloud was not. In the latter case the SCAM3 overestimated the LWP almost by a factor of three. Although the single-column version does not compare exactly to the CAM-Oslo, it suggests that overestimation of LWP may be a problem in the CAM-Oslo as this too is developed from the standard NCAR CAM3.0 model.

Too high liquid water amounts may be caused by several factors. An underestimated auto conversion rate will lead to little loss of water through

precipitation. Another possibility is too little conversion from liquid water to ice particles. It may also be caused by an overestimated transport of moisture into the region or by stably stratified conditions allowing model clouds to become thicker than what occurs in nature. Ice water path (IWP) retrievals have very high uncertainties. Nevertheless, it should be mentioned that Shupe et al. (2005) found an IWP on the order of 42 g/m^2 and Morrison et al. (2003) found IWPs on the order of 34.6 g/m^2 for the SHEBA region. Our model result is 24.0 g/m^2. This may point to a bias in the conversion between liquid and solid particles or a bias in the distinction of solid particles in the model. Due to the limited amount of measurements in the Arctic combined with high uncertainties we can not conclude on the main cause of the high model liquid water path.

Cloud Forcing

The cloud forcing returned by the model is checked against the findings of Intrieri et al. (2002a). They present "An annual cycle of the Arctic surface cloud forcing at SHEBA" based on both measured allsky and modelled clear sky properties. The clear sky flux was modelled because of a lack of satisfying measurements of clear sky flux, especially during summer when cloud occurring frequencies were high. Using this approach they found an annually averaged cloud forcing at the surface of 23 W/m^2 including turbulent flux. This flux is not part of our calculations and is therefore removed from the annual cloud forcing mean. The CAM-Oslo surface cloud forcing was averaged over the SHEBA region for comparison (144°-169°W and 74°-81°N (Zhang and Lohmann, 2002)). Table 7 shows the annual, winter and summer mean of the cloud forcing measured at SHEBA and modeled over this region by CAM-Oslo.

The modeled cloud forcing at the surface differs significantly from what was measured at SHEBA, especially during summer. This is mainly caused by a large difference in SW cloud forcing between the modeled and the observed value. We know that the cloud cover is reproduced well by the model, and that this should not affect our result greatly. The discrepancy in the SW may therefore be caused either by a lower model surface albedo, an overestimation of the model cloud optical thickness or a combination of the above. As shown previously, the surface albedo used by Intrieri et al. (2002a) is lower than what is used in our model and may affect our results. However, the albedo is consistent with other observations and is likely to be within reasonable range.

Differences in SWCF may also be caused the model cloud optical thickness being larger than what is observed. This can happen because of an underes-

timation of $\bar{r}$ or an overestimation of LWP. The model effective radius of the clouds in this region has been shown to be reasonable, or if anything higher, not lower than what was observed at SHEBA. This excludes underestimation of $\bar{r}$ as an explanation for the discrepancy, and leaves the overestimation of model LWP as a plausible cause of the difference between modeled and observed cloud forcing in the SW.

The LW contribution to the total cloud forcing during summer is also of larger magnitude than what is observed (see Figure 7). Like in the SW this can have three different causes: a higher model cloud base temperature, a higher model cloud emissivity or a combination of the above. Higher model cloud base temperatures would lead to a higher allsky LW net flux at the surface and an increase of the LWCF. This could either be caused by discrepancies in vertical temperature profiles or in cloud base heights between model and observations. Unfortunately, without time averaged temperature profiles available from the SHEBA campaign, we cannot decide for sure whether temperature differences are influencing our model runs.

A higher cloud LW emissivity in the CAM-Oslo would increase the LW cloud forcing in our results. As the model effective radius does not appear to be underestimated, a higher emissivity is likely to be caused by the overestimated LWP.

To summarise the above findings, the model cloud forcing is too large in both wavelength ranges. The large negative SW surface cloud forcing may be caused by a lower model surface albedo or by a high model LWP. The discrepancy in LW forcing may be caused by higher model cloud base temperatures or by high model LWP. Surface albedo does not influence the LWCF and cloud base temperature does not affect the SWCF. Additionally, the difference in SWCF is larger than the difference in the LW. This fits with the clouds becoming optically thick at lower liquid water paths in the LW than in the SW. Adding water to a cloud would then have a tendency to influence the SW radiation more than the LW, for which the cloud may already be saturated. These findings suggest that modifications of the model LWP are necessary.

Model Version With Enhanced Validity

We tried to better align the model to the observations, first by tuning the auto conversion so that more water was lost through precipitation. We did this through modifying the auto conversion threshold radius form 15 to 10 and 7.5 μm. This radius decides the size that cloud particles must reach before the onset of precipitation and is described in Rasch and Kristjánsson (1998) (equation 21). In addition to this we changed the proportionality

factor $C_{l,aut}$ from $5.0C_{l,aut}$ to $0.5C_{l,aut}$ and $0.0C_{l,aut}$. This parameter is also described in equation (21) in Rasch and Kristjánsson (1998) and accounts for the decrease in collection efficiency in a cloud droplet distribution that has been modified by precipitation. The smaller the auto conversion threshold radius and the proportionality factor are, the more water is lost through precipitation. The NCAR CAM3.0 model uses an auto conversion threshold radius of 10 μm and a proportionality factor of 0.5. It thus loses more water through precipitation than the CAM-Oslo does originally.

The results of this tuning are seen as the light blue and the red line in Figure 6. These liquid water paths lie much closer to the observed values, but are still high.

For simplicity we then conducted several idealized experiments where we forced the LWP to be within the range of the observed values. This was done through reducing either the effective radius or the cloud droplet number concentration (CDNC). The liquid water path was divided by a factor three to a factor five in these experiments. The goal was to keep the LWP within the range the of the observations and simultaneously find what experiment gave the values of cloud forcing closest to the SHEBA measurements.

The columns to the right in Table 7 show the cloud forcing computed for some of the experiments, including one version of the tuned auto conversion. It is clear that reducing the LWP by a factor five through reducing the CDNC (holding $\bar{r}$ constant) greatly improves the model result for this specific area and gives the best fit to the observed surface cloud forcing. Here we keep the reasonable, but possibly somewhat high, effective radius. The differences still present may be caused by the albedo and temperature effects discussed above. Using the second approach, where we reduce the LWP by reducing the effective radius, leads to much higher forcing than reducing it through reducing the CDNC. This is as expected, as we know that both LW emissivity and SW cloud albedo increase with decreasing radius.

In chapter 6 results from the best fit version of CAM-Oslo, referred to as the forced model version, are investigated further.

	SHEBA	CAM-Oslo	CAM-Oslo LWP/5 ΔCDNC	CAM-Oslo LWP/5 Δr	CAM-Oslo LWP/3 ΔCDNC	CAM-Oslo LWP/3 Δr	Tuned autoconv. no.1
Annual average							
LWCF	35 to 41	39.1	35.8	38.2	38.3	39.5	38.3
SWCF	-10.5 to -9.5	-23.1	-13.6	-16.8	-16.6	-19.0	-20.4
Net CF	25 to 30	16.0	22.1	21.4	21.7	20.5	17.9
Winter average							
LWCF	25 to 30	28.4	27.2	28.7	28.7	29.4	27.1
SWCF	-1 to 0	-4.7	-2.5	-3.0	-3.0	-3.4	-3.5
Net CF	24 to 30	23.7	24.7	25.7	25.7	26.0	23.6
Summer average							
LWCF	45 to 50	60.7	52.9	57.3	57.4	59.5	60.7
SWCF	~ -25	-60.0	-36.0	-44.5	-43.9	-50.2	-54.2
Net CD	~ 20	0.7	16.9	12.8	13.5	9.3	6.5

Figure 7: Cloud forcing [W/m^2] as given by measurements made during SHEBA and by different versions of the CAM-Oslo in the SHEBA region. Note that a turbulent heat flux of approximately -6 W/m^2 has been subtracted from the SHEBA total cloud forcing described here.

5 Results and Discussion: One Dimensional Model

In this chapter we will present results from the one dimensional simulations on how changes in cloud droplet effective radius and liquid water path alter the cloud forcing. We will focus on three questions when presenting the results. First, does the radiation scheme show changes in cloud forcing with changes in $\bar{r}$ and LWP in accordance with what is expected from section 3.4 (theory on indirect effects)? Secondly, for what clouds is the forcing most susceptible to change with pollution and why? Thirdly, is the LW part of the radiation scheme capable of reproducing findings of Garrett and Zhao (2006) when using their averaged observed change in effective radius and LWP as input? We will start by looking at the results of simulations in the LW. We will then discuss changes in shortwave and total cloud forcing with effective radius and LWP. The main focus of our discussion will be on cloud forcing at the surface. At the end of this section we will look briefly at changes in cloud forcing at the top of the atmosphere with increased aerosol amounts.

5.1 Longwave Cloud Forcing at the Surface

In this section we will present 1D model results of LW cloud forcing at the surface. We will show output from the winter season only. However, our results have the same general behaviour and magnitude in both seasons, as can be expected from section 3.2 (cloud forcing).

In section 3.4 (indirect effects) we explained how the emissivity, and hence the LW cloud forcing, generally increases with indirect effects. Figure 8 shows the simulated LW cloud forcing at the surface for the winter season as a function of effective radius and liquid water path. The forcing is positive and increases for clouds with larger liquid water paths and smaller effective radii. Results from the LW radiation scheme thus behave in accordance with what is expected from the section on indirect effects.

We will now consider what clouds are most susceptible to create change in forcing with an increase in liquid water path. First of all, clouds with liquid water paths greater than 40 to 50 g/m^2 are close to black bodies in the LW. Increasing the LWP beyond these values will not influence the LW radiation budget. For liquid water paths smaller than 40 to 50 g/m^2, however, an increased water amount will influence the LW emissivity and therefore the LW cloud forcing. From Figure 8(a) it is clear that the increase in LW cloud forcing with LWP depends on the amount of water already in the cloud. This behaviour is explained by the LW emissivity not changing linearly with LWP (see Equation 2). The smaller the liquid water path is initially the larger the change in ϵ is with a given ΔLWP. The surface LW cloud forcing of thin

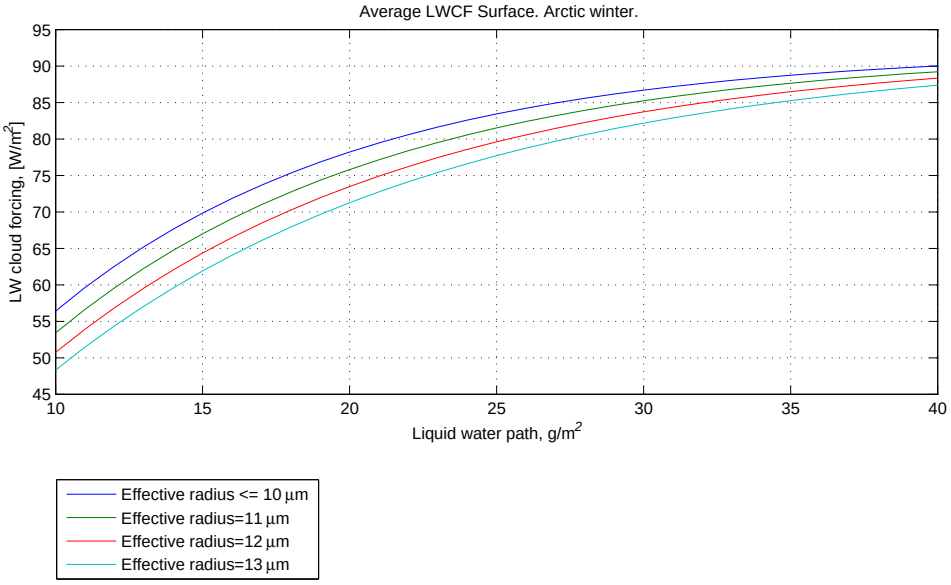

(a)

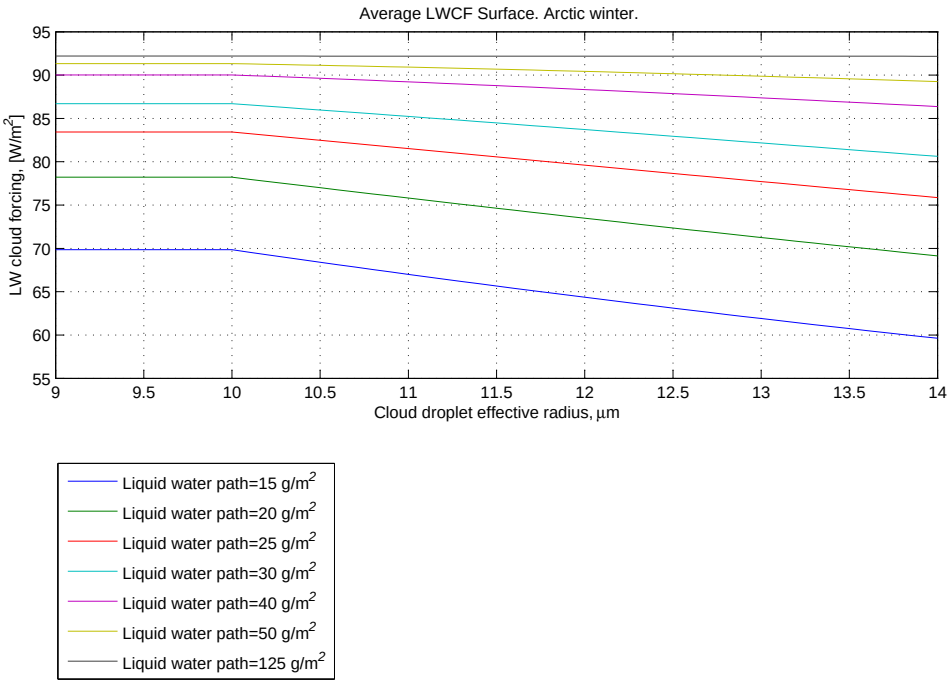

(b)

Figure 8: LW cloud forcing at the surface for January as a function of (a) liquid water path and (b) effective radius.

clouds is thus more susceptible to change with LWP than clouds with large liquid water paths.

Figure 9 shows how the LW cloud forcing at the surface changes with effective radius as a function of LWP. Notice how the influence of a change in $\bar{r}$ reaches maximum for clouds with liquid water paths between 10 and 15 g/m^2. We will now show that this maximum is directly linked to the shape of the emissivity curve and is not a model artifact. The change in emissivity between effective radii $\bar{r}_1 > \bar{r}_2$ is given by:

$$\begin{aligned} \Delta\epsilon &= (1 - e^{-1.66 * k_{abs}(\bar{r}_2) * LWP}) - (1 - e^{-1.66 * k_{abs}(\bar{r}_1) * LWP}) && (40) \\ &= (1 - e^{-\alpha * LWP}) - (1 - e^{-\beta * LWP}) && (41) \\ &= e^{-\beta * LWP} - e^{-\alpha * LWP}, && (42) \\ k_{abs} \propto \frac{1}{\bar{r}} \quad &so \quad \alpha > \beta \\ &\Rightarrow \quad \Delta\epsilon > 0 \end{aligned}$$

We take the derivative of this to find the maximum difference in emissivity.

$$\frac{d}{d(LWP)}\Delta\epsilon = -\beta e^{-\beta * LWP} + \alpha e^{-\alpha * LWP} \qquad (43)$$

With absorption coefficients from the winter case, Equation 43 equals zero for liquid water paths between 10 and 15 g/m^2. The physical explanation for the maximum is that the change in emissivity with $\bar{r}$ goes to zero both for large LWP ($\epsilon \to 1$ for all $\bar{r}$) and for small LWP ($\epsilon \to 0$ for all $\bar{r}$). This behaviour leaves clear maxima for intermediate liquid water paths.

Figure 9 and the above calculations show that a given change in $\bar{r}$ will affect the LW cloud forcing the most for cloud with liquid water paths between 10 and 15 g/m^2. A stratiform cloud has a typical liquid water content of 0.1 g/m^3 (Rogers and Yau, 1989). A liquid water path of 10 to 15 g/m^2 then corresponds to a cloud thickness of 100 to 150 m ($\Delta z \approx \frac{LWP}{LWC}$). It is clear that clouds with LWP of this magnitude are very thin. The figure shows, however, that even for thicker clouds the cloud forcing may change significantly with reductions in effective radius. At a LWP of 30 g/m^2 the longwave cloud forcing at the surface may increase by almost 5 W/m^2 during winter if $\bar{r}$ goes from 13 to 10 μm.

In section 3.1 (radiation theory and clouds) we explained how the LW absorption coefficient is constant for droplet effective radii below 10 μm. Figure 8 b shows how this influences the surface LW cloud forcing - for $\bar{r}$ smaller than 10 μm a change in effective radius will not affect the LWCF.

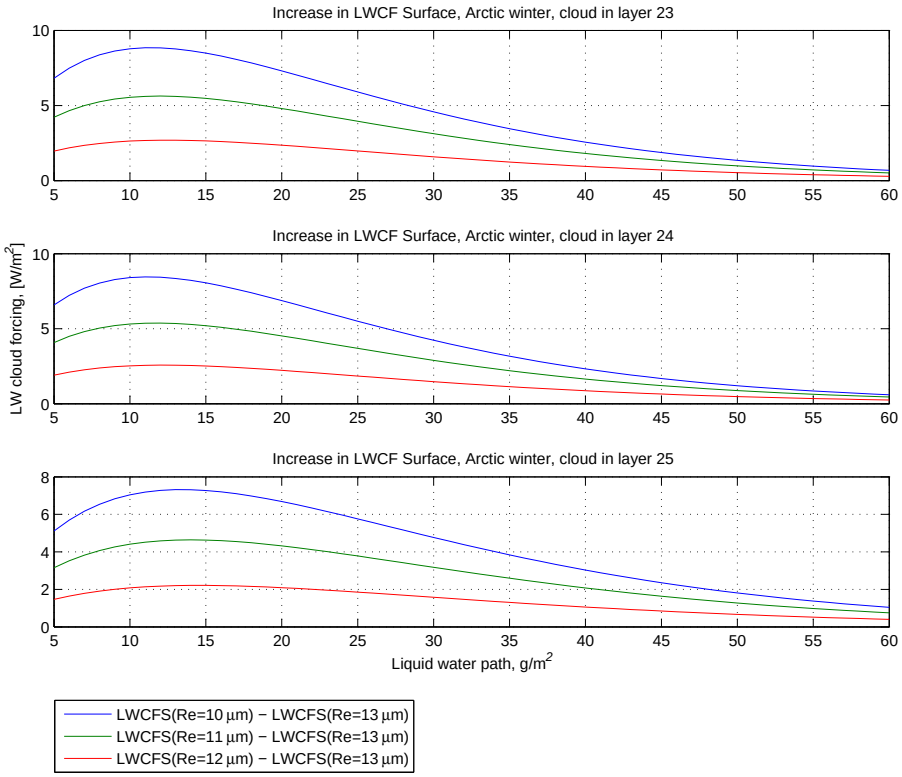

Figure 9: Change in average surface LW cloud forcing with effective radius as a function of liquid water path. High numbered cloud layers corresponds to layers close to the surface. The cloud base temperature increases with cloud height. Note that scales differ.

This result is important in limiting the possible radiative impact of the *first* indirect effect through increased pollution. If this effect is to influence the LW cloud forcing, the effective radius of the cloud in question must be greater than 10 μm.

In addition to the above, the change in LW cloud forcing with indirect effects is directly influenced by the temperature of the cloud base. Our results suggest that the absolute change is large for clouds with high base temperatures (see Figure 9). This behaviour can be explained by studying the change in LWCF with indirect effects for different cloud base temperatures. Using the Stefan-Boltzmann law (Equation 1), the change in emission of LW radiation towards the surface for a given change in effective radius and LWP

is given by:

$$\begin{aligned} \Delta F_{\downarrow} &= \epsilon(\bar{r}_1, LWP_1) * \sigma T^4 - \epsilon(\bar{r}_2, LWP_2) * \sigma T^4 && (44) \\ &= [\epsilon(\bar{r}_1, LWP_1) - \epsilon(\bar{r}_2, LWP_2)] * \sigma T^4 && (45) \\ &= \Delta\epsilon * \sigma T^4 && (46) \end{aligned}$$

From Equation 2 we know that for water clouds $\Delta\epsilon$ is constant for a given change in $\bar{r}$ and LWP and that it is independent of cloud base temperature, T. Equation 46 thus tells us that clouds with high temperatures will have high changes in LW cloud forcing when subject to pollution. The height of the cloud base is therefore likely to affect the sensitivity for changes in forcing with pollution.

Results from model runs with two cloud layers show that the top layer has little influence on the LW cloud forcing at the surface. Radiation emitted by this top layer is largely absorbed by the bottom layer (depending on the emissivity of the bottom cloud) and therefore has little influence on the surface radiative balance.

Summary of the key findings in this section:

- LWCF is most sensitive to changes in LWP if this is initially low.
- LWCF is most sensitive to changes in $\bar{r}$ for LWP between 10 and 15 g/m^2.
- LWCF changes more with indirect effects if the cloud base temperature is high. The height of the cloud base is therefore likely to affect the change in LW cloud forcing with pollution.
- LWCF at the surface is mainly affected by the bottom cloud layer.

5.1.1 Comparison with Earlier Findings

In this section we will investigate whether the one dimensional model can reproduce the findings of Garrett and Zhao presented in Nature in 2006. We will study whether the LW radiation scheme used in our models reacts to indirect effects as observed in nature.

To reproduce the earlier findings we forced the simulated clouds to be similar to the ones observed; The clouds are at low levels (tops below 1.5 km) and are all liquid. We then used the averaged observed change in effective radius and liquid water path as input in our simulations. Garrett and Zhao found a change in $\bar{r}$ of 3μm, from 12.9μm in pristine air to 9.9μm in polluted conditions. For the same scenarios they observed an average change in LWP from 31.1 to 33.5 g/m^2.

Results from the 1D simulations show slightly more moderate changes in LW cloud forcing with pollution than what was found by Garrett and Zhao. Our results show changes on the order of 2.1 to 2.6 W/m^2 depending on cloud base height and season, while they found changes of 3.3 to 5.2 W/m^2 for the same type of clouds.

There are several reasons to expect discrepancies between our simulated and their observed results. While the study by Garrett and Zhao is based on data from a small region around Barrow, Alaska, our study is based on input averaged over the entire Arctic region. It is therefore likely that the vertical profiles used in our study differ from the environment studied by Garrett and Zhao. It was shown in the previous section that the temperature of the cloud base will influence the change in LW cloud forcing with pollution. A difference in vertical profiles will therefore cause our results to differ from the observed quantities.

Another reason to expect results to differ is that Garrett and Zhao study the effects of pollution for all seasons, while our study covers the summer and the winter season only.

Despite these differences, our results are the same order of magnitude and are consistent with the findings of Garrett and Zhao (2006). This result suggests that the LW radiation scheme used both in the 1D and the 3D model reacts to indirect effects in accordance with observations. The scheme is therefore well suited for studying the radiative impact of changes in cloud parameters with pollution.

5.2 Shortwave Cloud Forcing at the Surface

In this section we will present the 1D model results of SW cloud forcing at the surface. We will consider the summer season only and only present results from the case with single cloud layers. The case with two layers behaves similarly to what is presented here.

Figure 10 shows the simulated SW cloud forcing at the surface for the month of July as a function of effective radius and liquid water path. The SW forcing is negative and its magnitude increases with increasing liquid water path and decreasing effective radius. We know from section 3.4 on indirect effects that this is the expected behaviour of the SW cloud albedo and therefore of the SW cloud forcing. The SW radiation scheme thus reproduces the general pattern of change in SW cloud forcing with indirect effects.

Figure 10 also shows two aspects of SW cloud forcing that differ from the LW case. First, the increased magnitude of SW cloud forcing with LWP continues after the cloud has become a black body in the LW. SW effects of increasing the LWP beyond 50 g/m^2 are therefore assumed to dominate as

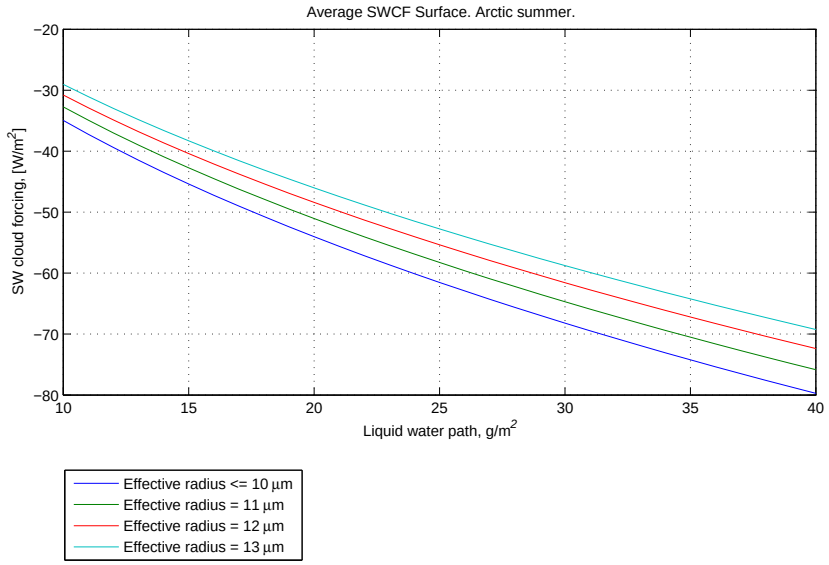

(a)

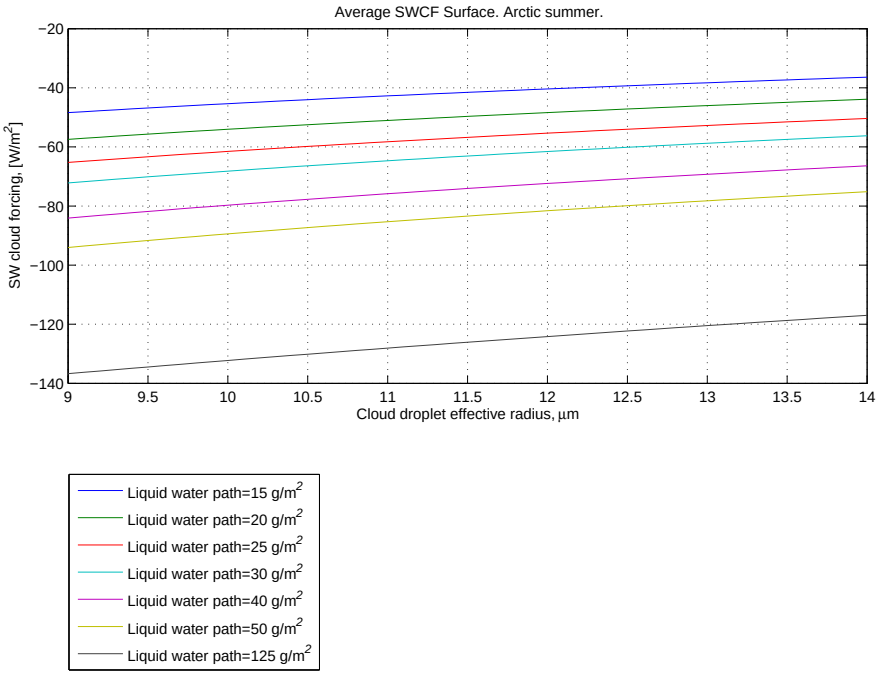

(b)

Figure 10: SW cloud forcing at the surface for the month of July as a function of liquid water path (a) and effective radius (b).

clouds are already saturated in the LW. This corresponds well with results of Shupe and Intrieri (2004). Secondly, the SW cloud forcing is affected by changes in cloud droplet size when the effective radius is smaller than 10 μm. This implies that changes in forcing with $\bar{r}$ when the cloud has a lot of small droplets will be dominated by SW effects as the LW cloud forcing is constant for radii $<$ 10 μm.

We will now consider what clouds are most sensitive to indirect effects in the SW. We will start by looking at how the SWCF changes with LWP. Similarly to the LW case, a given change in liquid water path will change the SW cloud forcing most if the cloud contains little water to begin with (see Figure 10). This is because the SW cloud albedo does not change linearly with LWP (see Equations 8 and 15). The less water the cloud holds initially the larger the change in SW cloud forcing with a given increase in LWP.

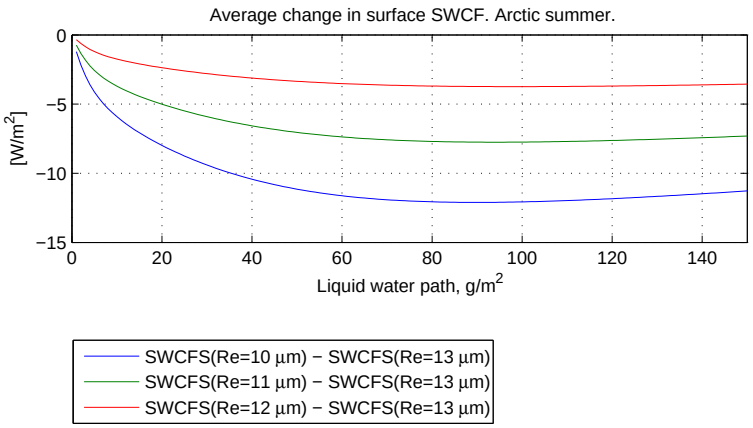

Figure 11: Change in average surface SW cloud forcing with effective radius as a function of liquid water path.

Figure 11 displays how changing the effective radius of cloud droplets affects the surface SW cloud forcing for different LWPs. Notice how the influence of a decrease in $\bar{r}$ reaches maxima for LWPs of approximately 90 g/m^2. Like in the LW case we will show that these maxima are not model artifacts by investigating for what LWP the SW cloud albedo changes most with $\Delta\bar{r}$. We start by expressing the SW cloud albedo as a function of

effective radius and liquid water path:

$$A = \frac{(1-g)\tau}{1+(1-g)\tau} \quad (47)$$

$$= \frac{1}{1+\frac{1}{(1-g)\tau}} \quad (48)$$

$$= \frac{1}{1+\frac{\gamma}{\tau}}, \quad (49)$$

$$where\ \gamma = \frac{1}{1-g} \quad (50)$$

Inserting for the optical depth, $\tau = \frac{3}{2}\frac{LWP}{\rho_L \bar{r}}$:

$$A = \frac{1}{1+\frac{2}{3}\gamma\rho_L\frac{\bar{r}}{LWP}} \quad (51)$$

The change in albedo for clouds with different effective radii is then given by:

$$\Delta A = A(\bar{r}=10,11,12\mu m) - A(\bar{r}=13\mu m) \quad (52)$$

$$= \frac{1}{1+\frac{2}{3}\gamma_2\rho_L\frac{\bar{r_2}}{LWP}} - \frac{1}{1+\frac{2}{3}\gamma_1\rho_L\frac{\bar{r_1}}{LWP}} \quad (53)$$

$$where\ \gamma_1,\gamma_2 = \frac{1}{1-g(\bar{r}_1,)}, \frac{1}{1-g(\bar{r}_2,)} \quad (54)$$

The derivative with respect to liquid water path shows for what water amount the SW cloud albedo is most sensitive to changes in effective radius. (Found where Equation 55 = 0).

$$\frac{d}{d(LWP)}\Delta A = \frac{2}{3}\frac{\rho_L}{LWP^2}\left(\frac{\gamma_2\bar{r}_2}{(1+\frac{2}{3}\gamma_2\rho_L\frac{\bar{r}_2}{LWP})^2} - \frac{\gamma_1\bar{r}_1}{(1+\frac{2}{3}\gamma_1\rho_L\frac{\bar{r}_1}{LWP})^2}\right) \quad (55)$$

For asymmetry factors around 0.9 (see section 3.1), the LWP of maximum sensitivity to changes in $\bar{r}$ fits with the maximum found in the results presented here - around 90 g/m^2.

Reducing the cloud droplet effective radius influences the cloud albedo through increasing the optical depth of the cloud. Physically, the maximum influence of such a reduction is controlled by two competing factors. First, the cloud albedo dependence on optical depth levels off as the cloud gets close to saturation in the SW. A continued increase in τ through reducing the effective radius will therefore affect the albedo and the surface SW cloud forcing less as the water amount increases beyond a certain level.

On the other hand, an increase in τ will affect the SW cloud albedo if the cloud is not saturated and the increase in optical depth with $\Delta\bar{r}$ is larger for large liquid water paths than it is for small. This is because a certain change in $\bar{r}$ influences the total droplet cross section most if the water amount in the cloud is large. We will now show this second factor in some detail.

Consider a change in effective radius from $\bar{r}_a$ to $\bar{r}_b$ where $\bar{r}_a > \bar{r}_b$. This occurs for two different cloud liquid water amounts $X_1 > X_2$. For these amounts, changing the effective radius leads to a change in the total droplet cross sections of (see section 3.4.1):

$$\Delta\sigma_1 = \pi\bar{r}_b^2 N_{1b} - \pi\bar{r}_a^2 N_{1a} \quad (56)$$

$$\Delta\sigma_2 = \pi\bar{r}_b^2 N_{2b} - \pi\bar{r}_a^2 N_{2a} \quad (57)$$

The two water amounts are given by:

$$X_1 = \frac{4}{3}\pi\bar{r}_a^3 N_{1a} = \frac{4}{3}\pi\bar{r}_b^3 N_{1b} \quad (58)$$

$$X_2 = \frac{4}{3}\pi\bar{r}_a^3 N_{2a} = \frac{4}{3}\pi\bar{r}_b^3 N_{2b} \quad (59)$$

We solve these expressions for the droplet number concentrations N_{1a}, N_{1b}, N_{2a} and N_{2b} and insert these into the expressions for $\Delta\sigma$:

$$\Delta\sigma_1 = \frac{3}{4}\frac{\bar{r}_a - \bar{r}_b}{\bar{r}_a\bar{r}_b} X_1 \quad (60)$$

$$\Delta\sigma_2 = \frac{3}{4}\frac{\bar{r}_a - \bar{r}_b}{\bar{r}_a\bar{r}_b} X_2 \quad (61)$$

Since $X_1 > X_2$ the change in cross sectional area is larger for the large water amount, X_1, than it is for X_2. The optical depth is therefore more influenced by changes in $\bar{r}$ if the LWP is large than if the LWP is small.

Combined the two factors above explain why there is a maximum in the influence of changes in $\bar{r}$. For large LWP a change in$\bar{r}$ affects the τ more than for small LWP. The cloud albedo, however, is less sensitive to this increase in τ the larger LWP is initially.

In addition to ΔLWP and $\Delta\bar{r}$, the LW cloud forcing was found to be affected by cloud base height through temperature. In the SW, on the other hand, cloud forcing is not affected by cloud height and temperature directly. Cloud temperature does, however, affect the cloud optical properties through affecting the ice fraction. For mixed phase clouds, height is therefore of importance. For identical water clouds the only possible change in SW forcing with cloud height is due to the amount of scattering by particles in the

atmosphere above or below the cloud. The effect of this change in scattering, however, is assumed to be small compared to the forcing from the cloud itself.

Results from model runs with two cloud layers show that adding an additional cloud layer significantly increases the SW cloud forcing at the surface. Independent of cloud height or layer number, clouds will reflect a portion of the incoming solar energy and reduce the amount of SW radiation reaching the surface. The SW cloud forcing is therefore likely to increase in magnitude when multiple cloud layers are present and depends little on the height of these layers.

In addition to the observed behaviour of the results, the magnitude of the forcing modelled is of importance. Shupe and Intrieri (2004) found that the monthly average maximum in SW cloud forcing at the Arctic surface occurred during July and reached a value of approximately 60 W/m^2. If we assume an average LWP for this month of 60 - 70 g/m^2 from the SHEBA results, Figure 10 shows that our results are substantially higher than the findings by Shupe and Intrieri for all effective radii. However, this is not surprising when considering what assumptions were made when running this model. As mentioned above, the Arctic region used here is extending far southwards and therefore covers a lot of open sea. This reduces the surface albedo and therefore enhances the influence of clouds on the radiation balance.

Summary of the key findings in this section:

- SWCF is most sensitive to changes in LWP if this is low initially.
- SWCF is most sensitive to changes in $\bar{r}$ for clouds with LWP around 90 g/m^2.
- Contrary to LWCF, SWCF changes with ΔLWP and $\Delta\bar{r}$ if the LWP is above 50 g/m^2 initially. SWCF also changes with $\Delta\bar{r}$ is $\bar{r}$ is below 10 μm initially.
- SWCF is affected by cloud height to a minor degree.
- All cloud layers between the top of the atmosphere and the surface will influence the SW cloud forcing.

5.3 Net Cloud Forcing at the Surface

We will now present results from the 1D model simulations of net cloud forcing. The total effect of change in cloud parameters with pollution will depend on what dominates this forcing - increased surface flux due to LW effects or decreased surface flux due to effects in the SW. In this section

there will be a main focus on net cloud forcing during summer as the SW contribution during winter is considered negligible.

Figure 12 displays net cloud forcing for July as a function of effective radius and liquid water path. Notice how it is positive for small to moderate liquid water paths, but negative for LWPs above 50 to 65 g/m^2. It was explained in section 5.1 how the change in LW forcing with LWP levels off with increasing liquid water paths. The continued increase in SW cloud forcing with LWP eventually lets SW effects dominate the net radiation balance. As found by Zhang et al. (1996), the combined effect leaves a maximum cloud forcing at moderate liquid water paths. In our simulations of the July case, the maximum CF occurs for LWP between 14 and 20 g/m^2. The LWP retrieved from the SHEBA campaign showed average values of around 65 g/m^2 in July (see Figure 6). For this water amount, the average simulated net cloud forcing is around 0 to -10 W/m^2 depending on cloud droplet effective radius.

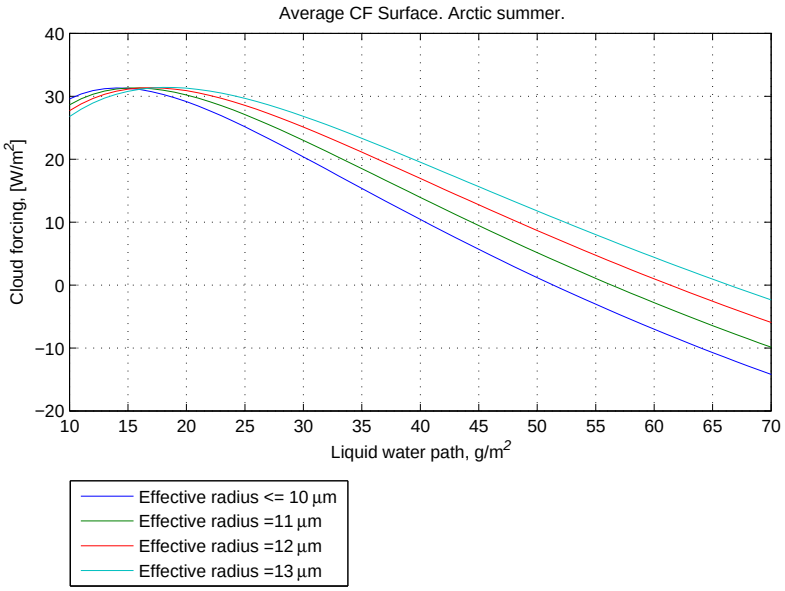

Figure 12: Net cloud forcing for different effective radii as a function of liquid water path for July.

We will now consider the change in net surface cloud forcing with liquid water path. Like in the LW and the SW case, the change in forcing with LWP is affected by the amount of water in the cloud initially. For very small initial LWPs the change in forcing is dominated by LW effects. Increasing the LWP increases the net cloud forcing. However, for liquid water paths

above ∼15 g/m^2 SW effects dominate and increasing the LWP will reduce the net cloud forcing (see Figure 12). Both the LW and the SW sensitivity to change in LWP decrease with increasing initial liquid water path. The net effect, however, behaves differently. The largest sensitivity of net cloud forcing to changes in LWP is for liquid water paths between 35 and 50 g/m^2. This is shown as the steepest inclination of the forcing with liquid water path in Figure 12. Clouds with liquid water paths between 35 and 50 g/m^2 are therefore most susceptible to create change in net cloud forcing with LWP.

The net cloud forcing will also be affected by changes in effective radius. Figure 13 shows that the net surface cloud forcing during July decreases with decreasing $\bar{r}$ for LWP greater than about 15 g/m^2. This behavior is consistent with the findings of Zhang et al. (1996) and is of great importance to our study. From the SHEBA measurements we know that a typical LWP in the Arctic during July is ∼65 g/m^2 (Figure 6). The above result therefore suggests that introducing an increased amount of anthropogenic sulfate aerosols into this region during summer is likely to decrease the net radiative flux at the surface.

Figure 13 also shows that the maximum increase in surface cloud forcing with decreasing $\bar{r}$ occurs for a LWP around 7 g/m^2, while the maximum decrease occurs around 90 g/m^2. This water amount is where changing $\bar{r}$ affects SW cloud forcing the most and it shows the SW dominance of forcing from clouds of such liquid water paths.

Our 1D simulations do not include changes in the direct effect due to an increased aerosol concentration. In reality, an increase in cloud condensation nuclei is likely to reduce the SW clear sky net flux because aerosols themselves scatter and absorb radiation. The change in SW cloud forcing between a polluted and a clean emission scenario is given by:

$$\begin{aligned} \Delta SWCF &= NetSW_{allsky,polluted} - NetSW_{clearsky,polluted} \\ &\quad -(NetSW_{allsky,clean} - NetSW_{clearsky,clean}) \\ \Delta SWCF &= NetSW_{allsky,polluted} - NetSW_{allsky,clean} \\ &\quad -NetSW_{clearsky,polluted} + NetSW_{clearsky,clean} \end{aligned} \tag{62}$$

The SW cloud forcing is increasingly negative with pollution: $\Delta SWCF < 0$. Because of a larger direct effect in a polluted regime, $\mathrm{NetSW}_{clearsky,polluted} < \mathrm{NetSW}_{clearsky,clean}$. The magnitude of change in SW cloud forcing with pollution therefore decreases if we include the direct effect. In the most polluted scenario some of the SW radiation is blocked by aerosols and the presence of clouds will therefore have less influence on the radiation reaching the surface than it will in a clean scenario. Changing the albedo of a cloud in a polluted environment will therefore affect the SW cloud forcing less than

the same change in albedo in a pristine environment. If the change in direct effect is ignored the change in SW cloud forcing will be overestimated. This overestimation will affect the change in net forcing with $\bar{r}$ and LWP to be too affected by SW effects.

Based on the findings above it may seem like introducing particles into the Arctic stratus in summer will not lead to an increase in the surface radiative flux, but rather to a reduction in this due to increased SW cloud forcing effects. This is unless the cloud is very thin. However, one must keep in mind that the 1D simulations are affected by the low model surface albedo. In areas where this is high, the SW forcing will be of less importance and the LW effects may dominate for LWPs larger than what we see in the July case presented here. One must also consider that the direct effects are not accounted for. Additionally, the SW cloud forcing is at its peak in July. During spring and autumn the SW radiation is less dominant and the LW effects may dominate for larger liquid water paths than what was found in the July case.

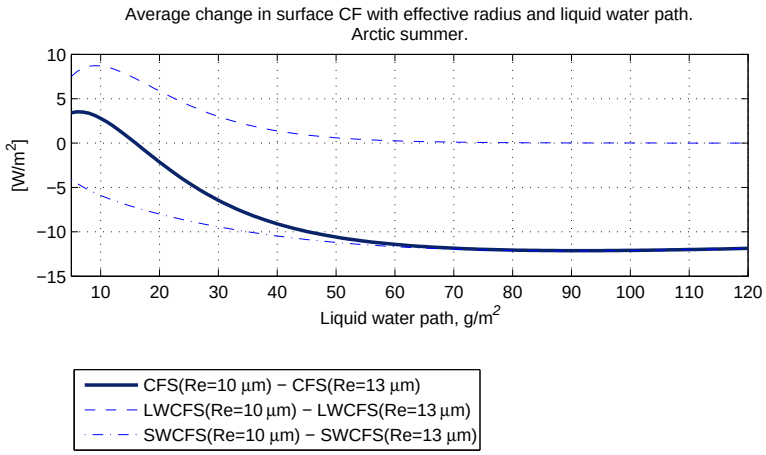

Figure 13: Change in average surface cloud forcing with effective radius as a function of liquid water path.

From the above findings it is clear that conditions outside as well as within the cloud itself will affect the cloud forcing. If conditions allow for large SW cloud forcing through low solar zenith angles, low surface albedos and sufficiently large LWP, the total forcing will be dominated by the cooling effect clouds have when interfering with the SW radiation. If conditions are right for large LW cloud forcing through lack of sunlight, temperature inversions and LWPs around 50 g/m^2, the LW warming effect of clouds will dominate the cloud forcing completely.

Summary of the key findings in this section:

- Net CF is most sensitive to changes in LWP for intermediate initial LWP (35 to 50 g/m^2 depending on $\bar{r}$).
- For clouds with LWP above $\sim$ 15 g/m^2, a reduction in effective radius will decrease the cloud forcing.
- Net CF increases most with reductions in $\bar{r}$ for clouds with LWP around 7 g/m^2 and decreases most for clouds with LWP around 90 g/m^2.
- The sign of the net CF depends on conditions outside as well as within the cloud itself. External factors are primarily solar zenith angle and surface albedo. Internal factors are cloud liquid water path, effective radius and temperature of the cloud base.

5.4 Cloud Forcing at the Top of the Atmosphere

In this section we will briefly present and discuss how changes in the low level arctic stratus affect the radiation budget at the top of the atmosphere (TOA). Here it is assumed that the radiation entering the earth atmosphere system is constant. The downward components of the net cloud forcing then cancel and the CF at the TOA depends only on radiation received from below.

$$\begin{aligned} CF &= Netflux_{allsky} - Netflux_{clear} && (63)\\ &= F{\downarrow}_{allsky} - F{\uparrow}_{allsky} - F{\downarrow}_{clear} + F{\uparrow}_{clear} && (64)\\ &= F{\uparrow}_{clear} - F{\uparrow}_{allsky} && (65) \end{aligned}$$

In the SW case this is the solar radiation reflected by the earth surface or by clouds and particles in the atmosphere. Clouds have high albedos and thus reflect a large portion of incoming SW radiation - usually more than the underlying surface. This leads to negative SW cloud forcing at the TOA, as confirmed by Figure 14.

The amount of LW radiation reaching the TOA depends on the temperature and the emissivity of the surface of the emitting body, whether that surface is the ground or a cloud. Usually the ground emits more radiation than a cloud top, leading to positive longwave cloud forcing. This is, however, often reversed in the Arctic because of the temperature inversions common to this area during winter. Figure 15 shows the average LW cloud forcing at the top of the atmosphere for both January and July. During January the cloud top is warmer than the underlying surface and the forcing is negative - more radiation is lost to space with clouds present than without. In the July

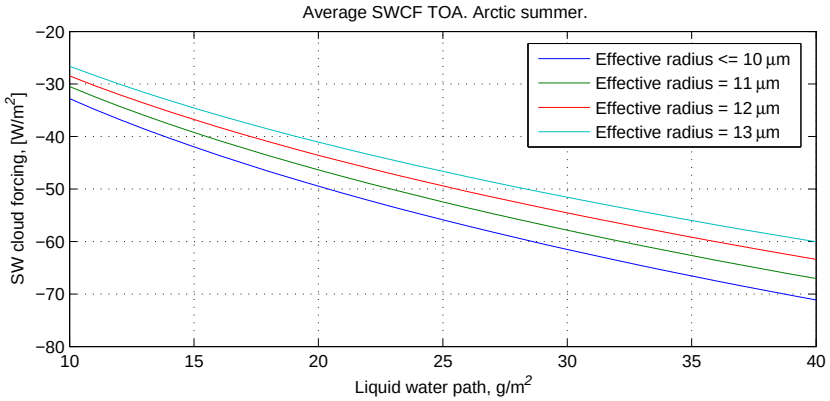

Figure 14: SW cloud forcing at the top of the atmosphere for the month of July as a function of liquid water path and effective radius.

simulations the average temperature of the cloud tops is colder than the surface. Clouds thus lead to more radiation being kept in the earth-atmosphere system.

The figures presented in this section show the same characteristics as results in the surface case - the cloud forcing increases in magnitude with increasing liquid water path and decreasing effective radius. These effects alter the cloud SW albedo and the LW emissivity as described earlier. The higher the cloud albedo the more radiation is reflected and the larger the magnitude of the SW cloud forcing at the TOA. The higher the cloud emissivity, the more of the surface LW radiation is absorbed in the cloud and the larger the portion of radiation emitted at the cloud top. Changes in forcing with indirect effects thus behave precisely the same way at the TOA as as they do in the sections describing surface cloud forcing. Cloud forcing sensitivity to changes in cloud parameters is also as described for the surface case.

5.5 One Dimensional Model: Summary

Results from the 1D model show that the radiation scheme simulates changes in cloud forcing with $\bar{r}$ and LWP in accordance with what is expected from the section on indirect effects (3.4). In this chapter the 1D model has been used to find what clouds are most susceptible to create change in forcing with indirect effects. Key findings of this investigation are summarized at the end of each section. Furthermore, in section 5.1.1 we concluded that the LW radiation scheme is well suited to study the radiative impact of changes in cloud properties due increased levels of pollution.

The model input has been taken from observations when this was possible,

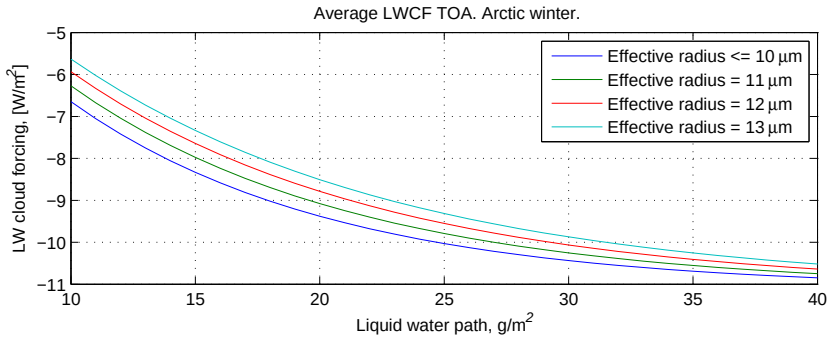

(a)

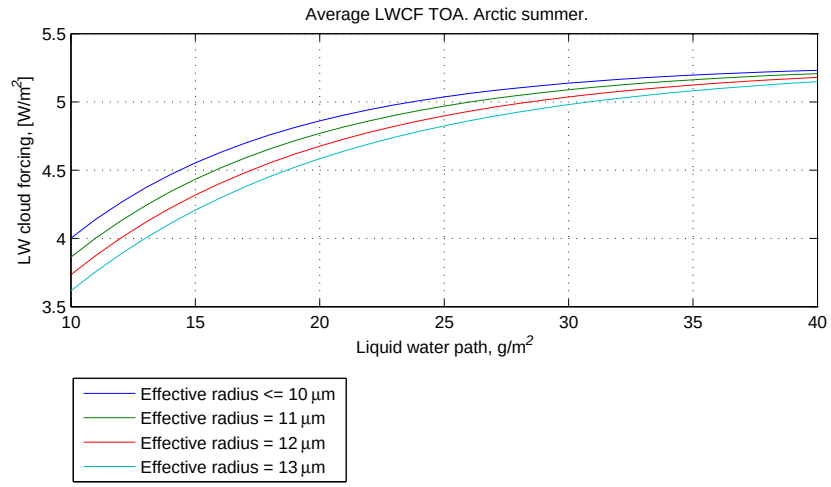

(b)

Figure 15: LW cloud forcing at the top of the atmosphere as a function of liquid water path and effective radius. a) January. b) July.

the rest from climate model output. Because of this the results given by this model are plausible. It is clear that if releasing an amount of pollution into the Arctic leads to cloud changes in the way modeled here, it may affect the radiation balance of the region by a fair amount. Results from the 3D model should help determine whether pollution finds it way into the Arctic and whether this leads to the indirect effects seen above. From these results one may conclude further as to whether the magnitude of the changes in surface flux is of any importance.

6 Results and discussion: Three Dimensional Model

In this chapter we will show and discuss results from the three dimensional model. We will investigate whether cloud properties change according to theory on indirect effects and study how this affects the radiative balance in the region. There will be a focus on seasonal trends and whether conditions are right for a change in cloud forcing with increased aerosol levels. We will start by looking at LW cloud forcing at the surface and go on to discuss the SW and the net forcing at the same level. At the end of the chapter we will briefly discuss the changes in cloud forcing at the top of the atmosphere with increased concentrations of sulfate.

When presenting our results, we will show results from the off-line calculations only (see section 4.3.1). A student T-test was conducted on results from the on-line simulations and there was found no statistically significant change in forcing with pollution. This lack of significant results is caused by the large variations in forcing due to the difference in meteorology between the runs. Small changes caused by pollution are hidden by large changes caused by weather events. This was the case even when running the model for a fifteen year period.

6.1 Longwave Cloud Forcing at the Surface

We will now examine the change in longwave cloud forcing at the surface between different emission scenarios. There will be a focus on magnitude and time of year. At the end of the section we will compare our results to the findings of Garrett and Zhao (2006) and Lubin and Vogelmann (2006). We will start by looking at the simulated changes between present day and pre-industrial times (*case* 1), and then look at the changes between the hypothetical 2SOx scenario and present day (*case* 2). The focus of this section will be on the area north of 71°N. This is because of relatively large signals over continental Europe that would interfere with our averages if we include regions south of this latitude.

6.1.1 LWCF at the Surface, Present Day Compared to Pre-industrial emissions

Figure 16 displays the annually averaged change in LW cloud forcing for both the original CAM-Oslo and the modified 3D model with forced LWP. The results from the original code shows an average increase of 0.11 W/m^2 in the LW surface flux in case 1. This low signal of change is consistent with clouds

in this model version holding enough water to be close to saturation in the LW. The cloud emissivity is practically insensitive to changes in $\bar{r}$ and LWP. There will be no further discussion of results from the original model in this section.

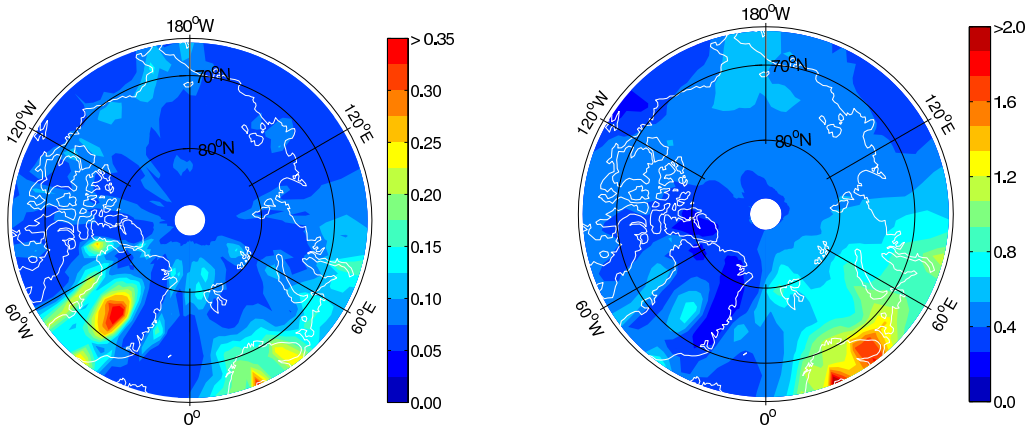

(a) ΔLWCF. Original CAM-Oslo

(b) ΔLWCF. Forced model

Figure 16: Annually averaged change in LW cloud forcing at the surface [W/m^2] for the original model code and the version with forced LWP. (PRES - PIND) Note that scales differ.

The forced model version shows larger changes in LW cloud forcing under different aerosol regimes than the original code. The average LWP of this model version is relatively low (section 4.3.3) and the LW emissivity is therefore sensitive to changes in cloud parameters, as shown in section 5.1. The annually averaged change in surface LWCF is **0.64 W/m^2** north of 71 °N. From this we know that the increase in anthropogenic sulfate concentrations has lead to an average 1.5 percent increase in the LW cloud forcing at the surface from pre-industrial times until today.

Results show that there is a significant seasonal variation in the change in LWCF with anthropogenic aerosol emissions (Figure 17)(seasons are defined in section 4.3.1). Averaged north of 71°N the LW cloud forcing changes by **1.16 W/m^2** during summer, while it changes by only **0.39 W/m^2** during winter time. The large changes in LW cloud forcing during summer may be caused by several factors. Figure 17 (c) and (d) show that the cloud liquid water path changes much more in summer than it does in winter. However, our results also show that the LWP itself is large in summer. High initial LWP leaves the clouds less sensitive in the LW to changes in this parameter during summer than during winter (see section 5.1). Despite this, the very

low changes in LWP during winter are likely to contribute to larger changes in surface LW flux in summer than in winter.

The large summer signals may also be caused by larger simulated changes in effective radius during this season than during winter (not shown here). Our results show, however, that this property is smaller during summer than during winter and clouds will therefore be less sensitive to these changes as well as to changes in LWP.

In addition, the change in LW cloud forcing with pollution may be highly influenced by the fraction of low clouds being larger during the summer season than during winter (Figure 18). According to Shupe and Intrieri (2004), clouds that are important to the LW radiation balance at the Arctic surface typically have bases at low altitudes (below 4 km). A high fraction of these clouds allows changes in cloud radiative properties to occur often and affects the LW radiation budget more than less frequent changes during winter.

The importance of changes in the low level clouds can be illustrated by comparing vertical cross sections of the change in LW cloud forcing and the change in in-cloud liquid water mixing ratio along 30°E. Between 75 and 80°N in Figure 19 one can see a minimum of change in liquid water amount at low levels co-located with a minimum of change in LW cloud forcing at the surface. The change in water amount at low levels clearly affects the change in surface LW cloud forcing greatly.

One additional aspect that may cause the change in forcing to be larger in summer than in winter is the temperature profiles. Our results show that the average Arctic temperature profiles generally have higher temperatures in summer than in winter at altitudes where clouds are frequently present. As shown in section 5.1 cloud bases with high base temperatures will lead to a larger change in LW cloud forcing with a given change in cloud properties than clouds with low base temperatures. This behavior may affect the signals of change in LW cloud forcing with anthropogenic aerosols to be larger during summer than during winter.

Despite the seasonal variation, some signals persist for both seasons. An example of this is a relatively strong signal of change occurring over central Greenland. This is the region that holds the lowest amount of water originally and is therefore very sensitive to changes due to increased aerosol amounts (see section 5.1). From our results we know that there is a large frequency of mid and high leveled clouds in this region throughout the year (40-50 percent). Although the liquid water amount does not change much at these altitudes, the effective radius in general changes more here than close to the surface. Optically thin clouds combined with relatively large changes in effective radius at these levels make the LW cloud forcing at the surface

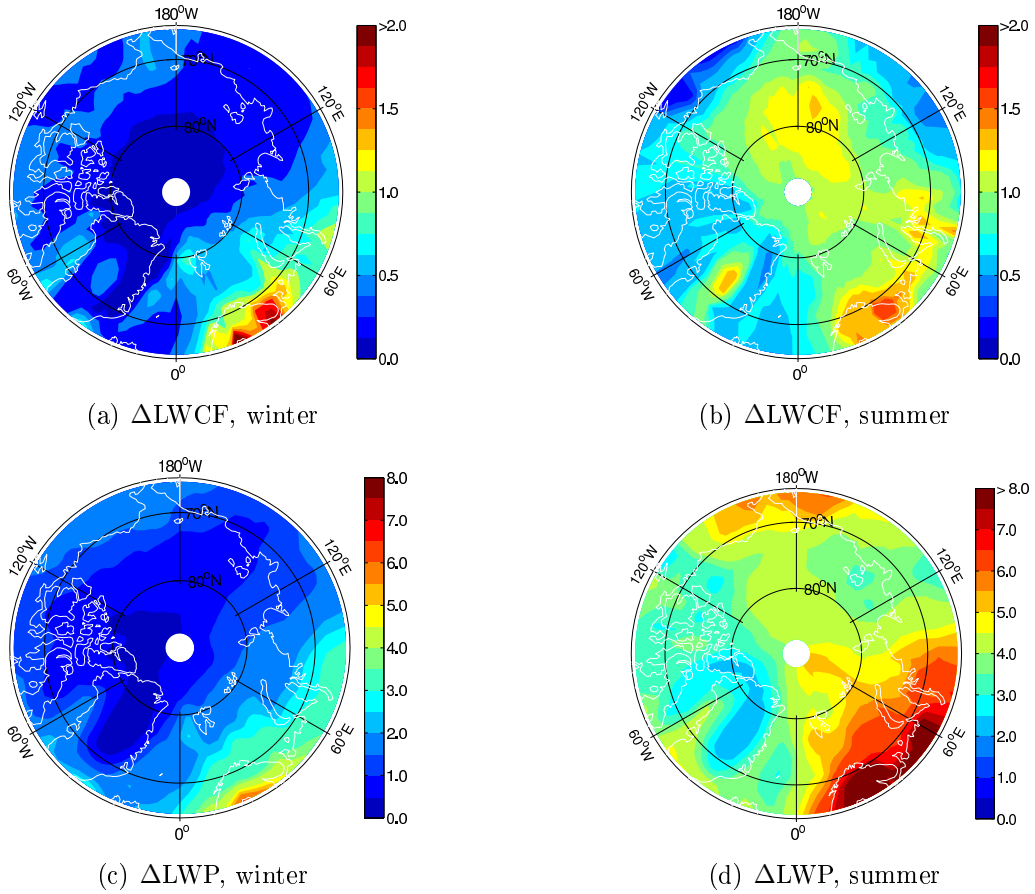

(a) ΔLWCF, winter

(b) ΔLWCF, summer

(c) ΔLWP, winter

(d) ΔLWP, summer

Figure 17: Change in LW cloud forcing at the surface [W/m^2] and in liquid water path [g/m^2]. (PRES - PIND) Forced model version.

change here in both seasons.

Our results suggest that there has been as increase in the LW radiative surface flux in the Arctic due to anthropogenic sulfate aerosols. This increase is larger in summer than it is during winter. This is due to larger changes in cloud properties with pollution, larger fractions of low level clouds and higher cloud base temperatures in summer than in winter.

6.1.2 Changes in Parameters that Affect the LW Cloud Forcing

The increase in LWCF from pre-industrial times until today is caused by changes in different parameters. Since the meteorology is the same in all model runs, the clouds will be identical in location and extent. Only changes in properties within each cloud can affect the LW cloud emissivity and there-

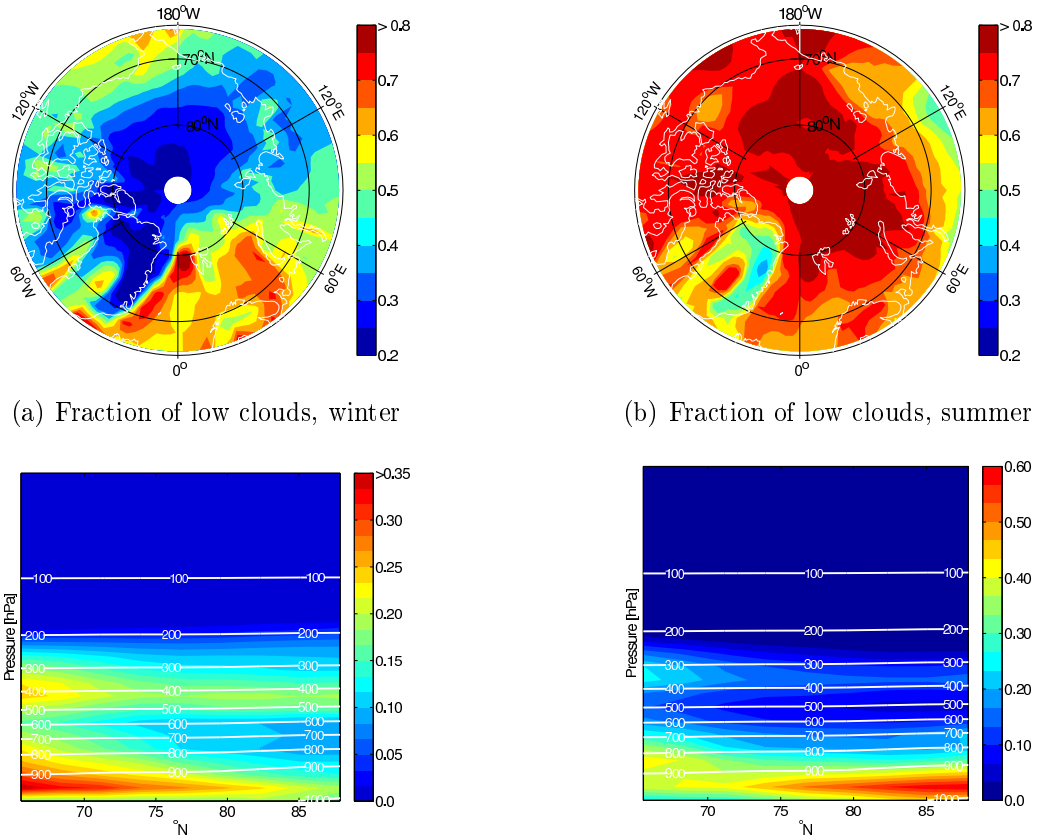

(a) Fraction of low clouds, winter

(b) Fraction of low clouds, summer

(c) Average cloud fraction, winter

(d) Average cloud fraction, summer

Figure 18: The fraction of low clouds above and the annually averaged Arctic cloud fraction below. Forced model version. Note that scales differ in c) and d).

fore the model cloud forcing. These changes occur when an increase in the aerosol concentration influences the effective radius and/or liquid water path. We will start by looking at how the concentration of sulfate changes in case 1 and go on to study how this affects the effective radius and the cloud liquid water path. While doing this we will comment on how these changes may influence the LW surface cloud forcing. At the end of this section we will mention some aspects of the 3D model and our methods that may influence the simulated LWCF.

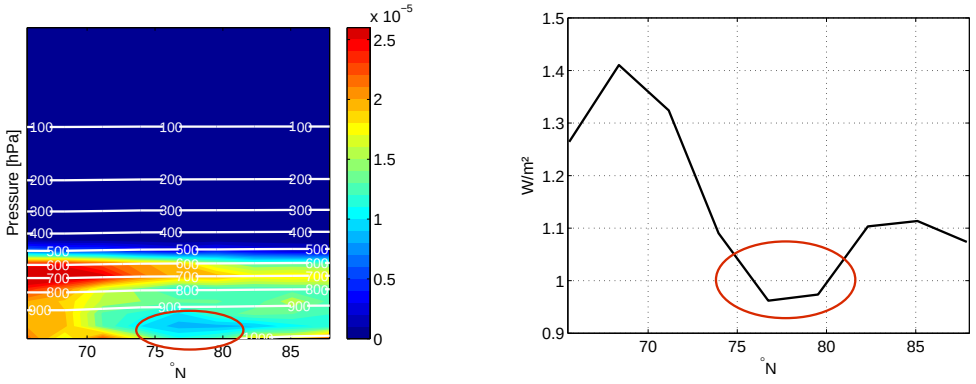

(a) ΔLWMR (b) ΔLWCF

Figure 19: Changes in in-cloud liquid water mixing ratio (LWMR) [kg/kg] and LW cloud forcing along 30°E during summer. (PRES - PIND) Forced model version.

Sulfate Concentration

The only input parameter that changes between the simulations is the aerosol concentration. Figure 20(a) shows the increase in column integrated concentration of sulfate from pre-industrial times until today. Notice how the spatial pattern of change has similarities with the pattern of change in LW cloud forcing at the surface (Figure 16(b)). The increase in sulfate amount is largest over the European continent where the concentration itself is largest in present day (Figure 4(a)). The large increase in this area is not surprising as northern Eurasia is a source region of anthropogenic sulfate precursors (section 3.3).

Figure 20(b) shows the vertical distribution of change in sulfate for case 1 annually averaged over the Arctic region. The largest changes in concentration occur in layers around 900 hPa. However, there are relatively large signals of change both above and below this value. (The large changes south of 70 to 75°N is due to the large increase in SO_4 concentrations over northern Europe.) From section 5.1 we know that the LW cloud forcing at the surface will mainly be affected by the bottom cloud layer, as radiation emitted from layers above is partially or fully absorbed by the bottom cloud. Intrieri et al. (2002b) found that the Arctic clouds often lie close to the surface (bases below 1 km). This tendency is reproduced by the 3D simulations (Figure 18). Combined, the two effects suggest that the changes seen in aerosol concentration close to the surface is of crucial importance for a change in surface LW cloud forcing with anthropogenic aerosols.

We will like to mention that due to the importance of the bottom cloud layer, an inaccurate vertical placement of aerosols will influence the LW cloud forcing especially. However, in section 4.3.3 we found no evidence to suggest that the model sulfate is misplaced in the vertical.

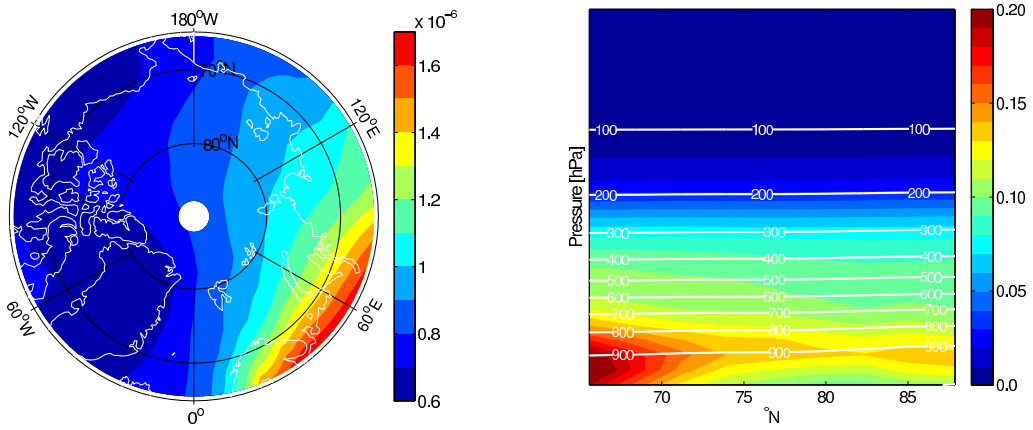

(a) ΔSO_4 (b) ΔSO_4

Figure 20: Changes in SO_4 concentrations, annual mean. a) column SO_4 [kg S/m^2]. b) Vertical concentration, Arctic average [μg S/m^3]. (PRES - PIND) Forced model version.

Effective Radius

A change in the sulfate concentration changes the concentration of cloud condensation nuclei. From section 3.4 on indirect effects we know that a increase in CCN is likely to affect the size of the cloud droplets. The simulated effective radius averaged annually over the cloud droplet number concentration decreases from 13.7μm in pristine conditions to 11.5μm in the polluted present day regime. This is consistent with observations by Garrett and Zhao (2006), who find an average decrease in effective radius from 12.9μm to 9.9μm between clean and polluted regimes. It appears that the first indirect effect is present in our simulations and that it is of the same order of magnitude as observed values.

It was explained in the last subsection how the LW cloud forcing is affected by the height of the change in cloud properties. The effective radius described in the last paragraph is averaged in height and therefore do not give any information about the vertical distribution of the change in cloud droplet size. Figure 21(a) displays a vertical cross section of the annually averaged effective radius over the Arctic region. This figure shows that the layers

below 500 to 600 hPa are sensitive to the *first* indirect effect in the LW as the $\bar{r}$ of these layers is above 10μm (see section 3.1).

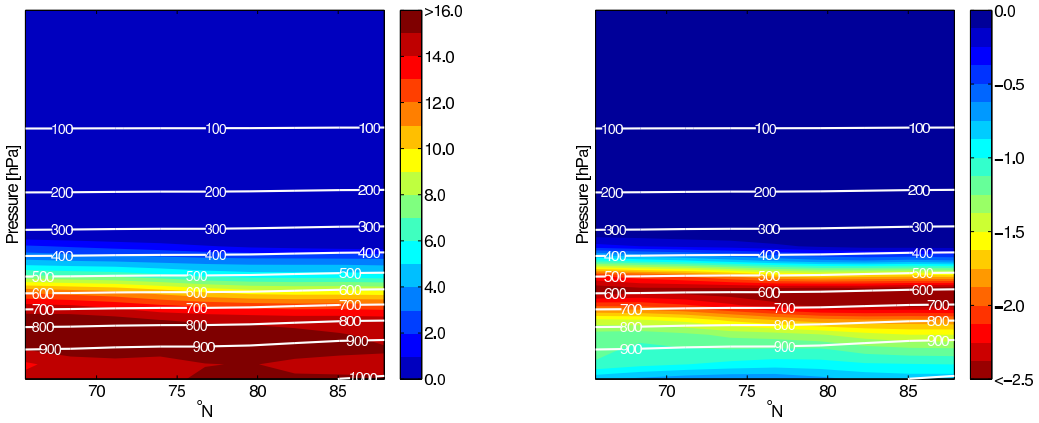

(a) Annual Arctic mean of $\bar{r}$.

(b) Annual Arctic mean of $\Delta\bar{r}$.

Figure 21: Annual Arctic mean of effective radius [μm] in present day and change in this parameter between the PRES and the PIND scenarios. Forced model version

Figure 21(b) displays the change in effective radius between the PRES and the PIND emission scenarios. It is clear that the simulated effective radius changes the most in a layer around 600 hPa, while the changes are smaller close to the surface. The absolute change in effective radius is large if the $\bar{r}$ is large initially and there is a large increase in the cloud droplet number concentration. This is what creates the maximum around 600 hPa. Above this level the initial $\bar{r}$ is small, while below there are small changes in the cloud droplet number concentration (not shown here).

The largest changes in effective radius happens well above the layers of the highest average cloud fraction (Figure 18) and are therefore not likely to influence the surface LW cloud forcing much. However, the decrease in $\bar{r}$ of between 0.6 and 1.0 μm close to the surface will increase the surface LW cloud forcing when going from the pre-industrial to the present day emission scenario.

Liquid Water Path

As displayed in Figure 22(a) the spacial pattern of annually averaged change in LWP between the PRES and the PIND scenarios has similarities with both the change in SO_4 and the change in LW cloud forcing at the surface (especially over northern Europe and around Spitsbergen). Notice that the LWP

increases in the more polluted regime. This is an expected manifestation of the second indirect effect.

The average increase in liquid water path between the two scenarios is about 2.6 g/m^2 north of 71°N, going from 32.4 to 35.1 g/m^2. This is within the same range as the change found by Garrett and Zhao (2006) of 2.4 g/m^2, from 31.1 in pristine conditions to 33.5 g/m^2 in a atmosphere with high aerosol concentrations. It is important to note that the clouds of the pre-industrial aerosol regime have liquid water paths in the same range as the average clean cloud observed by Garrett and Zhao. We found in section 5.1 that the LW emissivity does not change linearly with LWP. A certain ΔLWP will therefore affect the cloud forcing differently depending on the amount of water in the cloud initially.

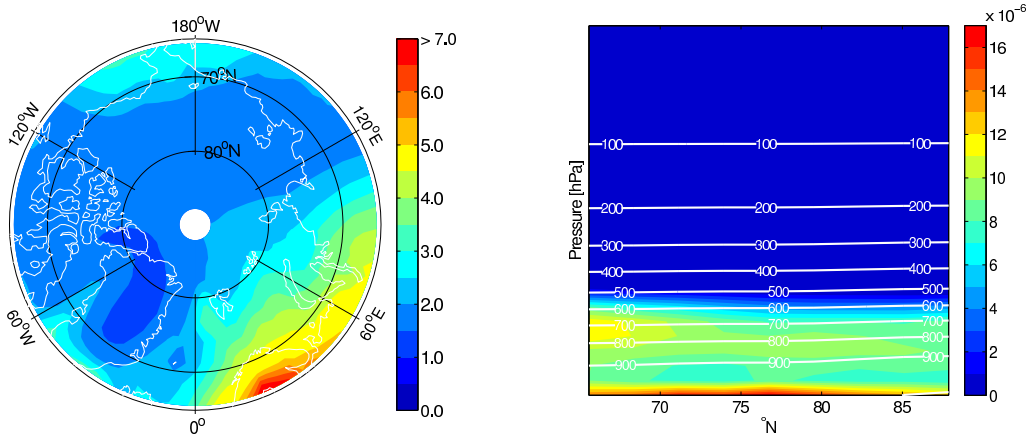

(a) ΔLWP annual mean

(b) ΔLWMR annual Arctic mean

Figure 22: Change in liquid water path [g/m^2] and in in-cloud liquid water mixing ratio [kg/kg] between the present day and the pre-industrial scenario. Forced model version

As in the case of the effective radius, the changes in LWP described above are two dimensional. A vertical cross section of changes in in-cloud liquid water mixing ratio (LWMR) averaged annually over the Arctic region is shown in Figure 22(b). Contrary to the changes in effective radius, the LWMR changes most in layers close to the surface. The reason for this is that the liquid water amount is largest in surface layers in pre-industrial times (not shown here). These layers are therefore where the onset of precipitation is most likely to be suppressed with a change in cloud properties. Although a small change in CDNC leads to only small changes in effective radius at these levels, this change may still be large enough to affect the model auto-

conversion. Hence the amount of water lost through precipitation decreases.

Note that there is a second layer of change at altitudes around 800 hPa. The liquid water mixing ratio decreases steadily with height, but is still large enough at 800 hPa to be affected by changes in effective radius, which increases with height up to 600 hPa. Combined, this leaves a second maximum around 800 hPa.

The average liquid water path described so far in this section says nothing about the thickness of each individual cloud simulated by the 3D model. There may be episodes of very low or very high LWPs that affect this average greatly. One might therefore question whether clouds are thin enough to be affected by indirect effects in the LW. Clouds with LWP higher than 50 g/m^2 have emissivities close to unity and the LW cloud forcing will not be affected by indirect effects (section 5.1). Figure 23 shows the present day fraction of time that has vertically integrated LWPs below 50 g/m^2 when cloud are present. It reaches a minimum in August, simultaneously with the maximum in average LWP (Figure 6). The fraction is never below 55 percent and we conclude that a large portion of clouds in the present day regime is non-opaque and therefore sensitive to changes in effective radius and liquid water path with anthropogenic sulfate. The pre-industrial fraction of clouds that are sensitive will be even higher as these clouds are thinner in general - leaving even more clouds sensitive to changes due to indirect effects.

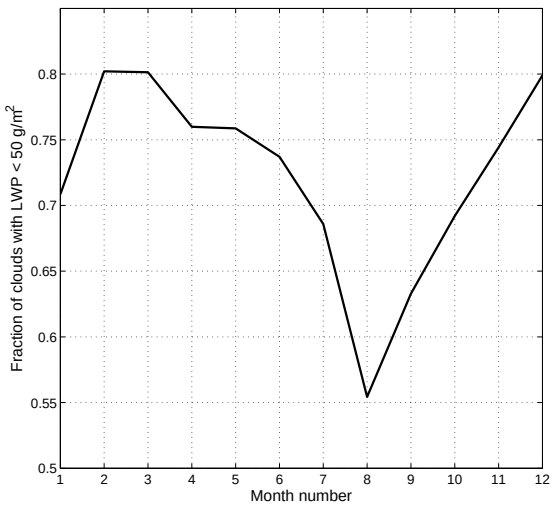

Figure 23: Fraction of time when clouds are present with vertically integrated LWP below 50 g/m^2. Forced model version

In this subsection we have found that our simulated change in average

LWP between the present day and the pre-industrial scenarios is consistent with earlier findings. We have also found that a large fraction of clouds are sensitive to changes in $\bar{r}$ and LWP and that the largest changes in liquid water amount occur in layers that are likely to affect the LW cloud forcing at the surface.

Limitations in the 3D Model and in Our Methods

We will now go through some aspects of the 3D model and of our methods that may influence the simulated changes in surface LWCF.

Vertical Resolution
Menon et al. (2002) have found that the vertical resolution of climate models is particularly important when simulating the cloud indirect effects. This is because of sharp gradients in aerosol concentrations with height and the detailed vertical distribution of clouds in the lower troposphere. In order to accurately simulate the change in cloud forcing with pollution Menon et al. find that a better vertical treatment of atmospheric conditions and cloud properties is needed than what is used in most climate models. The coarse vertical resolution used in the CAM-Oslo model do not include vertical treatment of properties as suggested by Menon et al. (2002). This may cause our results to be inaccurate.

Liquid Water vs. Ice Particles in Mixed-phase Clouds
In section 4.3.3 our results pointed to a possible overestimation of the fraction of liquid water in mixed-phase clouds. A biased amount of water versus ice particles will affect the change in LW cloud forcing with pollution, as aerosols in this study affect droplet nucleation only. However, the average liquid water path in our study is expected to be within the range of observed values. If there is an underestimation of ice relative to water it therefore means that the clouds holds too little water in total and may be somewhat thin. An underestimation like this may therefore cause our cloud emissivity to be too sensitive to changes in $\bar{r}$ and LWP and cause our estimated change in LW surface cloud forcing to be too high.

Cloud Lifetime Effect
As we are running the model off-line, changes in cloud parameters are not allowed to influence the further evolution of the meteorology. Whether there exists a cloud lifetime effect associated with suppressing precipitation is uncertain (see section 3.4.2). If there is such an effect, it would not be included in our off-line simulations, and would therefore be a source of uncertainty in

our results.

6.1.3 Comparison with Earlier Findings

In section 6.1.1 we found an annually averaged increase in surface LW cloud forcing of 0.64 W/m^2 from the pre-industrial to the present day emission scenario. This increase is *one order of magnitude* less than what is suggested by Garrett and Zhao (2006) and Lubin and Vogelmann (2006). In the two Nature articles, there were found increases in the LW radiative flux at the surface of between 3.3 and 8.2 W/m^2 when going from pristine to polluted conditions under cloudy skies (see chapter 2). In section 5.1.1 we concluded that the LW radiation scheme is well suited for simulating the radiative impact of changes in cloud parameters with pollution. Although there are elements of uncertainty in our study not linked to the LW radiation scheme, we find no evidence to suggest that our results are unreasonable. We will in the following discuss possible reasons for the significant discrepancy between our and earlier findings.

The low average change in LWCF in our study may either be caused by low average changes in cloud parameters between different emission scenarios or by clouds being less sensitive to these changes in our study than clouds studied in the background articles. We found in the previous section that our average initial LWP is consistent with observations by Garrett and Zhao. This should leave clouds sensitive to changes in $\bar{r}$ and LWP. In the same section we found that the changes in $\bar{r}$ and LWP averaged in height are also consistent with the above mentioned observations. Although the integrated LWP include changes at all altitudes (Figure 22(b)), the liquid water amount changes most close to the surface and is therefore expected to influence the change in LW cloud forcing. The effective radius, on the other hand, changes much less in surface layers than it does averaged in height. While Garrett and Zhao found a decrease in $\bar{r}$ of 3 μm between the pristine and the polluted regime, our results show a change of 0.6 to 1.0 μm in layers important to the surface LWCF. We thus do find average changes in cloud parameters lower than in the Garrett and Zhao study.

The low average change in $\bar{r}$ and LWP may help explain the noted discrepancy in results. We believe that these averages are highly influenced by differences in the approach used in this and the background studies.

One important aspect that is very likely to influence the results is that the earlier studies mentioned have looked at specific conditions for cloud type and pollution. By only looking at non-opaque clouds and episodes of particularly high or low aerosol levels Garrett and Zhao and Lubin and Vogelmann should find only the largest changes in surface flux caused by

anthropogenic emissions. It may be that these favorable conditions are met too seldom or over too short time periods to affect the annual mean of our results. If this is the case, instantaneous results should include signals of change that are significantly larger than our seasonal average. The fraction of time with change in surface LW cloud forcing above 3.3 W/m^2 is plotted in Figure 24. 3.3 W/m^2 is the lower boundary of the increase in surface flux found in the background articles. Except for the month of May, changes of this magnitude do occur between the present day and the pre-industrial emission scenario. The 3D model thus simulates changes consistent with the range observed by both Garrett and Zhao and Lubin and Vogelmann. The fraction of time when this occurs, however, is very limited, with a peak of approximately 4 percent in late summer/early fall.

It is difficult to decide whether this alone is enough to explain why our average results are lower than the earlier findings, as there is no information on the fraction of time studied in the background articles. We can, however, show that the fraction of time included in the earlier studies will be significantly smaller than in our study. Lubin and Vogelmann use the lowest and the highest 25th percentiles of pollution found in their data set and thus excludes one half of the time with data available. Following this they only study times when there are clouds present and exclude the cases where clouds are black bodies. There is no information on the fraction of clouds co-incident with high and low pollution events or on the fraction of clouds that are black bodied. This means that the fraction of time they are left studying is below 50 percent, but how much below is unclear.

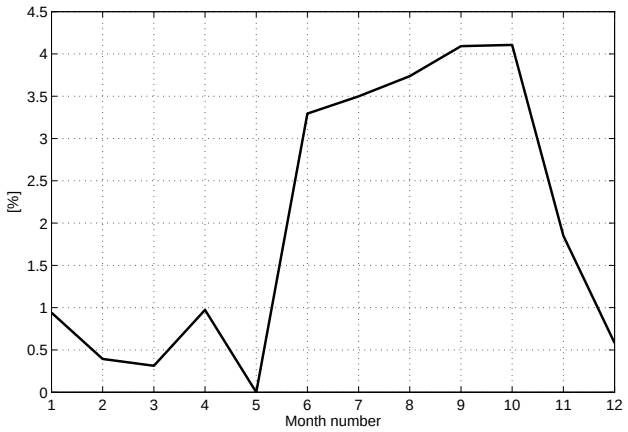

Figure 24: Fraction of time with change in LW cloud forcing at the surface greater than 3.3 W/m^2 (PRES - PIND). Forced model version

It should also be mentioned that the examples and demonstrations used in the Lubin and Vogelmann (2006) article are of clouds with LWP in the interval between 10 and 15 g/m^2. This is the interval where the LWCF is most sensitive to changes in effective radius (section 5.1). Signals of change with the first indirect effect should therefore be large.

Another possible explanation for the discrepancy between our results and earlier findings is that our average present day scenario will not have aerosol concentrations as high as the highly polluted regimes studied by Garrett and Zhao (2006) and Lubin and Vogelmann (2006). The polluted regimes in the earlier studies only include the highest 25 percent of the present day aerosol concentration. Our study, on the other hand, compare an average of all pollution events in the present day regime to the clean pre-industrial scenario. We are not comparing a low to a high, but a low to an "average" pollution scenario.

Additionally both background studies were carried out in Alaska and their findings may not be representative for the Arctic in general. However, the modeled change in surface LW cloud forcing found in Figure 16(b) does not show larger values over this region than over other areas within the Arctic.

One last aspect that will lead to discrepancies in results is that there may be differences in the weather and temperature anomalies of the model and the observed cases. In section 5.1 we showed that cloud bases with high temperatures give large changes in cloud forcing with changes in $\bar{r}$ and LWP. If the temperature profiles differ, it will affect the results. However, large systematic biases in this property are needed for this to influence the results greatly. We found in the model verification that the LW cloud forcing simulated by the forced model version compares fairly well to observations, and that we have no reason to suggest that the temperature profiles used are unreasonable. Additionally, it should be mentioned that the results shown in this section are averaged over five years and no particular meteorological event or temperature anomaly will affect the average results.

It is clear that there are significant differences between this and earlier studies of change in surface LWCF with increased aerosol levels. While our study shows the overall importance of the phenomenon, the background studies show the maximum possible influence of the increased levels of pollution. The average increase in LW cloud forcing found in our study is *significantly* lower than the high increase in surface LW flux found by Garrett and Zhao (2006) and Lubin and Vogelmann (2006).

6.1.4 LWCF at the Surface, 2SOx Compared to Present Day

In this section the simulated change in LW cloud forcing at the surface between the hypothetical 2SOx scenario and the present day emissions will be examined.

The annually averaged increase in LWCF at the surface is 0.35 W/m^2 north of 71°N (Figure 25(a)). The magnitude of this change is 0.29 W/m^2 lower than the change found in case 1 due to indirect effects, and implies that the change in the LW emissivity is lower. This can be a result of either lower changes in the parameters that influence the emissivity, effective radius and LWP, or of clouds being less sensitive to changes in these parameters. This would be the case if the clouds are already optically thick.

In the case studied here the regime of low aerosol concentrations is the present day regime. This emission scenario has a significant aerosol concentration and clouds have higher emissivities than clouds in the pre-industrial simulations. This implies that the clouds in the low aerosol regime in this case will be less sensitive to changes in effective radius and liquid water path than they were in case 1. Figure 23 shows, however, that the fraction of clouds sensitive to changes in cloud properties is never below 55 percent.

In addition to clouds having higher emissivities initially in case 2 than in case 1, the simulated changes in effective radius at all levels are smaller in the 2SOx - PRES case than in case 1. While this decrease is on the order of 2.2 μm in case 1 (13.7 to 11.5 μm), in case 2 the average effective radius decreases by only 0.6 μm (11.5 to 10.9 μm). Small changes in the effective radius in turn lead to a reduced suppression of precipitation. The change in LWP (Figure 25(b)) is therefore also smaller between the scenarios studied here than in case 1. The spacial pattern of change in this parameter is, however, similar to the previous case.

Both the effective radius and the cloud liquid water path are influenced by the amount of aerosols already available in the atmosphere. A clean environment will in general have smaller LWP and larger $\bar{r}$ than a polluted environment. The effect of a given increase in sulfate aerosols will therefore depend on the initial aerosol concentration. Results from the 3D model show that the absolute increase in the sulfate concentration is of the same order of magnitude in both cases studied, with a maximum concentration around $1.6*10^{-6}$ to $1.8*10^{-6}$ kg S/m^2. The reduced sensitivity of the present day clouds compared to the cleaner pre-industrial conditions leads to a lower change in both effective radius and LWP in case 2 than in case 1.

Lastly, we would like to mention that if the emission of SO_2 is over a certain magnitude, clouds saturate and can not take up more of this chemical compound. SO_4 is produced through oxidation of SO_2 that has reacted with

water and through clear air oxidation. If clouds are saturated with SO_2, the production of SO_4 may therefore be low even if the emission of its precursors increase (personal communication with Terje Berntsen).

The 2SOx - PRES scenario shows that the sensitivity of Arctic clouds to changes in LWCF with pollution is approaching saturation. High initial liquid water paths combined with small initial effective radii leads to low changes in surface LW cloud forcing with increased amounts of anthropogenic sulfate aerosols.

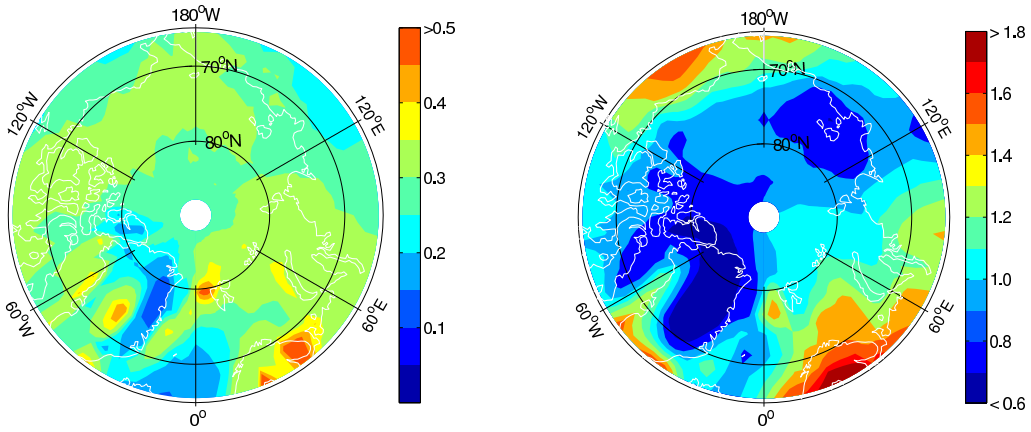

(a) ΔLWCF (b) ΔLWP

Figure 25: Annual change in LW cloud forcing at the surface [W/m^2] and LWP [g/m^2] between 2SOx and PRES scenario. Forced model version.

6.1.5 Summary of Changes in LW Cloud Forcing at the Surface

Results from the 3D model show that there is an annually averaged increase in surface LW cloud forcing of 0.64 W/m^2 when going from the pre-industrial to the present day concentration of aerosols. We also find that the increase is larger during summer (1.16 W/m^2) than during winter (0.39 W/m^2). This is due to larger changes in LWP and $\bar{r}$, a larger fraction of low clouds and higher cloud base temperatures during summer than during winter. Additionally, we found changes in both aerosol concentrations, liquid water path and effective radius in layers important to the surface LW cloud forcing, although the largest changes in $\bar{r}$ occur in layers too high to be of influence.

The annually averaged changes in surface LW cloud forcing simulated by the 3D model is one order of magnitude less than the increase in this forcing found by Garrett and Zhao (2006) and Lubin and Vogelmann (2006) when

going from pristine to polluted conditions under cloudy skies. The earlier studies have found the maximum influence of anthropogenic emissions under favorable conditions, while we study the average impact of anthropogenic sulfate emissions on the surface LW cloud forcing in the Arctic region. Our results suggest that the overall importance of increased LW surface flux is not as high as can be expected from the results of the studies by Garrett and Zhao and Lubin and Vogelmann.

Lastly we found that the sensitivity of the Arctic clouds to changes in LWCF with pollution is approaching saturation.

6.2 Shortwave Cloud Forcing at the Surface

The background articles that were a motivating factor for conducting this study consider LW effects only. It is clear, however, that as long as solar radiation is present, changes in $\bar{r}$ and LWP will affect the magnitude of the SW surface cloud forcing as well as the LW. In the following we will look at the average changes in the SW surface cloud forcing created by an increase in the anthropogenic sulfate concentrations. First the effects of going from pre-industrial to present day emissions will be examined. We will then study the changes occurring when further increasing the emissions to the hypothetical 2SOx regime.

6.2.1 SWCF at the Surface, Present Day Compared to Pre-industrial Emissions

Figure 26 displays the annually averaged change in SW cloud forcing between the present day and the pre-industrial emission scenarios both for the original model code and the forced model version. Results from the original model code give an annually averaged change in SWCF at the surface of -0.98 W/m^2 north of 71°N.

For the forced model version the increased magnitude of the surface SW cloud forcing averages to **-0.99 W/m^2** north of 71°N. This is a 6.5 percent increase in the SW cloud forcing from pre-industrial times until today. However, the change in forcing simulated with this model version is not much stronger than the results given by the original model code and the relative change is not as large as the change between the two model versions in the LW. This is because clouds saturate for higher LWPs in the SW than in the LW. The SWCF is therefore sensitive to indirect effects even for the large LWP found in the model originally. The SW cloud forcing itself, however, is much stronger in the original model version than in the version with reduced

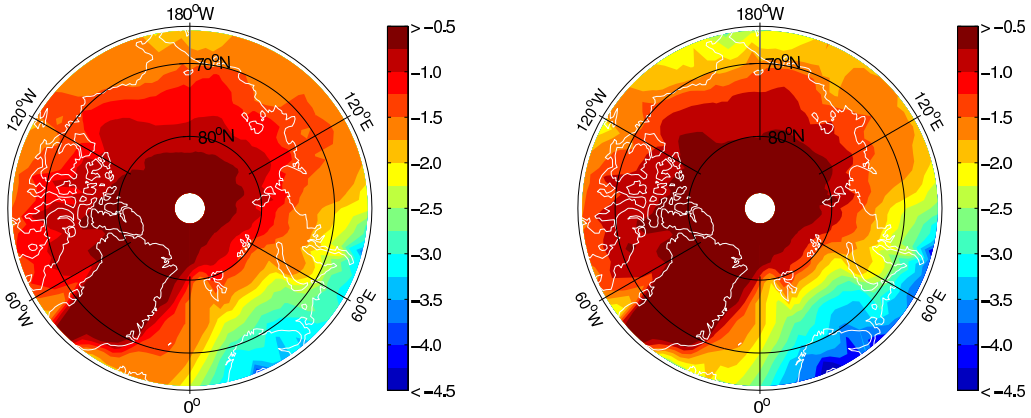

(a) ΔSWCF. Original CAM-Oslo

(b) ΔSWCF. Forced model

Figure 26: Annually averaged change in SW cloud forcing at the surface [W/m^2] for the original model code and the model version with forced LWP. (PRES - PIND)

LWP. There will be no further discussion of results from the original model in this section.

The seasonal variation in change in SWCF at the surface with anthropogenic emissions is much stronger in the SW than in the LW. This is caused by the sun being absent or at high solar zenith angles through most of the winter season. Because of the low signals during winter, we will now focus on the summer season.

The change in surface SW cloud forcing during summer has an average of **-2.53 W/m^2** north of 71°N. From Figure 27(a) it is clear that the changes are larger towards lower latitudes. This happens for two reasons. First, the solar zenith angle is lower here and the radiation more energetic, leaving a larger possible impact of the clouds on the radiation budget. However, Figure 27(b) shows that during this time of the year, the cloud fraction increases toward the north. The total influence of this effect is therefore lower than it would have been if the clouds had been evenly distributed within the Arctic region.

Secondly, areas around the North Pole and over Greenland are covered by surface and sea ice. The increased albedo of clouds subject to indirect effects will be less important here as the clouds are above highly reflective surfaces. The clouds thus have relatively little influence on the amount of radiation reflected to space. The importance of this phenomenon is underlined by the decreasing change in SW cloud forcing when approaching the edge of the multiyear ice (Figure 28). While the surface in these areas is highly reflective in the beginning of summer, as the ice melts the surface albedo

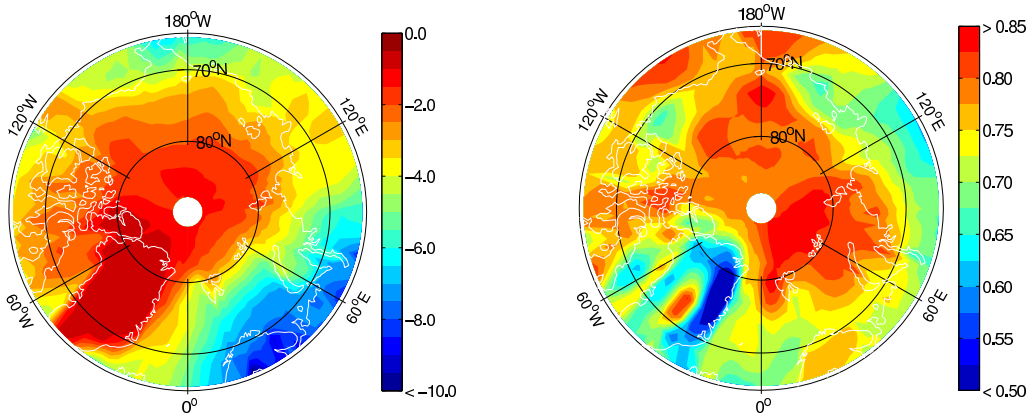

(a) ΔSWCF, summer (b) Total cloud fraction, summer

Figure 27: (a) Change in SW cloud forcing [W/m^2] at the surface between PRES and PIND scenario. (b) Simulated total cloud fraction. Summer season. Forced model version.

decreases and the impact of changes in cloud albedo becomes larger. This leads to the pattern of decreasing change in surface SW cloud forcing when moving towards the area covered by multiyear sea ice located around the North Pole.

The magnitude of both the relative and the absolute change in SW cloud forcing at the surface during summer is larger than the magnitude of change simulated for the LW case. There are several reasons for this large change in the SWCF with anthropogenic emissions. In section 5.3 we showed that during mid July a given change in $\bar{r}$ or LWP will affect the SW cloud forcing more than its LW counterpart for initial LWPs above 15 g/m^2. The changes in SW cloud albedo are more abrupt than the changes in LW emissivity. The simulated average of LWP is well above 15 g/m^2 during summer (55 g/m^2). Depending on the surface albedo it is likely that the SW cloud forcing during this season will change more with a given Δr and ΔLWP than the LW surface cloud forcing.

Another reason for the large SW signals of change is that changes in cloud albedo at any altitude will affect the amount of SW radiation received at the surface (section 5.2). In section 6.1.2 we showed that the annual average of change in $\bar{r}$ is largest in a layer around 600 hPa when going from pre-industrial to present day emissions (Figure 21(b)). Our results show that the main changes during summer season occur in the same levels, or in levels a bit higher in altitude. In the same section (6.1.2) it was found that the liquid water mixing ratio also experience change at levels well above the surface

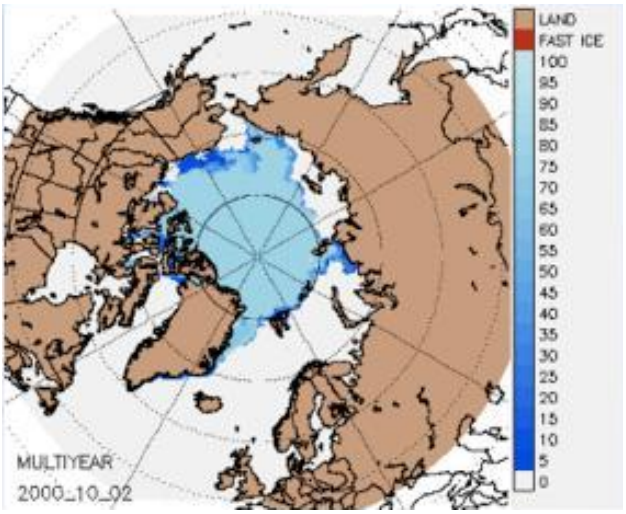

Figure 28: Multiyear ice cover (2000). Figure from NSIDC (2009b).

(800 hPa, Figure 22(b)). In summer, the changes around this altitude are approximately 50 percent larger than the annual average. In the LW case, changes at these altitudes were found to have little influence on the surface cloud forcing. The SW surface cloud forcing is affected by changes in cloud albedo at all altitudes and will be affected by the changes in cloud droplet size and water amount occurring at high levels as well as low. This may add to the reasons why the signal of change in SW cloud forcing is larger than the change in the LW.

Additionally, since clouds are saturated at higher LWPs in the SW than in the LW, a larger fraction of clouds have radiative properties sensitive to changes in $\bar{r}$ and LWP. This is likely to create larger changes in SW than in LW surface cloud forcing with pollution.

We want to point out that the changes in in-cloud liquid water amount and effective radius at high *latitudes* (Figures 22(b) and 21(b)) are not reflected in the SW cloud forcing results. This is again because of the highly reflective surface in this part of the Arctic region.

It is important to point out that the results presented here are of changes within the clouds only - the optics in clear sky is the same in all model runs and the direct effect unchanged. This means that the SW clear sky net flux is the same for both pre-industrial, present day and 2SOx simulations. In reality, however, this net flux will decrease with increased amounts of sulfate present in clear sky (section 5.3). Thus, the amount of solar radiation reaching the surface under clear skies in the more polluted scenarios will be less than under pristine conditions. With less radiation reaching the ground

in general, the SW cloud forcing will decrease. The net or total effect of introducing a given increase in the SW cloud albedo would therefore be less in present day, and even more so in the 2SOx case, than in the cleaner pre-industrial scenario. Including the direct effect in our simulations reduces the annual change in surface SW cloud forcing between the PRES and the PIND scenarios from -0.99 W/m^2 to -0.56 W/m^2 and the summer average from -2.53 W/m^2 to -1.50 W/m^2. Ignoring the change in direct effects between the scenarios thus influences the SW results significantly. In this study, however, we are investigating changes in the radiative balance at the surface due to indirect effects and focus on how increased levels of anthropogenic sulfate aerosols change the amount of radiation emitted from or passing through the clouds. Including the changes is direct effects highlights the overall change in importance of clouds and their properties in polluted versus clean conditions. It does, however, conceal changes occurring within clouds due to interaction with increased aerosol levels.

Lastly, we would like to mention that the elements that may affect the accuracy of the LW results will be equally important in the SW (see section 6.1.2).

The changes in SW cloud forcing due to indirect effects from pre-industrial times until today are significant. During summer the magnitude of the decrease in SW radiative flux is of the same order as the average increase in surface flux resulting from anthropogenic emissions of greenhouse gases (-2.5 vs. 2.3 W/m^2 (IPCC, 2007)).

6.2.2 SWCF at the Surface, 2SOx Compared to Present Day

From Figure 29 it is clear that the spacial pattern of change in SW cloud forcing between the 2SOx and the PRES scenarios is nearly the same in this case as in case 1. The magnitude is, however, much smaller in the case studied here. North of 71 °N the change in SW forcing averages to -1.29 W/m^2 during summer time and -0.51 W/m^2 annually. The lower signal of change in case 2 than in case 1 may, like in the LW case, be caused by several factors. We found that both the effective radius and the liquid water amount change less in this case than in case 1 (see section 6.1.4). This leads to weaker signals of change in the SW cloud forcing.

We also found that the clouds were optically thicker in the "low pollution" scenario in case 2 than in case 1. This leaves the clouds less sensitive to changes in surface SW cloud forcing with ΔLWP and $\Delta\bar{r}$ and may help explain the low signals of change between the 2SOx and the PRES scenario.

We would like to point out that the SW cloud albedo is most sensitive to changes in effective radius for LWP around 90 g/m^2 (section 5.2). The

initial clouds containing more liquid water may therefore make the cloud albedo more sensitive to changes in this parameter. However, this does not seem to affect our results greatly.

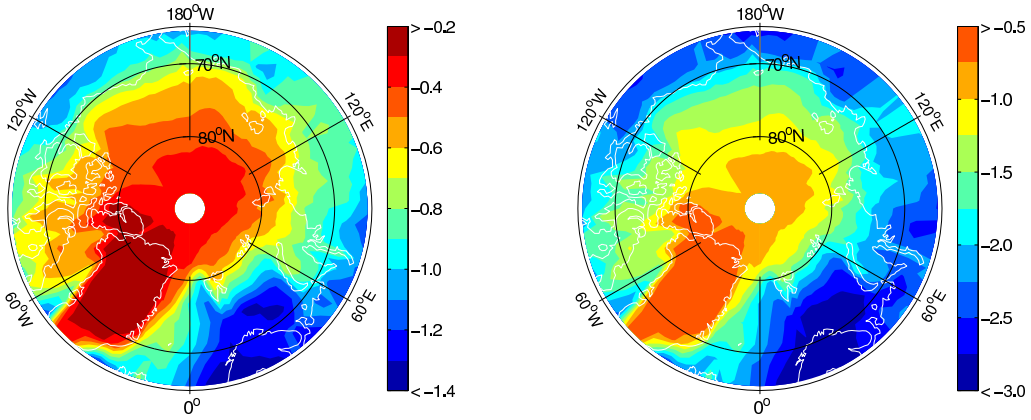

(a) ΔSWCF. Annual average

(b) ΔSWCF. Summer season

Figure 29: Annual change in SW cloud forcing [W/m^2] at the surface between 2SOx and PRES scenario. Forced model version.

6.2.3 Summary of Changes in SW Cloud Forcing at the Surface

Results from the 3D model show that the SW cloud forcing at the surface decreases by 0.99 W/m^2 due to indirect effects when going from pristine conditions in pre-industrial times to the polluted conditions found in the Arctic today. Our results also show that the change in SW cloud forcing during summer averages to -2.53 W/m^2. This large change in surface SWCF is caused by the high sensitivity of the SW cloud albedo to changes in $\bar{r}$ and LWP, combined with changes in cloud albedo at all altitudes affecting the surface SW cloud forcing. During summer, the increase in anthropogenic sulfate aerosols from pre-industrial times to present day will significantly decrease the surface SW radiative flux under cloudy skies in the Arctic region.

Lastly we found that the sensitivity of the Arctic clouds to changes in SWCF with pollution is lower today than it was pre-industrially.

6.3 Net Cloud Forcing at the Surface

The changes in cloud forcing in both the LW and the SW have now been examined. Here, we will study the total influence of increased aerosol levels interfering with Arctic clouds and examine the net change in cloud forcing

at the surface. We will start by looking at the present day compared to the pre-industrial scenario in some detail, and continue to describe changes in net cloud forcing at the surface between the 2SOx and the PRES scenario.

6.3.1 Net Cloud Forcing at the Surface, Present Day Compared to Pre-industrial Emissions

Figure 30(a) shows that the annually averaged surface net cloud forcing is positive over the entire Arctic region in the present day scenario. The areas where the net forcing is strong are either areas where the surface SW cloud forcing is weak (eg. over Greenland - due to high surface albedo) or areas where the surface LW cloud forcing is particularly strong (eg. the west coast of Spitsbergen - due to a high fraction of low clouds throughout the year). Areas of weak net cloud forcing are co-located with areas of strong surface SW cloud forcing - at low latitudes and areas of low surface albedo due to open water. The magnitude of the annually averaged surface net cloud forcing is 25.9 W/m^2 north of 71° in present day ($LWCF + SWCF = 42.0$ W/m^2 - 16.1 W/m^2).

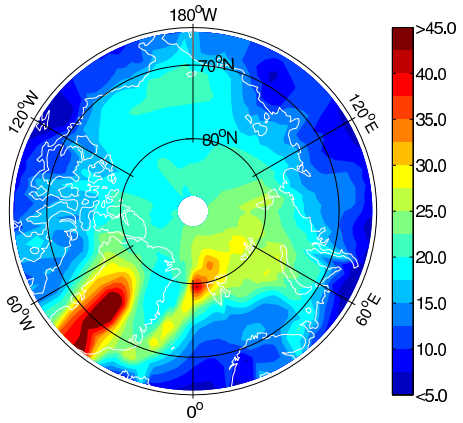

(a) Net CF at the surface. Annual average

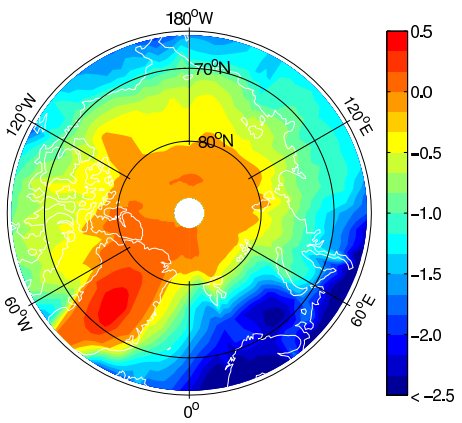

(b) ΔCF at the surface. Annual average

Figure 30: a) Net cloud forcing [W/m^2] at the surface in present day simulations. b) Change in net surface cloud forcing [W/m^2] between the PRES and the PIND scenarios. Forced model version.

Despite the overall positive net cloud forcing found in this region, the annually averaged change in this forcing between the PRES and the PIND scenario is negative. The change in surface net cloud forcing is shown in Figure 30(b). On an annual basis, the increase in cloud optical thickness due

to anthropogenic pollution is simulated to give a **0.35 W/m^2** decrease in the positive cloud forcing typical of the Arctic region. This confirms that the increased magnitude of SW cloud forcing with pollution is larger than the increased warming by clouds due to LW effects (see section 6.2.1).

The annual average gives information on the overall importance of the change in net cloud forcing from pre-industrial times to present day, but gives little insight into the seasonal variability of change in forcing with pollution. During summer the net cloud forcing in present day is positive over ice covered surfaces, while the areas of open water and the southern regions of the Arctic experience negative cloud forcing (Figure 31(a)). The LW component thus dominates where the surface albedo is high, as can be expected from section 5.3 (net cloud forcing, 1D), and the average net cloud forcing is 19.1 W/m^2 north of 71°N. The change in surface net cloud forcing with indirect effects is, on the other hand, negative over most of the Arctic region during summer (Figure 31(b)). The large change in SW cloud forcing dominates the change in net forcing completely, even over areas covered by surface ice (see Figure 28). The change in net surface cloud forcing averages to **-1.38 W/m^2** north of 71°N during this season. The increased amount of anthropogenic aerosols in clouds thus leads to an overall decrease in the surface radiative flux under cloudy skies in summer.

In winter, the SW cloud forcing is of less importance than in summer and the net surface cloud forcing is positive everywhere. It averages to 29.3 W/m^2 north of 71°N (Figure 31(c)). The change in net forcing with pollution is also controlled by LW effects. From Figure 31(d) it is clear that the increased LW component of the surface cloud forcing dominates during this season. Anthropogenic aerosols interacting with clouds lead to a net increase in the surface flux on the order of **0.16 W/m^2** north of 71°.

The magnitude of the change in surface net cloud forcing during winter can be put into perspective by using findings of Rothrock et al. (1999). They suggest that an approximate increase of 6.5 W/m^2 in the net radiation at the Arctic surface for one year is enough to decrease the thickness of the sea ice by 1.4 meters. Our winter period lasts for $\frac{2}{3}$ of the year, meaning that an increased net flux of $\sim$7.0 W/m^2 ($\frac{6.5}{1.4} * \frac{3}{2}$) throughout this period could lead to a one meter decrease in sea ice thickness. Our net increase of 0.16 W/m^2 during the winter season should therefore be enough to decrease the sea ice thickness by approximately 2 cm ($\frac{0.16}{7.0} \approx 0.02$). During summer the change in net cloud forcing with indirect effects is negative and is therefore expected to inhibit or delay the ice melt.

The results presented in this section do not include the change in the direct effect between the two scenarios. The change in this effect will influence the change in net surface cloud forcing through its influence on the SW

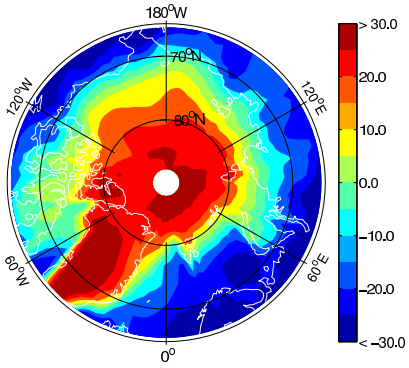

(a) Net CF at the surface. Summer

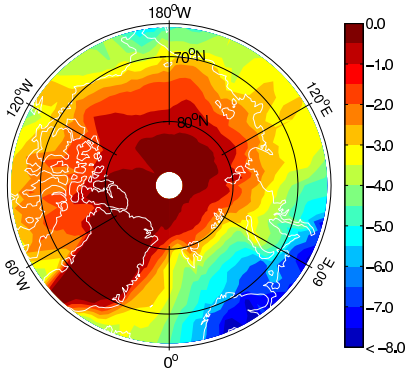

(b) ΔCF at the surface. Summer

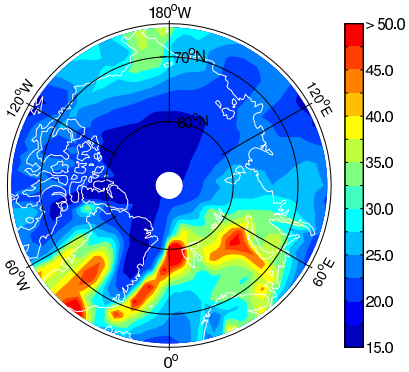

(c) Net CF at the surface. Winter

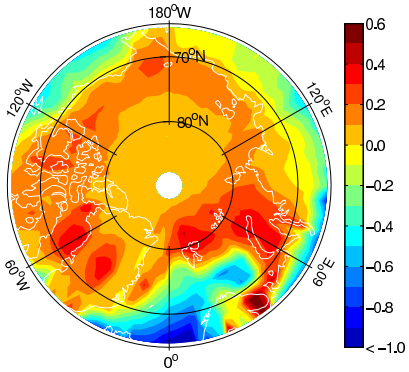

(d) ΔCF at the surface. Winter

Figure 31: Net cloud forcing [W/m^2] at the surface in present day simulations (left) and the change in this between the PRES and the PIND scenario (right). Forced model version.

component. The annually averaged change in surface cloud forcing in case 1 increases from -0.35 W/m^2 to +0.08 W/m^2 when including the change in direct effect. The summer average increases from -1.38 W/m^2 to -0.35 W/m^2 and the winter average from 0.16 W/m^2 to 0.30 W/m^2. The change in the net surface cloud forcing for simulations including both the direct and the indirect effects is thus positive. The increase in anthropogenic sulfate aerosols from pre-industrial times to present day leads to an overall increase in the warming effect of clouds in the Arctic. The increased direct effect with this increase in pollution will, on the other hand, act to reduce the radiative flux at the Arctic surface.

6.3.2 Net Cloud Forcing at the Surface, 2SOx Compared to Present Day

The change in surface net cloud forcing between the 2SOx and the present day scenario shows the same behaviour as in case 1. The magnitude of this change is low because of the small changes in both the LW and the SW cloud forcing between these scenarios. As shown earlier, these low signals of change are mainly due to small changes in the parameters that affect the LW cloud emissivity and the SW cloud albedo, combined with high initial optical thickness.

The annual average of change in surface net cloud forcing between the 2SOx and the PRES scenarios is -0.16 W/m^2 north of 71°N, while the winter mean is 0.09 W/m^2 and the summer mean -0.66 W/m^2. These low values of change further confirms that the clouds are less sensitive to increases in aerosol levels today than they were in pre-industrial times.

Our findings suggest that clouds in the Arctic are approaching saturation. Despite this, an increased amount of sulfate aerosols will continue to increase the direct effect of the aerosols and decrease the SW clear sky flux. This will decrease the magnitude of change in SW cloud forcing between the 2SOx and the PRES scenario. Including the change in direct effect in simulations of change in net surface flux in case 2 leads to the following results: Annual increase in surface cloud forcing of 0.19 W/m^2, winter increase of 0.22 W/m^2 and a summer *increase* in the surface cloud forcing with pollution of 0.14 W/m^2. The increased direct effect of the aerosols reduces the increased magnitude of the SW cloud forcing enough for LW effects to dominate, also during summer.

6.3.3 Summary of Changes in Net Cloud Forcing at the Surface

To summarize, our results show that the net surface cloud forcing is positive over much of the Arctic. Introducing increased amounts of sulfate aerosols into the Arctic clouds will lead to a *decrease* in the amount of radiation reaching the surface under cloudy skies (-0.35 W/m^2). During summer, the magnitude of the increased SW component dominates completely and the surface flux under cloudy skies decreases significantly (-1.38 W/m^2). In winter time, on the other hand, the magnitude of increased LW flux emitted by the clouds subject to pollution is most important (+0.16 W/m^2). *An increased cloud thickness due to increased amounts of anthropogenic aerosols will therefore in sum lead to a slight decrease in the net radiative flux at the surface, but will during winter lead to increased surface warming by the Arctic clouds.*

6.4 Cloud Forcing at the Top of the Atmosphere

Traditionally when discussing cloud forcing and indirect effects, the focus is on the top of the atmosphere. The change in radiative flux at this level over cloudy skies describes the total change in flux within the earth-atmosphere system. It tells us how much more or less energy is kept in the system with clouds present than without. We will now briefly discuss the change in cloud forcing at the top of the atmosphere with pollution as simulated by the forced version of the CAM-Oslo climate model. We will consider the present day versus the pre-industrial emissions only.

LW Cloud Forcing at the TOA

In the LW the average simulated cloud forcing at the TOA is positive for all seasons (Figure 32(a)). Averaged annually clouds increase the energy kept in the climate system by 14.7 W/m^2 north of 71°N. This can be explained by studying the clouds common in the Arctic region.

Figure 18(c) and 18(d) show that the largest fraction of clouds in the Arctic is found close to the surface. In summer, the simulated temperatures of these layers are very close to the surface temperature. Cloud tops in these layers will therefore emit approximately the same amount of energy as the surface and should contribute little to LW cloud forcing at the TOA. In winter, on the other hand, there are temperature inversions in the Arctic. Cloud tops are therefore often warmer than the underlying surface and the LW cloud forcing from these clouds should be negative at the TOA. Clouds close to the surface can therefore not explain the relatively large positive LW cloud forcing at the top of the atmosphere.

Figure 18(c) and 18(d) also show that a second cloud layer of much greater altitude is common both in summer and in winter (around 400 hPa). Clouds around this altitude have temperatures much lower than the temperatures at the surface (230-240 K vs. 255-270 K) and decrease the LW radiation reaching the TOA greatly. These clouds are what lead to the positive cloud forcing at the top of the atmosphere.

The change in LW cloud forcing at the TOA with pollution is very small (0.1 W/m^2 annually, Figure 32(b)). There are two main reasons for this. First, the high cloud layer important to the LW cloud forcing is primarily made up of ice particles. An increased amount of aerosols will only affect cloud droplet nucleation in our simulations and will therefore have little influence on this layer.

Secondly, the clouds at low levels have temperatures very close to the surface temperature. Changing the emissivity of these clouds will therefore

have little influence on the amount of radiation emitted towards the top of the atmosphere. Additionally, the main changes simulated both in effective radius and in liquid water path occur below the high cloud layer (see section 6.1.2). This reduces the possible influence of a change in LW emissivity with ΔLWP and $\Delta\bar{r}$ as the radiation emitted at levels where changes occur will be partially absorbed by the clouds above.

Combined, small changes in cloud radiative properties of high leveled clouds and little importance of changes occurring at low levels, lead to small changes in LW cloud forcing at the top of the atmosphere with increased amounts of anthropogenic sulfate.

SW Cloud Forcing at the TOA

The average SW cloud forcing at the TOA is negative for all seasons and averages to -14.1 W/m^2 north of 71°N on an annual basis (Figure 32(c)). The SW cloud forcing at this level is negative because clouds in general reflect more energy than the underlying surface. The average change in SWCF at the top of the atmosphere averages to -1.1 W/m^2 on an annual basis (Figure 32(d)). This signal of change is much greater than the change in LWCF at the TOA.

The SWCF is not affected directly by the temperature of the cloud top and therefore not by the height of the cloud layer (section 5.2). A given change in cloud albedo will affect the cloud forcing equally, independent of the height of the cloud layer. We just found that the cloud layer common around 400 hPa experiences little change in cloud parameters with pollution. This cloud layer is, however, not always present and because it is a thin layer with low average water content (not shown here) it is not likely to be optically thick in the SW. Changes in cloud albedo in levels below the top cloud layer are therefore likely to cause the relatively large changes in SWCF at the top of the atmosphere.

Net Cloud Forcing at the TOA

Simulations of the net cloud forcing at the top of the atmosphere shows that the forcing it self has both large positive and large negative values depending on surface albedo (Figure 32(e)). SW effects dominate over open water while LW effects dominates over ice covered surfaces. Averaged annually north of 71°N the TOA net cloud forcing is 0.6 W/m^2.

The average change in TOA net cloud forcing with increased aerosol levels is negative both during summer and winter season. Small changes in LWCF at the TOA lead to the net forcing being completely dominated by SW effects

(Figure 32(f)).

Increasing the concentration of anthropogenic aerosols in the Arctic clouds in the way simulated in this study has a decreasing effect on the net cloud forcing at the top of the atmosphere. More sulfate thus leads to more energy leaving the Earth-Atmosphere system.

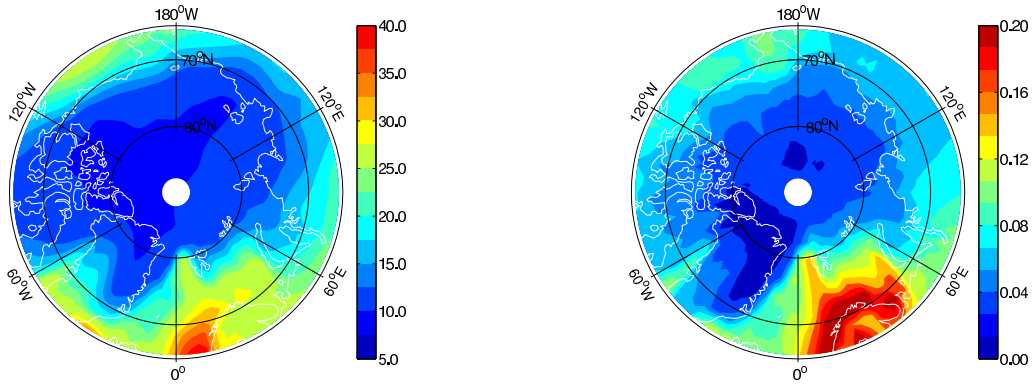

(a) LWCF TOA (b) ΔLWCF TOA

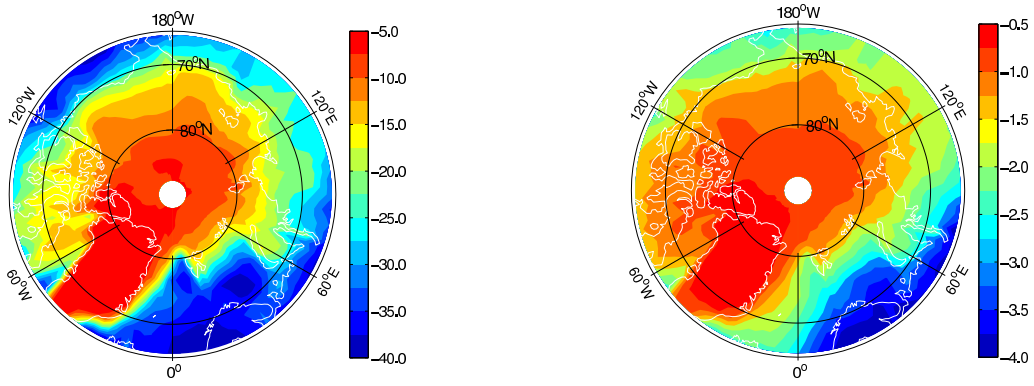

(c) SWCF TOA (d) ΔSWCF TOA

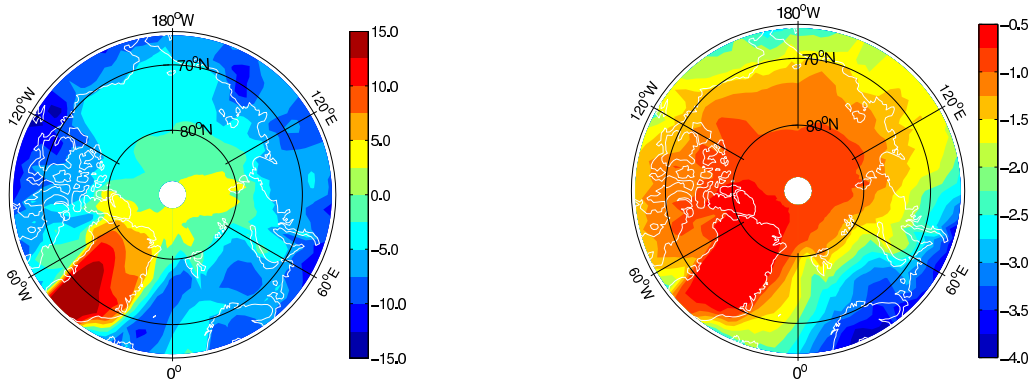

(e) Net CF TOA (f) ΔNet CF TOA

Figure 32: Cloud forcing at the top of the atmosphere [W/m^2], annual average. Forced model version. Note that scales differ.

7 Summary and Conclusions

In this thesis we have studied simulated changes in the radiative properties of Arctic clouds with pollution and how these changes affect the radiative balance at the surface. Our results show that the indirect effects of increased amounts of anthropogenic aerosol are close to the same magnitude in the LW and the SW wavelength ranges and nearly cancel on an annual basis.

The Arctic region is highly sensitive to climate change (Wang and Key, 2005) and the increase in air temperature near the surface is almost twice as large here as in the rest of the world (Graversen et al., 2008). Studies by Garrett and Zhao (2006) and Lubin and Vogelmann (2006) suggest that there are large increases in the LW radiation emitted towards the surface when going from pristine to polluted conditions under cloudy skies. They find an increase in surface radiative flux of 3.3 to 8.2 W/m^2, which is significantly larger than the average estimated increase due to the anthropogenic emissions of greenhouse gases (2.3 W/m^2) (IPCC, 2007). We found it important to study the overall effect of changes in cloud radiative properties with anthropogenic aerosols because of these earlier findings and the high sensitivity of this region to climate change. Additionally, it is important to study indirect effects in general as these are a major source of uncertainty in projections of future climate by the IPCC (IPCC, 2007).

The CAM-Oslo climate model was used to study the overall importance of the indirect effects. This model was verified by using observations from the SHEBA campaign (Intrieri et al. (2002b)). While the cloud fraction and the effective radius were reproduced well by the model, the magnitude of the liquid water path and the cloud forcing were both overestimated. Results presented in this thesis are from a forced version of the CAM-Oslo where the LWP has been reduced by a factor five through reducing the cloud droplet number concentration. This version is what gave the LWP and the cloud forcing closest to the observed SHEBA values.

Summary of key findings in this thesis:

- Results from the 1D model show that the cloud forcing of clouds with small initial liquid water paths is most susceptible to change with pollution. Changes in surface LWCF increase with increasing temperature of the cloud base. Changes in SWCF with pollution are large if the albedo of the underlying surface is low. The behaviour of the net cloud forcing depends on whether LW or SW effects dominate. This depends on the time of year, the underlying surface, the temperature of the cloud base and properties within the cloud - the effective radius and the liquid water path.

- The 1D model is capable of reproducing observed changes in LW cloud forcing with pollution. The LW radiation scheme, which is similar in the 1D and the 3D model, is therefore well suited for studying the LW radiative impact of changes in cloud properties with increased levels of anthropogenic sulfate aerosols.

- The simulated increase in LW cloud forcing at the surface due to anthropogenic sulfate aerosols averages to 0.64 W/m^2 annually. The increased LW surface flux is larger in summer (1.16 W/m^2) than in winter (0.39 W/m^2). This behavior is caused by larger changes in cloud emissivity with pollution in summer than in winter, combined with high fractions of low clouds and high cloud base temperatures in summer.

- The 3D model results of changes in LWCF due to indirect effects are *one order of magnitude* lower than the findings of Garrett and Zhao (2006) and Lubin and Vogelmann (2006). These background studies focused on cloud and aerosol conditions favorable to create changes in surface LWCF with pollution. Our study includes all conditions at all times of the year. While Garrett and Zhao and Lubin and Vogelmann find the maximum possible change in LW radiative flux due to anthropogenic aerosols in Arctic clouds, we find the overall radiative impact of changes in clouds with pollution.

- The simulated SWCF at the surface increases in magnitude due to indirect effects. The decrease in surface flux because of increased cloud albedo averages to -0.99 W/m^2 annually and -2.53 W/m^2 in summer.

- Results from the 3D model show an annual change in surface net cloud forcing of -0.35 W/m^2 due to indirect effects. Introducing more sulfate aerosols into clouds in the Arctic thus leads to an overall decrease in the radiative flux at the surface under cloudy skies. This decrease is not nearly large enough, however, to lead to negative net cloud forcing. During summer, the ability of clouds to increase the radiative flux at the surface decreases by 1.38 W/m^2 due to indirect effects. In winter, on the other hand, LW effects dominate and a changes in cloud properties due to anthropogenic aerosols increase the surface radiative flux by 0.16 W/m^2.

- Our simulations only include changes in cloud properties with pollution. An increase in anthropogenic sulfate aerosols will also influence the direct effect and the amount of energy reaching the surface under clear skies. Including the changes in direct effects between pre-industrial

times and present day reduces the change in SWCF significantly. The simulated change in net cloud forcing then averages to $+0.08$ W/m^2 on an annual basis. The overall effect of introducing increased amounts of anthropogenic sulfate aerosols into the Arctic is thus a slightly increased warming effect of clouds in this region (assuming that the direct and indirect effects dominate over other possible effects of such an increase).

Results from the hypothesised scenario where the emissions of SO_2 from fossil fuel combustion were doubled are not included in the summary above. We now know that the emissions of this sulfate precursor have decreased in Europe and Russia over the last years (Karnieli et al., 2009). One can therefore question whether this scenario is realistic. However, results from simulations using these emissions are informative. They show that an absolute increase in SO_4 concentrations of the same magnitude as the increase from pre-industrial times till today will affect the cloud forcing less than when the initial concentrations were lower. It shows that the system is closer to saturation today than in pre-industrial times.

The simulated overall change in surface net cloud forcing is negative due to the strong SW contribution where the surface albedo is low. In recent years the extent of the sea ice over the North Pole has decreased, reaching a minimum in September 2007 (NSIDC, 2009a). Because of the ice-albedo feedback and an expected further increase in Arctic surface temperatures many expect further reductions in the polar ice cap. This reduction is coincident with a reduction in surface albedo and it is likely that the importance of the SW component of cloud forcing is increasing. The indirect effects in the Arctic will thus have a larger negative influence on the surface net cloud forcing in the future than today. During winter time, however, the lack of sunlight ensures that the LW component of change in surface cloud forcing with pollution will still be positive.

Based on our findings and the sensitivity of the Arctic climate, the indirect effects in the Arctic should be studied further. Several measures can be made in order to deepen our understanding of these effects and get more precise answers. First of all, the accuracy of climate models needs to be improved, especially in dealing with cloud water amount and conversion between liquid water and solid phased particles. Secondly, a higher frequency and larger geographical spread in Arctic measuring campaigns are needed. The current lack of comprehensive observations limits the possibility of verifying and improving current climate models.

The empirical studies conducted by Garrett and Zhao and Lubin and Vogelmann on the topic of indirect effects in the Arctic show a potentially *large* increase in LW surface flux when polluted air and clouds interact. In this

thesis we find that indirect effects may lead to an increase in the LW surface flux, but our study nevertheless concludes that the overall effect of increased levels of anthropogenic aerosols under cloudy skies is a small *decrease* in surface radiative flux.

References

Barrie, L. A. (1986). Arcitc air pollution: An overview of current knowledge. *Atmospheric Environment*, 20, 643–663.

Curry, J. A. and E. E. Ebert (1992). Annual Cycle of Radiation Fluxes over the Arctic Ocean: Sensitivity to Cloud Optical Properties. *Journal of Climate*, 5, 1267–1280.

Curry, J. A., P. V. Hobbs, M. D. King, D. A. Randall, P. Minnis, G. A. Isaac, J. O. Pinto, T. Uttal, A. Bucholtz, D. G. Cripe, H. Gerber, C. W. Fairall, T. J. Garrett, J. Hudson, J. M. Intrieri, C. Jakob, T. Jensen, P. Lawson, D. Marcotte, L. Nguyen, P. Pilewskie, A. Rangno, D. C. Rogers, K. B. Strawbridge, F. P. J. Valero, A. G. Williams, and D. Wylie (2000). FIRE Arctic Clouds Experiment. *Bulletin of the American Meteorological Society*, 81, 5–29.

Curry, J. A., W. B. Rossow, D. Randall, and J. L. Schramm (1996). Overview of Arctic Cloud and Radiation Characteristics. *Journal of Climate*, 9, 1731–1764.

Dreiling, V. and B. Friederich (1997). Spatial distribution of the arctic haze aerosol size distribution in western and eastern Arctic. *Atmospheric Research*, 44, 133–152.

Garrett, J. T., L. F. Radke, and P. V. Hobbs (2002). Aerosol Effects on Cloud Emissivity and Surface Longwave Heating in the Arctic. *Journal of the Atmospheric Sciences*, 59, 769–778.

Garrett, T. J. and C. Zhao (2006). Increased Arctic cloud longwave emissivity associated with pollution from mid-latitudes. *Nature*, 440, 787–789.

Graversen, R. G., T. Mauritsen, M. Tjernström, E. Källen, and G. Svensson (2008). Vertical structure of recent Arctic warming. *Nature*, 541, 53–57.

Hobbs, P. V. (1993). *Aerosol-Cloud-Climate Interactions*. Academic Press Inc.

Intrieri, J. M., C. W. Fairall, M. D. Shupe, P. O. G. Persson, E. L. Andreas, P. S. Guest, and R. E. Moritz (2002a). An annual cycle of Arctic surface cloud forcing at SHEBA. *Journal of Geophysical Research*, 107, 13,1–13,14.

Intrieri, J. M., M. D. Shupe, T. Uttal, and B. J. McCarty (2002b). An annual cycle of Arctic cloud characteristics observed by radar and lidar at SHEBA. *Journal of Geophysical Research*, 107, 5,1–5,15.

IPCC (2007). Climate Change 2007: The Physical Science Basis. Contribution of Working Group I to the Fourth Assessment Report of the Intergovernmental Panel on Climate Change. Summary for Policymakers. . Technical report, UN. *http* : *//ipcc* − *wg*1.*ucar.edu*/*wg*1/*Report*/*AR*4*WG*1$_P$*rint*$_S$*PM.pdf*..

Karnieli, A., Y. Derimian, R. Indoitu, N. Panov, R. C. Levy, L. A. Remer, W. Maenhaut, and B. N. Holben (2009). Temporal trend in anthropogenic sulfur aerosol transport from central and eastern Europe to Israel. *Journal of Geophysical Research*, 114, D00D19, 1–12.

Klein, S. A., R. B. McCoy, H. Morrison, A. S. Ackermann, A. Avramov, G. de Boer, M. Chen, J. N. S. Cole, A. D. Den Genio, M. Falk, M. Foster, A. Fridlin, J. C. Golaz, T. Hashino, J. Y. Harrington, C. Hoose, M. F. Khairoutdinov, V. E. Larson, X. Liu, Y. Luo, G. M. McFarquhar, S. Menon, R. A. J. Neggers, S. Park, M. R. Poellot, J. M. Schmidt, I. Sednev, B. J. Shipway, M. D. Shupe, D. A. Spangenberg, Y. C. Sud, D. D. Turner, D. E. Veron, K. von Salzen, G. K. Walker, Z. Wang, A. B. Wolf, S. Xie, K. M. Xu, F. Yang, and G. Zhang (2009). Intercomparison of model simulations of mixed-phase clouds observed during the ARM Mixed-Phase Arctic CLoud Experiment. I: Single-layer cloud. *Q. J. R. Meteorol. Soc.*, 135, 979–1002.

Kristjánsson, J. E., J. M. Edwards, and D. L. Mitchell (2000). Impact of a new scheme for optical properties of ice crystals on climates of two gcms. *Journal of Geophysical Research*, 105, 10063–10079.

Löhnert, U., G. Feingold, T. Uttal, A. S. Frisch, and M. D. Shupe (2003). Analysis of two independent methods for retrieving liquid water profiles in spring and summer Arctic boundary clouds. *Journal of Geophysical Research*, 108(D.7).

Lin, B., P. Minnis, A. Fan, J. A. Curry, and H. Gerber (2001). Comparison of cloud liquid water paths derived from in situ and microwave radiometer data taken during the SHEBA/FIREACE. *Geophysical Research Letters*, 28, 975–978.

Liou, K. N. (2002). *An Introduction to Atmospheric Radiation*. Academic Press, 2nd edition.

Lohmann, U. (2005). Indirect Effects: Aerosol and Cloud Microphysics. IPCC Expert Meeting on Aerosols, Geneva.

Lubin, D. and A. M. Vogelmann (2006). A climatologically significant aerosol longwave indirect effect in the Arctic. *Nature*, 439, 453–456.

Meador, W. E. and W. R. Weaver (1980). Two-Stream Approximations to Radiative Transfer in Planetary Atmospheres: A Unified Description of Existing Methods and a New Improvement. *Journal of the Atmospheric Sciences*, 37, 630–643.

Menon, S., A. D. Del Genio, D. Koch, and G. Tselioudis (2002). GCM Simulations of the Aerosol Indirect Effect: Sensitivity to Cloud Parameterization and Aerosol Burden. *Journal of the Atmospheric sciences*, 59, 692–713.

Morrison, H., R. B. McCoy, S. A. Klein, S. Xie, Y. Luo, A. Avramov, M. Chen, J. N. S. Cole, M. Falk, M. J. Foster, A. D. Del Genio, J. Y. Harrington, C. Hoose, M. F. Khairoutdinov, V. E. Larson, X. Liu, G. M. McFarquhar, M. R. Poellot, K. von Salzen, B. J. Shipway, M. D. Shupe, Y. C. Sud, D. D. Turner, D. E. Veron, G. K. Walker, Z. Wang, A. B. Wolf, K. M. Xu, F. Yang, and G. Zhang (2009). Intercomparison of model simulations of mixed-phase clouds observed during the ARM Mixed-Phase Arctic CLoud Experiment. II: Multilayer cloud. *Q.J.R. Meteorol. Soc.*, 135, 1003–1019.

Morrison, H., M. D. Shupe, and J. A. Curry (2003). Modeling clouds observed at SHEBA using a bulk microphysics parameterization implemented into a single-column model. *Journal of Geophysical Research*, 108.

NSIDC (2009a). National Snow and Ice Data Center. *http* : *//nsidc.org/arcticseaicenews/*2007*.html*.

NSIDC (2009b). National Snow and Ice Data Center. *http* : *//nsidc.org*.

Quinn, P. K., T. S. Bates, E. Baum, N. Doubleday, A. M. Fiore, M. Flanner, A. Fridlind, T. J. Garrett, D. Koch, S. Menon, D. Shindell, A. Stohl, and S. G. Warren (2008). Short-lived pollutants in the Arctic: their climate impact and possible mittigation strategies. *Atmospheric Chemestry and Physics*, 8, 1723–1735.

Quinn, P. K., G. Shaw, E. Andrews, E. G. Dutton, T. Ruoho-Airola, and S. L. Gong (2007). Arctic haze: current trends and knowledge gaps. *Tellus*, 59B, 99–114.

Rasch, P. J. and J. E. Kristjánsson (1998). A Comparison of the CCM3 Model Climate Using Diagnosed and Predicted Condensate Parameterizations. *Journal of Climate*, 11, 1587–1614.

Rogers, R. R. and M. K. Yau (1989). *A Short Course in Cloud Physics*, chapter 5. Butterworth - Heinemann, 3rd edition.

Rothrock, D. A., Y. Yu, and G. A. Maykut (1999). Thinning of the Arctic Sea-Ice Cover. *Geophys.res. lett.*, 26, 3469–3472.

Scheuer, E., R. W. Talbot, J. E. Dibb, G. K. Seid, L. DeBell, and B. Lefer (2003). Seasonal distributions of fine aerosol sulfate in the North American Arctic basin during TOPSE. *Journal of Geophysical Research*, 108, TOP 18–1, TOP 18–11.

Shupe, M. D. and J. M. Intrieri (2004). Cloud Radiative Forcing of the Arctic Surface: The Influence of Cloud Properties, Surface Albedo, and Solar Zenith Angle. *Journal of Climate*, 17, 616–628.

Shupe, M. D., S. Y. Matrosov, and T. Uttal (2005). Arctic Mixed-Phase Cloud Properties Derived from Surface-Based Sensors. *Fofteenth ARM Science Team Meeting Proceedings*.

Shupe, M. D., T. Uttal, S. Y. Matrosov, and A. S. Frisch (2001). Cloud water contents and hydrometeor sizes during the FIRE Arctic Clouds Experiment. *Journal of Geophysical Research*, 106, 15,015–15,028.

Slingo, A. (1989). A GCM Parameterization for the Shortwave Radiative Properties of Water Clouds. *Journal of the Atmospheric Sciences*, 46, 1419–1427.

Slingo, A. and H. M. Schrecker (1982). On the shortwave radiative properties of stratiform water clouds. *Quart. J. Roy. Meteor. Soc.*, 108, 407–426.

Talbot, R. W., A. S. Vijgen, and R. C. Harriss (1992). Soluble Species in the arctic summer troposphere: Acidic gases, aerosols, and precipitation. *Journal of Geophysical Research*, 97, 16,531 – 16,543.

Treffeisen, R., A. Rinke, M. Fortmann, K. Dethloff, A. Herber, and T. Yamanouchi (2005). A case study of the radiative effects of Arctic aerosols in March 2000. *Atmospheric Environment*, 39, 899–911.

Twomey, S. (1974). Pollution and the Planetary Albedo. *Atmospheric Environment*, 8, 1251–1256.

Twomey, S. (1977). The Influence of Pollution on the Shortwave Albedo of Clouds. *Journal of the Atmospheric Sciences*, 34, 1149–1152.

Wang, X. and J. R. Key (2005). Arctic Surface, Cloud, and Radiation Properties Based on the AVHRR Polar Pathfinder Dataset. Part I: Spatial and Temporal Characteristics. *Journal of Climate*, 18, 2558–2574.

Zhang, J. and U. Lohmann (2002). A new statistically based autoconversion rate parameterization for use in large-scale models. *Journal of Geophysical Research*, 107(D.24).

Zhang, T., K. Stamnes, and S. A. Bowling (1996). Impact of Clouds on Surface Radiative Fluxes and Snowmelt in the Arctic and Subarctic. *Journal of Climate*, 9, 2110–2123.